ISSN 1984-6428

APRIL-JUNE
2012
VOLUME 4
NUMBER 2

Orbital

The Electronic Journal of Chemistry

Hydrocortisone-loaded poly-ε-caprolactone nanoparticles

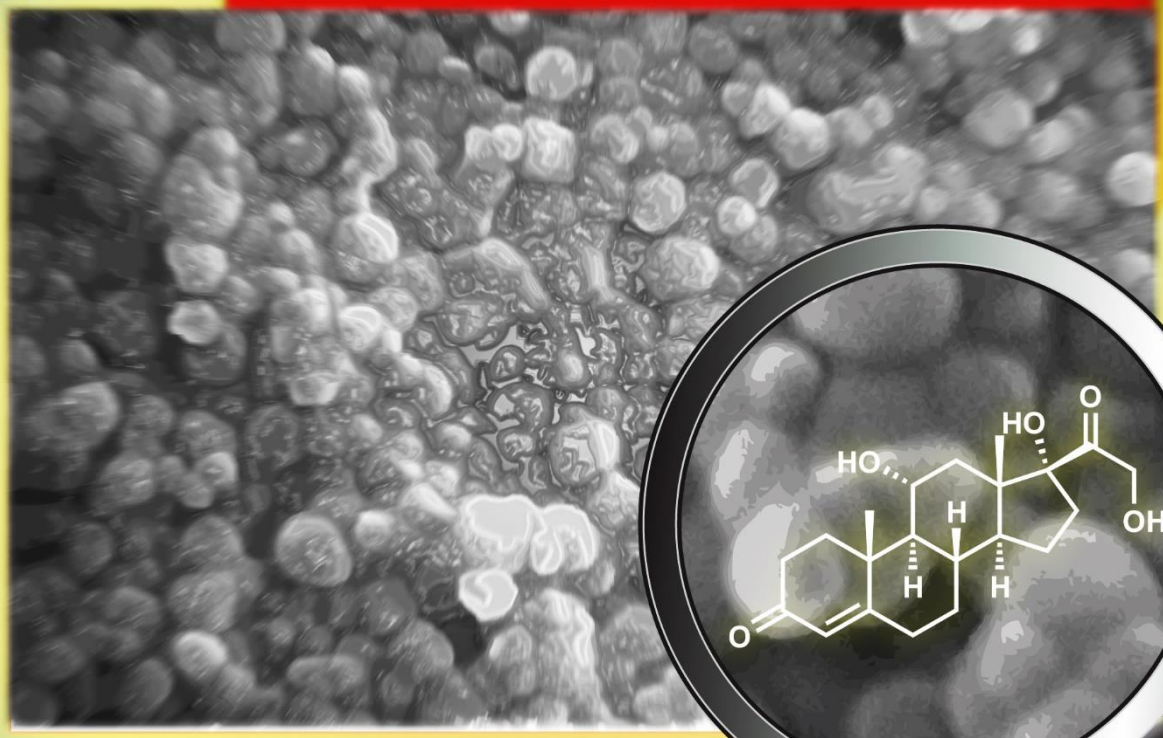

Published by the
Department of Chemistry of the Federal
University of Mato Grosso do Sul.
Campo Grande, BRAZIL

www.orbital.ufms.br

UFMS

Orbital - Vol. 4 No. 2 - April-June 2012

Table of Contents

EDITORIAL

FULL PAPERS

Orbital
The Electronic Journal of Chemistry

Editorial

Ethics in Science: Pleasure and obligation?

Dear Readers:

In this volume of Orbital - The Electronic Journal, we would like to promote a reflection about a highlighted theme in the scientific world - Ethics in Science. Over the last few decades we have verified a progressive increase in the flow of scientific production, reaching the mark of dozens of articles a day only in chemistry. Much of this increase in worldwide scientific production comes from the current technological landscape and sophisticated research instrumentation, which permit fast results with high impact. With an ever increasing flow of papers, we have established a dangerous level of requirements, an almost pathological necessity for good (or bad) results, which in the opinion of many researchers have destroyed a basic principle of science, the pleasure to practice science.

How much time should we invest in the production of a paper? Is there a defined time? Is this the correct way that we should do science, or are publications a natural consequence of matured results achieved with the pleasure of a great discovery/realization?

There is also much concern about the formation of our future scientists. Are our research centers actually making students aware and able to realize new discoveries, or are just teaching them how to produce a paper? These are important considerations that we would like present in this editorial, because they are directly connected to one of the biggest crises experienced by the scientific world, the crisis of ethics in science. There is no doubt that the whole essence of science - the pleasure of a discovery or an achieved target - has been lost among the uncontrolled requirements to produce ever increasing numbers. Young and also more established scientists have introduced false results into the literature or have performed plagiarism, which has caused confusion throughout the community. The question is: What is the pleasure of telling the world that something has been done or discovered if it is not true? There is no sense in the dissemination of science if it is not true. The Orbital team calls on the Brazilian and the worldwide scientific communities to establish a discussion about this theme, starting from the centers of knowledge production to the higher spheres of world science. Above all, we would like to transmit the message that the practice of ethics in science begins with small gestures and should spread to the whole scientific environment. There is no pleasure in having a name stamped on something that does not belong or that does not even exist.

Ética na Ciência: Um prazer e dever?

Orbital
The Electronic Journal of Chemistry

Caros leitores:

Neste volume da *Orbital – The Electronic Journal of Chemistry,* gostaríamos de promover uma reflexão diante de um tema em destaque no cenário científico mundial – Ética na Ciência. Nas últimas décadas assistimos a um progressivo aumento do fluxo de produção científica chegando à marca de dezenas de artigos/dia somente na área de química. Grande parte deste aumento na produção científica mundial advém do atual cenário tecnológico e de instrumentação que dinamizaram as pesquisas permitindo resultados rápidos e de valor elevado. Com um fluxo cada vez maior de trabalhos, temos verificado um nível perigoso de cobrança, de certa forma, uma necessidade quase patológica por resultados prontos, o que na opinião de muitos pesquisadores vêm removendo da ciência um princípio básico, o prazer de se produzir ciência.

Quanto tempo devemos investir na produção de um *paper*? Há definitivamente um prazo? É assim que devemos ponderar fazer ciência, ou publicar trabalhos deve ser uma consequência natural de resultados maduros alcançados com o prazer de uma grande descoberta/realização?

Fica ainda a preocupação de como estamos preparando nossos cientistas do futuro. Os nossos centros de pesquisa estão de fato produzindo conhecimento e pessoas capazes de fomentar novas descobertas no futuro, ou apenas estamos ensinando como se produzir um *paper*? Estas são reflexões importantes que gostaríamos de deixar neste editorial, pois estão diretamente ligadas a uma das maiores crises vividas pela ciência mundial, a crise da Ética na Ciência. Não há dúvidas de que toda a essência científica – o prazer de uma descoberta ou alvo alcançado – tem se perdido em meio à necessidade desenfreada de produzir números cada vez maiores. Cientistas jovens e também os mais consolidados têm lamentavelmente introduzido resultados falsos na literatura ou realizando plágio, o que tem provocado perplexidade em toda comunidade. A pergunta que fica é: Qual o prazer de dizer ao mundo que algo fora feito ou descoberto se "este algo" de fato não foi feito ou ainda não existe? Não há sentido em divulgar ciência se ela não é verdadeira. Nós do time da Orbital conclamamos a comunidade científica brasileira e mundial a uma discussão profunda sobre este tema, desde as pequenas células de produção do conhecimento até as esferas superiores da ciência mundial. Acima de tudo, deixamos a mensagem de que a prática da ética na ciência inicia-se com os pequenos gestos dentro das pequenas equipes e deve se alastrar para tudo que se faz e se produz no ambiente científico. Não há prazer algum em ter um nome estampado em algo que não lhe pertence ou que sequer existe.

Kleber Thiago de Oliveira (UFSCar)
Associate Editor, Orbital

ISSN 1984-6428
ONLINE
www.orbital.ufms.br

| Vol 4 | | No. 2 | | April-June 2012 |

Full Paper

Synthesis of some novel 3-[ω–(substituted phenoxy/anilino/thiophenoxy/2-pyridylamino) alkoxy] flavones

K. L. Ameta[a], R. S. Sodani[b], R. B. Bhandari[b] and B. L. Verma[b]*

[a]Department of Chemistry, Faculty of Arts Science and Commerce, MITS University, Lakshmangarh, Rajasthan-332311, India.
[b]Department of Chemistry, University College of Science, MLS University, Udaipur, Rajasthan-313001, India.

Received: 31 December 2011; revised: 15 March 2012; accepted: 07 May 2012. Available online: 07 July 2012.

ABSTRACT: *Several α-(3-flavonyloxy)-ω-bromoalkanes (**1**) on treatment with substituted phenols, anilines, thiophenols and 2-aminopyridine resulted novel potentially bioactive 3-[ω-substituted phenoxy (**3a-t**), anilino (**4a-h**), thiophenoxy (**5a-d**) and 2-pyridylamino (**7a-c**) alkoxy] flavones. The structures of the products have been elucidated by analytical and spectral data.*

Keywords: *flavone; α-(3-flavonyloxy)-ω-bromoalkanes; 2-aminopyridine*

Introduction

The flavones ring (2-phenyl-4H-1-benzopyran-4-one) constitutes a large segment of natural products. Currently the synthesis of flavones and their derivatives have attracted considerable attention due to their significant biochemical and pharmacological activities which are beneficial for human health [1], including biocidal [2], antioxidant [3], anti-cancer [4], anti-inflammatory [5] and anti-diabetic effects [6]. A number of flavones derivatives carrying a methoxy group at C-3 position and a hydroxyl group at C-5 position are found to be anti-cancer and anti-viral agents [7, 8]. In view of these observations and in continuation of our work on the chemistry of α-(3-flavonyloxy)-ω-bromoalkane [9] derivatives and therapeutic potential of flavonoids for making valuable targets for drug design [10-16], it was considered of interest to report the synthesis of some novel potentially bioactive 3-[ω-(substituted phenoxy/anilino/thiophenoxy/2-pyridyl

* Corresponding author. E-mail: klameta77@yahoo.co.in

amino alkoxy] flavones (**3a-t, 4a-h, 5a-d, 7a-c**) in this paper (Scheme 1).

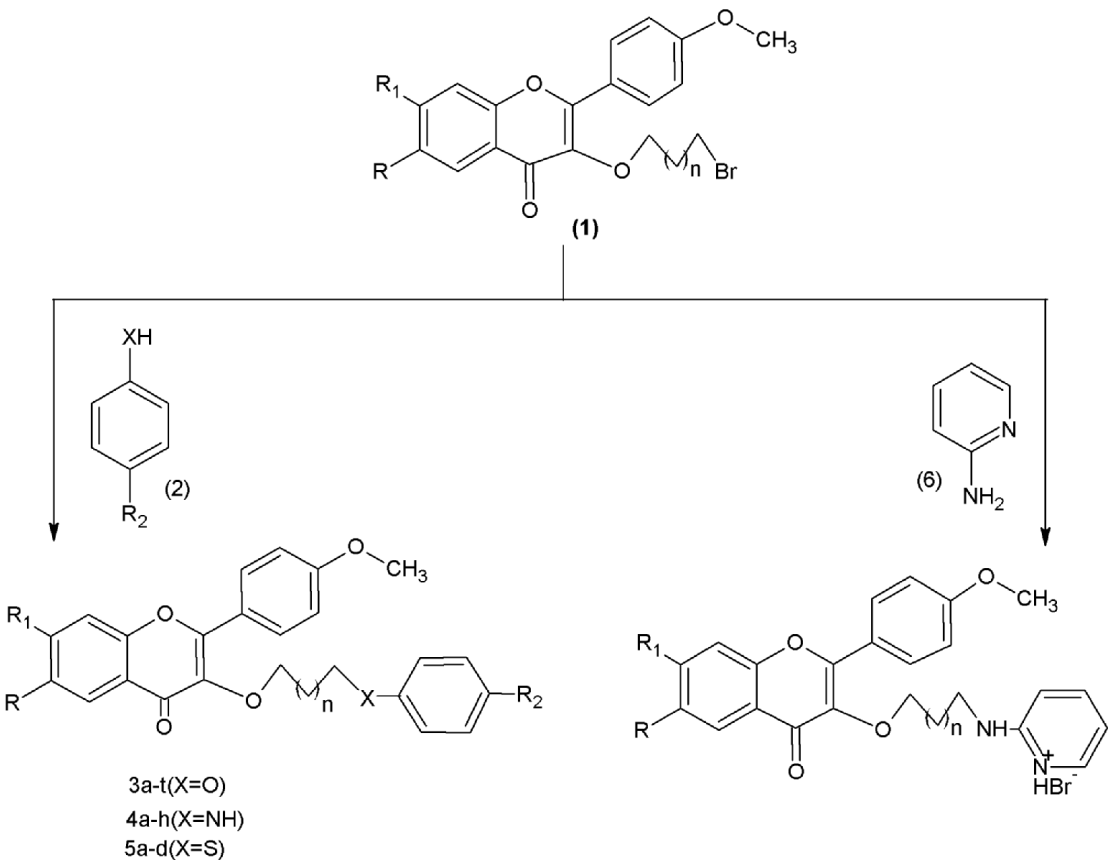

Scheme 1. Synthesis of substituted flavones

Material and Methods

All melting points were taken in open capillaries and are uncorrected. Purity of the samples was checked by TLC using silica gel-G plates using ethyl acetate-benzene (9:1, v/v) or benzene alone as solvent systems. Visualization of spots was done in iodine chamber or by spraying with aq. H_2SO_4 (10%). IR spectra (KBr) were recorded on DIGILAB FTS-14 or Perkin- Elmer 157 P spectrophotometer (ν_{max} in cm^{-1}). ^1H NMR spectra were recorded in $CDCl_3$ on a Varian CFT-20 and Brucker DRX-300 (300 MHz) spectrometer using TMS as internal standard (chemical shifts in δ, ppm). All compounds gave satisfactory elemental analysis. Synthesis of α-(3-flavonyloxy)-ω-bromoalkanes **(1)** was carried out as reported in our earlier communications [9].

General procedure for the synthesis of 3-[ω-(substituted phenoxy/thiophenoxy/alkoxy]-flavones (3a-t and 5a-d).

A mixture of α-flavonyloxy-ω-bromoalkane (0.01 mol), phenol/thiophenol (0.01 mol) and anhydrous potassium carbonate (0.02 mol) in dry acetone (100 mL) was refluxed (8-10 h) till the completion of the reaction (TLC). The solvent was distilled off under reduced pressure and the residue was triturated with dill NaOH and then with

water (3X50 mL). The separated solid was filtered, dried and recrystalization with proper solvent afford as the analytical samples (Table 1).

Analytical data

3a: IR (KBr) ν/cm^{-1} 1640 (C=O), 1260 (asym C-O-C), 1040 (sym C-O-C). ^{1}H NMR (CDCl3, 300 mHz): δ_H 2.11 (2H, t, -CH_2-), 2.45 (3H, s, CH_3), 3.45 (3H, s, 4'-OCH_3), 4.29 (4H, t, 2x -OCH_2-), 7.31-7.64 (11H, m, Ar-H).

3b: IR (KBr) ν/cm^{-1} 1640 (C=O), 1265 (asym C-O-C), 1040 (sym C-O-C). ^{1}H NMR (CDCl3, 300 mHz): δ_H 2.14 (2H, t, -CH_2-), 2.43 (3H, s, CH_3), 3.44 (3H, s, 4'-OCH_3), 4.26 (4H, t, 2x -OCH_2-), 7.35-7.74 (11H, m, Ar-H).

3c: IR (KBr) ν/cm^{-1} 1640 (C=O), 1260 (asym C-O-C), 1040 (sym C-O-C). ^{1}H NMR (CDCl3, 300 mHz): δ_H 2.13 (2H, t, -CH_2-), 2.45 (3H, s, CH_3), 3.45 (3H, s, 4'-OCH_3), 4.15 (4H, t, 2x -OCH_2-), 6.89-8.08 (11H, m, Ar-H).

3d: IR (KBr) ν/cm^{-1} 1640 (C=O), 1260 (asym C-O-C), 1040 (sym C-O-C). ^{1}H NMR (CDCl3, 300 mHz): δ_H 2.13 (2H, t, -CH_2-), 2.48 (3H, s, CH_3), 3.47 (3H, s, 4'-OCH_3), 4.16 (4H, t, 2x -OCH_2-), 7.02-8.14 (11H, m, Ar-H).

3e: IR (KBr) ν/cm^{-1} 1640 (C=O), 1260 (asym C-O-C), 1040 (sym C-O-C). ^{1}H NMR (CDCl3, 300 mHz): δ_H 2.12 (2H, t, -CH_2-), 3.77 (3H, s, 2x-OCH_3), 4.18 (4H, t, 2x -OCH_2-), 6.89-7.88 (11H, m, Ar-H).

3f: IR (KBr) ν/cm^{-1} 1640 (C=O), 1260 (asym C-O-C), 1040 (sym C-O-C). ^{1}H NMR (CDCl3, 300 mHz): δ_H 2.11 (2H, t, -CH_2-), 3.77 (3H, s, 2x-OCH_3), 4.29 (4H, t, 2x -OCH_2-), 7.31-7.68 (11H, m, Ar-H).

3g: IR (KBr) ν/cm^{-1} 1640 (C=O), 1260 (asym C-O-C), 1040 (sym C-O-C). ^{1}H NMR (CDCl3, 300 mHz): δ_H 2.14 (2H, t, -CH_2-), 3.79 (3H, s, 2x-OCH_3), 4.29 (4H, t, 2x -OCH_2-), 7.28-7.64 (11H, m, Ar-H).

3h: IR (KBr) ν/cm^{-1} 1640 (C=O), 1260 (asym C-O-C), 1040 cm^{-1} (sym C-O-C). ^{1}H NMR (CDCl3, 300 mHz): δ_H 2.18 (2H, t, -CH_2-), 3.77 (3H, s, 2x-OCH_3), 4.22 (4H, t, 2x -OCH_2-), 7.22-7.78 (11H, m, Ar-H).

3i: IR (KBr) ν/cm^{-1} 1640 (C=O), 1260 (asym C-O-C), 1040 (sym C-O-C). ^{1}H NMR (CDCl3, 300 mHz): δ_H 1.79 (4H, m, 2x-CH_2-), 2.49 (3H, s, CH_3), 3.79 (3H, s, 4'-OCH_3), 4.29 (4H, t, 2x -OCH_2-), 6.98-7.99 (11H, m, Ar-H).

3j: IR (KBr) ν/cm^{-1} 1640 (C=O), 1260 (asym C-O-C), 1040 (sym C-O-C). ^{1}H NMR (CDCl3, 300 mHz): δ_H 1.76 (4H, m, 2x-CH_2-), 2.46 (3H, s, CH_3), 3.79 (3H, s, 4'-OCH_3), 4.29 (4H, t, 2x -OCH_2-), 6.98-7.94 (11H, m, Ar-H).

3k: IR (KBr) ν/cm^{-1} 1640 (C=O), 1260 (asym C-O-C), 1040 (sym C-O-C). ^{1}H NMR (CDCl3, 300 mHz): δ_H 1.89 (4H, m, 2x-CH_2-), 2.48 (3H, s, CH_3), 3.77 (3H, s, 4'-OCH_3), 4.16 (4H, t, 2x -OCH_2-), 7.02-7.98 (11H, m, Ar-H).

3l: IR (KBr) ν/cm^{-1} 1640 (C=O), 1260 (asym C-O-C), 1040 (sym C-O-C). ^{1}H NMR (CDCl3, 300 mHz): δ_H 1.80 (4H, m, 2x-CH_2-), 2.48 (3H, s, CH_3), 3.89 (3H, s, 4'-OCH_3), 4.01 (4H, t, 2x -OCH_2-), 6.80-8.20 (11H, m, Ar-H).

3m: IR (KBr) ν/cm^{-1} 1640 cm^{-1} (C=O), 1260 (asym C-O-C), 1040 (sym C-O-C). ^{1}H NMR (CDCl3, 300 mHz): δ_H 1.88 (6H, m, 3x-CH_2-), 2.48 (3H, s, CH_3), 3.80 (3H, s, 4'-OCH_3), 4.19 (4H, t, 2x -OCH_2-), 6.92-7.98 (11H, m, Ar-H).

3n: IR (KBr) ν/cm^{-1} 1640 (C=O), 1260 (asym C-O-C), 1040 (sym C-O-C). ^{1}H NMR (CDCl3, 300 mHz): δ_H 1.64 (6H, m, 3x-CH_2-), 2.49 (3H, s, CH_3), 3.77 (3H, s, 4'-OCH_3), 4.10 (4H, t, 2x -OCH_2-), 7.02-7.68 (11H, m, Ar-H).

3o: IR (KBr) ν/cm^{-1} 1640 cm^{-1} (C=O), 1260 (asym C-O-C), 1040 (sym C-O-C). ^{1}H NMR (CDCl3, 300 mHz): δ_H 1.82 (6H, m, 3x-CH_2-), 2.46 (3H, s, CH_3), 3.78 (3H, s, 4'-OCH_3), 4.27 (4H, t, 2x -OCH_2-), 7.02-7.68 (11H, m, Ar-H).

3p: IR (KBr) ν/cm^{-1} 1640 (C=O), 1260 (asym C-O-C), 1040 (sym C-O-C). ^{1}H NMR (CDCl3, 300 mHz): δ_H 1.20-1.90 (6H, m, 3X-CH_2-), 2.45 (3H, s, CH_3), 3.85 (3H, s, 4'-OCH_3), 4.10 (4H, t, 2x -OCH_2-), 6.82-7.96 (11H, m, Ar-H).

3q: IR (KBr) ν/cm^{-1} 1640 (C=O), 1260 (asym C-O-C), 1060 (sym C-O-C). ^{1}H NMR (CDCl3, 300 mHz): δ_H 1.10-1.80 (8H, m, 4X-CH_2-), 2.46 (3H, s, CH_3), 3.75 (3H, s, 4'-OCH_3), 4.02 (4H, t, 2x -OCH_2-), 6.78-7.98 (11H, m, Ar-H).

3r: IR (KBr) ν/cm^{-1} 1640 (C=O), 1260 (asym C-O-C), 1060 (sym C-O-C). δ_H 1.20-1.92 (8H, m, 4X-CH_2-), 2.42 (3H, s, CH_3), 3.79 (3H, s, 4'-OCH_3), 4.29 (4H, t, 2x -OCH_2-), 6.38-7.92 (11H, m, Ar-H).

3s: IR (KBr) ν/cm^{-1} 1640 (C=O), 1260 (asym C-O-C), 1060 (sym C-O-C). ^{1}H NMR (CDCl3, 300 mHz): δ_H 1.76 (8H, m, 4X-CH_2-), 2.46 (3H, s, CH_3), 3.76 (3H, s, 4'-OCH_3), 4.49 (4H, t, 2x -OCH_2-), 6.64-7.98 (11H, m, Ar-H).

3t: IR (KBr) ν/cm^{-1} 1640 (C=O), 1260 (asym C-O-C), 1060 (sym C-O-C). ^{1}H NMR (CDCl3, 300 mHz): δ_H 1.10-1.80 (8H, m, 4X-CH_2-), 2.46 (3H, s, CH_3), 3.75 (3H, s, 4'-OCH_3), 4.02 (4H, t, 2x -OCH_2-), 6.78-7.98 (11H, m, Ar-H).

5a: IR (KBr) ν/cm^{-1} 1640 (C=O), 1240 (asym C-O-C), 1040 (sym C-O-C). ^{1}H NMR (CDCl3, 300 mHz): δ_H 2.20 (2H, m, -CH_2-), 2.95 (2H, t, -CH_2S-), 3.80 (3H, s, 4'-OCH_3), 4.25 (2H, t, -OCH_2-), 6.70-8.04 (8H, m, Ar-H).

Table 1. Characterization data of the synthesized compounds

Compd.	n	R	R_1	R_2	Mol. Formula	Mp (^{0}C)	Yield (%)	Colour of crystals*	Elemental analysis (%)Found (cald)		
									C	H	N
3a	1	CH_3	H	H	$C_{26}H_{24}O_5$ (416.0)	122	82	Colourless[1]	74.91 (75.00)	5.89 (5.76)	-
3b	1	CH_3	H	Cl	$C_{26}H_{23}O_5Cl$ (450.5)	127	91	Yellow neddle[1]	69.20 (69.25)	5.15 (5.10)	-
3c	1	CH_3	H	Br	$C_{26}H_{23}O_5Br$ (494.91)	134-135	60	Colourless[2]	62.90 (63.04)	4.68 (4.64)	-
3d	1	CH_3	H	NO_2	$C_{26}H_{23}O_7N$ (461.0)	144	82	Colourless[3]	67.64 (67.67)	5.03 (4.98)	3.07 (3.03)
3e	1	H	OCH_3	H	$C_{26}H_{24}O_6$ (432.0)	115	87	Colourless[4]	72.18 (72.22)	5.49 (5.55)	-
3f	1	H	OCH_3	Cl	$C_{26}H_{23}O_6Cl$ (466.50)	120	65	Colourless[4]	66.85 (66.88)	4.91 (4.93)	-
3g	1	H	OCH_3	Br	$C_{26}H_{23}O_6Br$ (510.91)	103	52	Colourless[4]	61.00 (61.06)	4.54 (4.50)	-
3h	1	H	OCH_3	NO_2	$C_{26}H_{23}O_8N$ (477.0)	118	72	Brown[4]	65.37 (65.40)	4.79 (4.82)	2.90 (2.93)
3i	2	CH_3	H	H	$C_{27}H_{26}O_5$ (430.0)	76	80	Light pink[4]	75.31 (75.35)	6.07 (6.04)	-
3j	2	CH_3	H	Cl	$C_{27}H_{25}O_5Cl$ (464.5)	115-116	90	Pink[4]	69.78 (69.75)	5.36 (5.38)	-
3k	2	CH_3	H	Br	$C_{27}H_{25}O_5Br$ (508.91)	94	75	Colourless[4]	63.68 (63.66)	4.98 (4.91)	-
3l	2	CH_3	H	NO_2	$C_{27}H_{25}O_7N$ (475.0)	161-162	90	Yellow[1]	68.24 (68.26)	5.29 (5.25)	2.99 (2.94)
3m	3	CH_3	H	H	$C_{28}H_{28}O_5$ (444.0)	77-78	80	Pink[4]	75.69 (75.67)	6.22 (6.30)	-
3n	3	CH_3	H	Cl	$C_{28}H_{27}O_5Cl$ (478.5)	104-105	90	Colourless[4]	70.10 (70.21)	5.53 (5.64)	-
3o	3	CH_3	H	Br	$C_{28}H_{27}O_5Br$ (523.91)	100	92	Pink[4]	64.10 (64.13)	5.19 (5.15)	-
3p	3	CH_3	H	NO_2	$C_{28}H_{27}O_7N$ (489.0)	135	91	Light yellow[2]	68.64 (68.71)	5.54 (5.52)	2.71 (2.86)
3q	4	CH_3	H	H	$C_{29}H_{30}O_5$ (458.0)	86-87	90	Pink[4]	76.07 (75.98)	6.61 (6.55)	-
3r	4	CH_3	H	Cl	$C_{29}H_{29}O_5Cl$ (492.5)	113-115	97	Pink[4]	70.59 (70.65)	5.82 (5.88)	-
3s	4	CH_3	H	Br	$C_{29}H_{29}O_5Br$ (536.91)	124-125	70	Orange[3]	65.85 (64.81)	5.33 (5.40)	-
3t	4	CH_3	H	NO_2	$C_{29}H_{29}O_7N$ (503.0)	129	92	Colourless[3]	69.02 (69.18)	5.69 (5.76)	2.88 (2.78)
4a	1	H	OCH_3	H	$C_{26}H_{25}O_5N$ (431.0)	95	50	Yellow[5]	72.47 (72.38)	5.84 (5.80)	3.24 (3.29)
4b	1	H	OCH_3	Cl	$C_{26}H_{24}O_5NCl$ (465.50)	105	50	Yellow[2]	67.08 (67.02)	5.19 (5.15)	3.10 (3.00)
4c	1	H	OCH_3	Br	$C_{26}H_{24}O_5NBr$ (509.91)	89	45	Colourless[4]	61.00 (61.18)	4.59 (4.70)	2.78 (2.74)
4d	1	H	OCH_3	NO_2	$C_{26}H_{24}O_7N_2$ (476.0)	128	50	Pale yellow[2]	65.58 (65.54)	4.89 (5.03)	5.80 (5.88)
4e	2	H	OCH_3	H	$C_{27}H_{27}O_5N$ (445.0)	85	55	Colourless[5]	72.52 (72.80)	6.27 (6.06)	3.26 (3.14)
4f	2	H	OCH_3	Cl	$C_{27}H_{26}O_5NCl$ (479.50)	90	72	Colourless[2]	67.52 (67.57)	5.57 (5.42)	2.99 (2.91)
4g	2	H	OCH_3	Br	$C_{27}H_{26}O_5NBr$ (523.91)	85	60	Colourless[4]	61.87 (61.84)	4.95 (4.96)	2.78 (2.67)
4h	2	H	OCH_3	NO_2	$C_{27}H_{26}O_7N_2$(490.00)	106	72	Yellow[2]	66.19 (66.12)	5.58 (5.30)	5.60 (5.71)
5a	1	H	OCH_3	H	$C_{26}H_{24}O_5S$ (448.0)	100	82	Colourless[4]	69.78 (69.64)	5.29 (5.35)	-
5b	1	H	OCH_3	Cl	$C_{26}H_{23}O_5SCl$ (482.50)	101	83	Colourless[4]	64.40 (64.66)	4.82 (4.76)	-
5c	2	H	OCH_3	H	$C_{27}H_{26}O_5S$ (462.00)	90	65	Colourless[4]	69.89 (70.12)	5.54 (5.62)	-
5d	2	H	OCH_3	Cl	$C_{27}H_{25}O_5SCl$ (496.50)	98	80	Colourless[4]	65.00 (65.25)	5.13 (5.03)	-
7a	1	CH_3	H	-	$C_{25}H_{25}O_4N_2Br$ (496.91)	199-200	60	Yellow[2]	60.15 (60.36)	5.13 (5.03)	5.29 (5.63)
7b	2	CH_3	H	-	$C_{26}H_{27}O_4N_2Br$ (510.91)	115-116	50	Pale yellow[2]	61.73 (61.06)	5.17 (5.28)	5.53 (5.48)
7c	3	CH_3	H	-	$C_{27}H_{29}O_4N_2Br$ (524.91)	102-105	60	Yellow[4]	61.77 (61.72)	5.47 (5.52)	5.02 (5.53)

*Solvent used for recrystalization (1) acetone + methanol (1:3; v/v) (2) ethanol + benzene (1:1; v/v) (3) methanol (4) ethanol (80%) (5) Benzene + petroleum ether ((40-60°) (1:1 v/v).

5b: IR (KBr) ν/cm^{-1} 1640 (C=O), 1240 (asym C-O-C), 1040 (sym C-O-C). ^{1}H NMR (CDCl3, 300 mHz): δ_H 2.26 (2H, m, -CH_2-), 3.10 (2H, t, -CH_2S-), 3.84 (3H, s, -OCH_3), 4.26 (2H, t, 2x -OCH_2-), 6.68-7.29 (8H, m, Ar-H).

5c: IR (KBr) ν/cm^{-1} 1640 (C=O), 1250 (asym C-O-C), 1035 (sym C-O-C). ^{1}H NMR (CDCl3, 300 mHz): δ_H 1.70 (4H, m, 2x-CH_2-), 2.80 (2H, t, -CH_2S-), 3.79 (3H, s, -OCH_3), 4.29 (2H, t, 2x -OCH_2-), 6.68-8.00 (8H, m, Ar-H).

5d: IR (KBr) ν/cm^{-1} 1640 (C=O), 1250 (asym C-O-C), 1035 (sym C-O-C). ^{1}H NMR (CDCl3, 300 mHz): δ_H 1.75 (4H, m, 2x-CH_2-), 3.02 (2H, t, -CH_2S-), 3.82 (3H, s, -OCH_3), 4.19 (2H, t, 2x -OCH_2-), 6.68-7.98 (8H, m, Ar-H).

General Procedure for Synthesis of 3-[ω-(substituted anilino (4a-h)/(2-pyridyl amino (7a-c) alkoxy]-flavones.

Equimolar mixture of 3-(ω-bromoalkoxy)-substituted flavone and substituted aniline/2-aminopyridine were refluxed in ethanol (100 mL) for 10-12 h. Completion of the reaction was monitored by TLC. The reaction mixture on concentration under reduced pressure result a semisolid mass which on repeated crystallization with proper solvents resulted the analytical samples (Table 1).

Analytical data

4a: IR (KBr) ν/cm^{-1} 3350 (NH), 1630 (C=O), 1260 (asym C-O-C), 1020 (sym C-O-C). ^{1}H NMR (CDCl3, 300 mHz): δ_H 1.86 (2H, t, -CH_2-), 4.27 (2H, t, -OCH_2-), 3.41 (2H, m, -NH-CH_2-), 4.15 (1H, s, NH), 3.84 (3H, s, -OCH_3), 6.85-7.78 (8H, m, Ar-H).

4b: IR (KBr) ν/cm^{-1} 3350 (NH), 1630 (C=O), 1260 (asym C-O-C), 1020 (sym C-O-C). ^{1}H NMR (CDCl3, 300 mHz): δ_H 1.89 (2H, t, -CH_2-), 4.16 (2H, t, -OCH_2-), 3.45 (2H, m, -NH-CH_2-), 4.10 (1H, s, NH), 3.77 (3H, s, -OCH_3), 7.38-8.00 (8H, m, Ar-H).

4c: IR (KBr) ν/cm^{-1} 3350 (NH), 1630 (C=O), 1260 (asym C-O-C), 1020 (sym C-O-C). ^{1}H NMR (CDCl3, 300 mHz): δ_H 2.10 (2H, t, -CH_2-), 4.10 (2H, t, -OCH_2-), 3.40 (2H, m, -NH-CH_2-), 5.0 (1H, s, NH), 3.91 (3H, s, -OCH_3), 6.35-7.78 (8H, m, Ar-H).

4d: IR (KBr) ν/cm^{-1} 3350 (NH), 1630 (C=O), 1260 (asym C-O-C), 1020 (sym C-O-C). ^{1}H NMR (CDCl3, 300 mHz): δ_H 2.10 (2H, t, -CH_2-), 4.10 (2H, t, -OCH_2-), 3.40 (2H, m, -NH-CH_2-), 4.20 (1H, s, NH), 3.79 (3H, s, -OCH_3), 3.32 (3H, s, 4'-OCH_3), 6.85-7.78 (8H, m, Ar-H).

4e: IR (KBr) ν/cm^{-1} 3350 (NH), 1630 (C=O), 1260 (asym C-O-C), 1020 (sym C-O-C). ^{1}H NMR (CDCl3, 300 mHz): δ_H 1.85 (4H, t, 2x-CH_2-), 4.29 (2H, t, -OCH_2-), 3.34 (2H, m, -NH-CH_2-), 4.36 (1H, s, NH), 3.86 (3H, s, -OCH_3), 6.68-8.02 (8H, m, Ar-H).

4f: IR (KBr) ν/cm^{-1} 3350 (NH), 1630 (C=O), 1260 (asym C-O-C), 1020 (sym C-O-C). ^{1}H NMR (CDCl3, 300 mHz): δ_H 1.48 (4H, t, 2x-CH_2-), 4.26 (2H, t, -OCH_2-), 3.30 (2H, m, -NH-CH_2-), 4.39 (1H, s, NH), 3.84 (3H, s, -OCH_3), 6.58-8.00 (8H, m, Ar-H).

4g: IR (KBr) ν/cm^{-1} 3350 (NH), 1630 (C=O), 1260 (asym C-O-C), 1020 (sym C-O-C). ^{1}H NMR (CDCl3, 300 mHz): δ_H 1.45 (4H, t, 2x-CH_2-), 4.22 (2H, t, -OCH_2-), 3.30 (2H, m, -NH-CH_2-), 4.37 (1H, s, NH), 3.78 (3H, s, -OCH_3), 6.68-7.98 (8H, m, Ar-H).

4h: IR (KBr) ν/cm^{-1} 3350 (NH), 1630 (C=O), 1260 (asym C-O-C), 1020 (sym C-O-C). ^{1}H NMR (CDCl3, 300 mHz): δ_H 1.45 (4H, t, 2x-CH_2-), 4.26 (2H, t, -OCH_2-), 3.30 (2H, m, -NH-CH_2-), 4.39 (1H, s, NH), 3.84 (3H, s, -OCH_3), 6.68-7.99 (8H, m, Ar-H).

7a: IR (KBr) ν/cm^{-1} 3400-3100 (broad NH) hydrobromide, 1660 (C=O), 1260 (asym C-O-C), 1030 (sym C-O-C). ^{1}H NMR (CDCl3, 300 mHz): δ_H 1.90 (2H, m, CH_2-), 4.01 (2H, t, OCH_2-), 3.61 (2H, m, -NH-CH_2-), 5.40 (1H, s, NH), 3.79 (3H, s, 4'-OCH_3), 2.48 (3H, s, CH_3), 6.81-7.94 (11H, m, Ar-H).

7b: IR (KBr) ν/cm^{-1} 3400-3100 (broad NH) hydrobromide, 1660 (C=O), 1260 (asym C-O-C), 1030 (sym C-O-C). ^{1}H NMR (CDCl3, 300 mHz): δ_H 1.48 (4H, m, 2xCH_2-), 4.29 (2H, t, OCH_2-), 3.46 (2H, m, -NH-CH_2-), 5.40 (1H, s, NH), 3.79 (3H, s, 4'-OCH_3), 2.46 (3H, s, CH_3), 6.81-7.98 (11H, m, Ar-H).

7c: IR (KBr) ν/cm^{-1} 3400-3100 (broad NH) hydrobromide, 1660 (C=O), 1260 (asym C-O-C), 1030 (sym C-O-C). ^{1}H NMR (CDCl3, 300 mHz): δ_H 1.18-1.80 (6H, m, 3x-CH_2-), 4.20 (2H, t, -OCH_2-), 3.42 (2H, m, -NH-CH_2-), 5.20 (1H, s, NH), 3.80 (3H, s, 4'-OCH_3), 2.43 (3H, s, CH_3), 6.90-8.20 (11H, m, Ar-H).

Results and Discussion

The starting material α-(3-flavonyloxy)-ω-bromoalkane **(1)** (n=1-4) was prepared by literature methods reported by us [9-11]. Reaction of compound 1 with different *para*-substituted phenols (2, X=O, R_2=H, Cl, Br or NO_2) anilines (2, X=NH, R_2= H, Cl, Br or NO_2) thiophenols (2, X=S, R_2=H or Cl) resulted phenoxy derivatives **(3a-t)**, anilino derivatives **(4a-h)** and thiophenoxy derivatives **(5a-d)** where as reaction of 1 (n=1-4) with 2-amino pyridine (6) resulted compounds **(7a-c)** (Scheme 1). For the synthesis of compounds **3a-t** an equimolar mixture of the reactants 1 and 2 was heated under reflux in dry acetone in the presence of anhydrous potassium carbonate (8-10 h). The reaction products, after purification from suitable solvents, afforded an analytically pure sample. The infrared spectra of these compound display characteristic absorption band in the regions 1640-1620 (C=O), 1280-1240 (C-O-C, asym) and 1060-1020 (C-O-C, sym) cm^{-1}. ^{1}H NMR of these compounds showed a multiplet in the range δ 1.10-2.3 for – $(CH_2)_n$-where (n=1-4) and a triplet in the range δ 4.00-4.29 for (2X-OCH_2-)

confirming the presence of polymethylenedioxy group (-OCH_2-$(CH_2)_n$-OCH_2-) in the resultant compounds. Characteristic singlets for methyl and methoxy group protons in the range δ 2.35-2.48 and δ 3.34-3.91 and aromatic ring protons as multiplet in the range δ 6.60-7.40 and δ 7.90-8.20 were also observed. Thiophenoxy derivatives **(5a-d)** were also similarly prepared and characterized by their analytical and spectral results. The synthesis of anilino **(4a-h)** and pyridyl amino derivatives **(7a-c)** was carried out by refluxing (8-10 h) the reactant 1 and para substituted anilines (2, X=NH) or 2-amino pyridines (6) in the presence of ethanol as solvent. The analytical and spectral data supported the proposed structures. Compounds **(7a-c)** were analyzed as their hydro bromides. The characteristic IR stretching frequencies of these compounds are in the regions 3200-3100 (NH), 1660-1640 (CO), 1610-1590 (C=C), 1270-1260 (C-O-C asym) and 1040-1020 (C-O-C sym) cm^{-1}.

Conclusion

In the present study we focused the synthesis of novel potentially bioactive 3-[ω-(substituted phenoxy **(3a-t)**/anilino **(4a-h)**/thiophenoxy **(5a-d)**/2-pyridylamino **(7a-c)** alkoxy] flavones.

Acknowledgments

The authors thank the Head, Department of Chemistry, University College of Science, M.L. Sukhadia University, Udaipur (Raj), India, for providing necessary laboratory facilities, financial assistance from CSIR and UGC to R.B.B. and R.S.S. respectively is also thankfully acknowledged. Thanks are also due to the Director CDRI Lucknow (U.P) for analytical and spectral data.

References

[1] Stavsteen, B. H. *Pharmacology and Therapeutic* **2002**, *9B*, 67. [CrossRef]
[2] Silva, A. M.; Borner, M. W.; Cavaleiro, J. A. S. *Mycol. Res*. **1998**, *102*, 638. [CrossRef]
[3] Rice-Evans, C. *Curr. Med. Chem.* **2001**, *8*, 797. [PubMed]
[4] Leu, Y. I.; Ho, D. K.; Cassady, J. M.; Cook, V. M.; Baird, W. M. *J. Nat. Prod*. **1992**, *55*, 357. [CrossRef]
[5] Deo, T. T.; Chi, Y. S.; Kim, J.; Kim, H. P.; Kim, S.; Park, H. *Bio-org. Med. Chem. Lett.* **2004**, *14*, 1165. [CrossRef]
[6] Verma, S. D.; Kinoshita, J. H. *Biochem. Pharmacol*. **1976**, *25***,** 2505. [CrossRef]
[7] Das, N. P. In: Flavonoids in biology and medicine (National University of Singapore Press Singapore). **1990**, 403.
[8] Bittner, M.; Silva, M.; Vargan, J.; Bohlmann, F. *Phytochemistry* **1983**, *22***,** 1523. [CrossRef]

[9] Sodani, R. S.; Bhandari, R. B.; Verma, B. L. *Chem. Ind.* (London) **1987**, 530.
[10] Sukhwal, S.; Ashawa, A.; Verma, B. L. *Asian J. Chem.* **1995**, *7***,** 615.
[11] Bhandari, R. B.; Sodani, R. S.; Chundawat, J. S.; Dulawat, S. S.; Verma, B. L. J. *Indian Chem. Soc*. **2006**, *83*, 1113.
[12] Sodani, R. S.; Chundawat, J. S.; Dulawat, S. S.; Verma, B. L. *Indian. J. Heterocyclic Chem.* **2007**, *17*, 145.
[13] Srivastava, Y. K.; Verma, B. L. J. *Indian Council Chem*. **1988**, *4*, 1.
[14] Srivastava, Y. K.; Sukhwal, S.; Ashawa, A.; Verma, B. L. J. *Indian Chem. Soc*. **1997**, *74*, 573.
[15] Srivastava, Y. K.; Ameta, K. L.; Verma, B. L. *Indian J. Heterocyclic Chem*. **2002**, *11*, 279.
[16] Sodani, R. S.; Choudhary, P. C.; Sharma, H.; Verma, B. L. *E. J. Chem*. **2010**, *7***,** 763.

ISSN 1984-6428
ONLINE
www.orbital.ufms.br

| Vol 4 | | No. 2 | | April-June 2012 |

Full Paper

Nanopartículas de poli-ε-caprolactona carregadas com hidrocortisona: preparação usando planejamento fatorial e sua avaliação

*Nayara A. Cazo[a], Edenir R. Pereira-Filho[a], Maria F. G. Fernandes da Silva[a], João Batista Fernandes[a], Paulo Cezar Vieira[a], Ana C. Puhl[b], Igor Polikarpov[b], Moacir Rossi Forim[a]**

[a]Departamento de Química, Universidade Federal de São Carlos, Rod. Washington Luiz, Km. 235, Caixa Postal 676, CEP 13.565-905, São Carlos, SP, Brasil
[b]Instituto de Física de São Carlos, Universidade de São Paulo, Av. Trabalhador São-carlense, 400, CEP 13.566-590, São Carlos, SP, Brasil

Received: 30 January 2012; revised: 13 April 2012; accepted: 20 June 2012. Available online: 07 July 2012.

ABSTRACT: *Polymeric-nanoparticle systems such as nanocapsules and nanospheres have a great potential in applications for nanoencapsulation of corticosteroids which show low solubility in water. The physicochemical characteristics of nanoparticle suspensions are important pre-requisites for the successful development of new dosage form. In this study, hydrocortisone-loaded poly-ε-caprolactone nanoparticles have been prepared by the interfacial deposition method. A 3-factor 2-level factorial design was used to study and optimize nanoparticles formulation. This factorial design was used to study the contrasts and effects of independent variables on particle size distribution, morphology, surface charge, drug content, entrapment efficiency and in vitro drug release profiles. The screened independent variables were: the concentration of hydrocortisone, poly-ε-caprolactone and isodecyl oleate. A High Performance Liquid Chromatography method was developed and validated for hydrocortisone quantification. Special attention was given to both absolute recovery and entrapment efficiency. The results of optimized formulations showed a narrow size distribution with a polydispersity index near to 0.200. The particle sizes were on average 109.2 and 236.5nm to nanospheres and nanocapsules, respectively. In the best formulations the zeta potential was higher than 30 mV (in module) and the absolute recovery and entrapment efficiency were higher 82% and nearly 60%, respectively. The main variables were the quantity of the polymer and of the oil. Nanoparticles observed by the Scanning Electron Microscope depicted extremely spherical shape. In vitro release studies were performed through dialysis with continuous stream. Nanocapsules and nanospheres showed a similar pure diffusion release mechanism according to Korsmeyer-Peppas's model.*

Keywords: *polymeric nanoparticles; hydrocortisone; factorial design; kinetic release*

* Corresponding author. E-mail: mrforim@ufscar.br

Introdução

Corticosteróides como a hidrocortisona (HC – Figura 1) possuem um amplo espectro de ação terapêutica com efeitos antiinflamatórios, imunossupressores, entre outros [1-4] Entretanto, tratamentos realizados com estes compostos frequentemente apresentam efeitos colaterais. Além disso, geralmente possuem baixa solubilidade em água comprometendo sua biodisponibilidade [4]. O corticosteróide hidrocortisona escolhido para este estudo possui uma baixa solubilidade em água com sua estabilidade afetada por mudanças nos valores de pH (solubilidade igual a $1{,}08 \times 10^{-3}$ mol L^{-1}).[3] A solução destas deficiências são alguns dos principais objetivos dos estudos com sistemas de liberação de fármacos os quais vêm sendo facilmente superados. Desde a introdução terapêutica dos corticosteróides, diversos grupos de pesquisa têm concentrado esforços para maximizar seus benefícios e minimizar os efeitos colaterais. Como resultado, diversos trabalhos demonstram técnicas para alteração estrutural do núcleo esteroidal básico e de seus grupos laterais, formulações específica, ou mais recente, descrevem técnicas de encapsulamento em sistemas de liberação controlada [5-8].

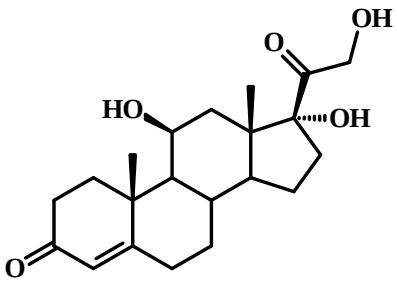

Figura 1. Estrutura da hidrocortisona.

Os sistemas de liberação podem ser subdivididos em micro ou nanopartículas. Não obstante, partículas submicrométricas oferecem uma série de vantagens sobre micropartículas incluindo a superior capacidade intracelular de captação do fármaco em relação às micropartículas [9]. Nanoencapsulação de fármacos envolve a formação de partículas carregadas em escala submicro podendo ou não ser biodegradadas [9]. O termo nanopartículas é o nome coletivo usado para nanocápsulas (NC) e nanoesferas (NS) quais diferem entre si segundo a composição e organização estrutural. Nanoesferas referem-se a partículas formadas por uma matriz polimérica onde o fármaco pode ficar retido ou adsorvido. As nanocápsulas são partículas constituídas por um invólucro polimérico disposto ao redor de um núcleo oleoso [9-10].

Nanopartículas preparadas por polímeros sintéticos ou naturais tem encontrado aplicações em vários segmentos tecnológicos e biomédicos decorrente da facilidade de controle das estruturas químicas, funcionalidades de superfície e do diâmetro de partícula [11]. A importância das técnicas de encapsulamento em sistemas de liberação para

fármacos com os corticosteróides pode ser avaliada observando a diversidade de técnicas descritas na literatura. Kristmundsdóttir e col. propuseram um complexo de inclusão de hidrocortisona em hidroxipropil-β-ciclodextrina com avaliação clínica em tratamentos orais [12]. Os autores destacam neste trabalho o aumento na solubilidade da hidrocortisona com a formação do complexo, a ausência de efeitos colaterais não notificados por pacientes, fácil uso e eficácia clínica comparada com outras preparações mais potentes. Filipović-Grčić e col. descrevem o preparo de complexos de inclusão do acetato de hidrocortisona em hidroxipropil-β-ciclodextrina por *Spray-Drying* qual resultou em microesferas [4]. Este complexo de microesferas originou um sistema com maior dispersão em água que o acetato de hidrocortisona não encapsulado.

Num outro trabalho, Jensen e col. descrevem um promissor sistema de liberação de corticosteróides para administração tópica de nanopartículas lipídicas sólidas [8]. Foi verificado o ganho na eficiência de encapsulamento e o perfil de liberação para as nanopartículas lipídicas sólidas. Cevc e Blume desenvolveram um carreador lipossomático para glucocorticosteroides de aplicação tópica quais, mesmo com a redução nas dosagens, asseguraram a eficácia terapêutica resultando num ganho de eficiência [6]. Nanosuspensões coloidais com hidrocortisona para aplicação ocular foram desenvolvidas por Ali e col. [13]. Diversos outros trabalhos descrevendo sistemas específicos para carreadores de corticosteróides podendo ser encontrados na literatura [8-15].

Desde a década de setenta, tem sido cada vez mais evidente que somente o desenvolvimento de novos fármacos não é suficiente para assegurar o progresso da terapia medicamentosa. Algumas razões para o insucesso da terapia convencional incluem: a) insuficiente concentração do fármaco resultado da pobre absorção, rápido metabolismo e eliminação ou distribuição do fármaco em tecidos não alvo com elevada toxicidade e b) baixa solubilidade dos fármacos que exclui administração de soluções aquosas [16].

Neste contexto, o presente trabalho teve como objetivo preparar e caracterizar nanopartículas de poli-ε-caprolactona (PCL) carregadas com o corticóide hidrofóbica hidrocortisona. Nanoparticulas contendo HC foram preparadas por deposição polimérica interfacial seguida pelo deslocamento do solvente, conhecido como nanoprecipitação, sendo um método inicialmente proposto por Fessi e col. [17]. Entre as novidades do trabalho se destaca o baixo custo e simplicidade de preparação de nanopartículas (formulação) contendo moléculas como, por exemplo, a hidrocortisona (composto alvo), alta capacidade de encapsulamento e dispersão em meio aquoso de moléculas pouco polares, elevada estabilidade das dispersões coloidais, as nanopartículas podem ser facilmente convertidas em pó solúveis, o polímero e o óleo empregados são biocompatíveis e biodegradáveis, etc. A formulação contendo hidrocortisona pode ser

facilmente escalonado para o setor industrial. Além disso, o presente trabalho destaca um método cromatográfico validado que pode ser aplicado em diversos ensaios quantitativos de hidrocortisona.

Resumidamente, este método envolve a precipitação de um polímero presente inicialmente numa fase orgânica, num meio aquoso contendo um surfactante. O polímero é dissolvido em um solvente miscível em água de polaridade intermediária (fase orgânica) juntamente com o composto ativo, outro surfactante e um óleo (somente para NC). A precipitação ocorre após a introdução e difusão da fase orgânica no meio aquoso, mantida sob agitação mecânica. A deposição polimérica ocorre na interface entre a água e o solvente orgânico causada pela rápida difusão do solvente, levando a formação instantânea da suspensão coloidal [9, 17, 18]. O desenvolvimento das formulações foi realizado através do planejamento fatorial 2^3 com três experimentos no ponto central, avaliando o efeito dos fatores selecionados sobre parâmetros físico-químicos e quantitativos.

Material e Métodos

Reagentes e padrões

A hidrocortisona foi adquirida da Sigma (lote n°. 103K06241). O polímero poli-ε-caprolactona (PCL) de peso molecular ponderal médio 65.000, monoestearato de sorbitano-60 (Span®60), polissorbato 80 (Tween®80) foram adquiridos da Sigma-Aldrich (St. Louis, EUA). Oleato de isodecila foi obtido da Importadora Química Delaware Ltda. (Porto Alegre, Brasil). Os solventes grau CLAE, bem como o ácido fosfórico e os sais NaCl, KCl, Na_2HPO_4 e KH_2PO_4 foram fornecidos pela J. T. Baker (Ecatepec, Mexico). Água ultra pura (18 Ω) foi obtida por osmose reversa num sistema Milli-Q (Millipore, Bedford, MA, EUA).

Preparo das nanopartículas em suspensão coloidal

Todas as nanopartículas, nanocápsulas e nanoesferas, foram preparadas pela técnica de nanoprecipitação de polímeros pré-formado (deposição interfacial) proposto por Fessi e col. [17]. Resumidamente, uma fase orgânica preparada pela dissolução do polímero, hidrocortisona, tensoativo de baixo equilíbrio hidrofílico-lipofílico (Span®60) e oleato de isodecila (somente em nanocápsulas) em acetona a 45 °C, foi vertida lentamente com o auxílio de uma bomba peristáltica (PumpPro TPM 600 55RPM, Waton-Marlow, Wilmington, Reino Unido), operada a 10% de sua capacidade, sobre uma fase aquosa contendo o Tween®80 sob agitação magnética moderada. As nanopartículas foram imediatamente formadas após difusão do solvente orgânico. O sistema foi mantido em agitação magnética por 10 min e em repouso durante 30 min. Após este período, o solvente orgânico e parte da fase aquosa foram removidos sob pressão reduzida

ajustando o volume final da dispersão coloidal em 50 mL.

Planejamento fatorial 2^3

Nanopartículas poliméricas contendo hidrocortisona foram obtidas com base no planejamento fatorial 2^3. A concentração de hidrocortisona (x_1), quantidade de polímero (x_2) e óleo (x_3) foram selecionados como variáveis independentes (Tabela 1). Os níveis das variáveis independentes foram estabelecidos de acordo com estudos prévios para desenvolvimento de nanopartículas com PCL. Cada variável foi analisada em dois diferentes níveis, inferior e superior transformados em valores (–1) e (+1), respectivamente. Definindo todas as possíveis combinações entre as variáveis independentes o planejamento fatorial completo resultou $2^3 = 8$ experimentos. A repetibilidade experimental foi investigada avaliando a dispersão dos resultados no ponto central (nível 0 para as variáveis, $n = 3$). O volume do solvente, fase aquosa e dos tensoativos utilizados na preparação foram mantidos constantes conforme valores descritos na Tabela 1. A avaliação dos efeitos foi realizada pelo *software* Microsoft Office Excel®2007 (Microsoft Corporation, EUA). Valores de pH, diâmetro de partículas (DP), potencial zeta (PZ), recuperação absoluta (Rec%) e eficiência de encapsulamento (EE%) foram os parâmetros de resposta ou as variáveis dependente. A descrição dos experimentos para o planejamento fatorial 2^3 e resultados obtidos correspondentes as variáveis dependente são descritos na Tabela 2.

O software OriginPro®8.0 foi utilizado para gerar e avaliar o planejamento experimental estatístico. Com a finalidade de otimizar o planejamento, os efeitos das variáveis independentes sobre as respostas obtidas foram modeladas usando um modelo linear matemático para descrever as variáveis independentes e suas interações com as várias respostas medidas que foram geradas pelo planejamento fatorial 2^3 sendo:

$$Y = \beta_0 + \beta_1.x_1 + \beta_2.x_2 + \beta_3.x_3 + \beta_4.x_1.x_2 + \beta_5.x_1.x_3 + \beta_6.x_2.x_3 + \beta_7.x_1.x_2.x_3 + \varepsilon \quad \text{(Eq.1)}$$

onde Y são as variáveis dependentes, enquanto β_i são os parâmetros do modelo (β_0 do intercepto e β_1, β_2, β_3, β_4, β_5, β_6 e β_7 são coeficientes de regressão) e ε o erro aleatório; x_1, x_2 e x_3 são as variáveis independentes; $x_1.x_2$, $x_1.x_3$, $x_2.x_3$ e $x_1.x_2.x_3$ são as interações entre as variáveis. Análise de variância (ANOVA) foi usada para investigação dos dados para obter a interação entre as variáveis processadas e as respostas. A qualidade do ajuste polinomial foi expressa pelo coeficiente de determinação (R^2) e sua significância estatística foi avaliada pelo Teste F no mesmo programa. Os termos do modelo foram avaliados para um valor de P (probabilidade) com um nível de confiança de 95% (α = 0,05).

Caracterização físico-química das nanopartículas

Quantificação da hidrocortisona

O conteúdo de hidrocortisona no sistema coloidal foi determinado por cromatografia líquida de alta eficiência (CLAE) utilizando um cromatógrafo a líquido Agilent 1200 Series (Agilent Technologies, Santa Clara, EUA) configurado com degaseificador G1322A, bomba quaternária G1311A, autoinjetor G1329A, forno de coluna G1316A e detector de ultravioleta G1314B. Foi utilizado uma coluna de fase reversa Zorbax Eclipse XDB®C18 (150 x 4,6 mm d.i., 5 µm diâmetro de partícula, P. N. 993967-902 Agilent, EUA) acoplada com uma pré-coluna de segurança Phenomenex® C18 (4x3 mm i.d., 5 µm particle size, Torrance, CA, EUA). O controle do equipamento CLAE, aquisição e processamento dos dados foram realizados pelo *software* Agilent Technologies EZCrom SI (G6702AA, s.n.08021502300).

As análises cromatográficas foram realizadas no modo de eluição isocrático. A fase móvel consiste de uma mistura de acetonitrila:água (70:30, v/v) com uma vazão de 1,0 mL min^{-1}. A temperatura da coluna foi mantida em 30 °C e o volume de injeção de 20 µL. Todos os experimentos foram realizados operando o detector de UV-Vis em 217 nm.

Preparo das amostras padrões e validação do método analítico

Uma solução estoque de 1,00 mg mL^{-1} de hidrocortisona foi preparada dissolvendo 10,0 mg de HC em metanol num balão volumétrico de 10,0 mL. A solução de trabalho (100 µg mL^{-1}) foi obtida após diluição da solução estoque. Sete soluções padrões (5,00; 10,0; 20,0; 40,0; 60,0; 80,0 e 100 µg mL^{-1}) foram preparadas diluindo a solução de trabalho com quantidades exatas de metanol (n = *3*). As soluções padrões foram utilizadas para: construção da curva de calibração por padronização externa, estabelecer a faixa linear de trabalho e determinar os limites de quantificação (LQ) e de detecção (LD) do método analítico. De modo similar, três outras soluções de validação (6,00; 50,0; e 95,0 µg mL^{-1}) foram preparadas (n = *5*) e analisadas em três dias não consecutivos (n = *3*) estabelecendo a exatidão e precisão do método. A linearidade foi determinada pelo cálculo da regressão linear pelo método dos mínimos quadrados após construção do gráfico da área do sinal analítico de todas as soluções padrão *versus* a concentração individual de cada uma. A linearidade também foi avaliada analisando o fator de resposta, isto é, dividindo a área da banda cromatográfica pela concentração individual de cada solução padrão.

A exatidão foi determinada calculando a porcentagem de recuperação da concentração média de HC e a precisão pode ser estabelecida através do cálculo do Desvio Padrão Relativo (DPR). Os limites de detecção e quantificação foram calculados através da relação entre o desvio padrão (dp) da curva de calibração e sua inclinação (S), utilizando o cálculo sugerido pela ICH standard [19]. Os LD e LQ foram calculados através das equações 02 e 03, respectivamente:

$$LOD = \left(\frac{3.3 \text{ x } dp}{S} \right) \quad \text{(Equação 2)} \qquad LOQ = \left(\frac{10 \text{ x } dp}{S} \right) \quad \text{(Equação 3)}$$

Pré-tratamento e análises de hidrocortisona em matrizes poliméricas

Inicialmente foi necessário desenvolver dois diferentes pré-tratamentos para análises quantitativas de hidrocortisona: um específico para determinação do teor total em suspensão coloidal e outro para determinar a quantidade associada às nanopartículas. A Rec% foi determinada após nanopartículas em suspensão coloidal serem submetidas ao seguinte procedimento: 0,9 mL de acetona foram adicionados e homogeneizados a 0,1 mL da suspensão coloidal mantendo posteriormente a solução em repouso por duas horas. Após dissolução do polímero, a solução foi centrifugada (Centrifuge 5810 R, Eppendorf®, Hamburg, Alemanha) a 14.000 rpm por 30 minutos a 25 °C. Em seguida, 0,5 mL do sobrenadante foram secos utilizando um *Speed vac* (Savant Speed vac Plus SC10A, Farmingdale, EUA). O extrato seco foi solubilizado em metanol e o teor total de HC determinado por CLAE.

A eficiência de encapsulamento nas nanopartículas foi determinada quantificando a concentração do composto livre no meio de dispersão (fase aquosa) da suspensão coloidal. Uma quantidade da suspensão coloidal (0,5 mL) foi filtrada usando tubos Corning® com filtros de acetato de celulose de poros 0,22 µm (Costar®Spin-X®, Corning Inc.) por centrifugação a 4.000 rpm por 20 min a 15 °C. As nanopartículas ficaram retidas no filtro sendo o filtrado, contendo a HC livre, posteriormente coletado. Uma quantidade de 0,3 mL do filtrado foi então seco e ressuspendido em 0,2 mL de metanol para análise por CLAE. A EE% foi calculada pela equação 04:

$$EE\ (\%) = \left(\frac{\text{Quantidade total de hidrocortisona} - \text{Quantidade livre de hidrocortisona}}{\text{Quantidade total de hidrocortisona}} \right) \text{x } 100 \qquad \text{(Equação 04)}$$

Caracterização das suspensões coloidais

Diâmetro de partícula e potencial zeta

As análises físico-químicas das nanopartículas foram realizadas imediatamente após a preparação das suspensões coloidais. Os parâmetros investigados foram: valor de pH usando um potenciômetro (B474 Micronal, São Paulo, Brasil); análise do diâmetro de partícula (DP) em nanômetros pela análise da difusão dinâmica da luz (PCS). As medidas de PCS foram obtidas a temperatura ambiente num ângulo fixo de 90°. Esta técnica possibilitou obter o diâmetro hidrodinâmico médio das nanopartículas e o índice de polidispersividade; investigação do potencial zeta (ζ) em milivolts. O diâmetro de partícula e potencial zeta foram determinados após diluir 0,1 mL de cada suspensão coloidal em 10 mL de água ultrapura e 10 mM NaCl, respectivamente, utilizando um

Zetatrac controlado pelo *software* Microtrac Flex V.10.5.0, ambos da Microtrac Inc., EUA.

Análise morfológica por Microscopia Eletrônica de Varredura

As nanopartículas foram secas sobre suportes metálicos de alumínio, posteriormente recobertos com uma fina camada de ouro e sua morfologia examinada por Microscopia Eletrônica de Varredura (MEV) (Philips XL 30 FEG, Holanda) a 5 kV com ampliações de até 50.000 vezes.

Estudos de liberação in vitro das nanopartículas

Os estudos de liberação *in vitro* das nanopartículas em suspensão coloidal foram realizados pela técnica de difusão de bolsas de diálise proposta por Levy e Benita [20]. Bolsas de diálise (Dialysis tubing cellulose membrane, 1,0 cm largura, Sigma) com 1,0 mL da suspensão coloidal foram seladas e adicionadas em 1,0 L de tampão fosfato (PBS) num pH = 7,4. Esta solução foi mantida em constante agitação. O tampão PBS foi preparado dissolvendo as seguintes quantidades dos sais: 8,00 g NaCl; 0,20 g KCl; 1,44 g $Na_2HPO_4.2H_2O$ e 0,24 g de KH_2PO_4 para cada litro de água. O sistema foi mantido a 35 °C com um fluxo contínuo de 3,0 mL min^{-1} controlado por uma bomba peristáltica (PumpPro TPM 600 55RPM, Waton-Marlow, Wilmington, Reino Unido). Em intervalos de tempo específicos, uma bolsa de diálise era retirada do meio e o conteúdo de HC e analisado por CLAE. A cinética de liberação foi determinada após o cálculo do valor de *n* (ordem de cinética) proposto por Korsmeyer-Peppas [21] pela seguinte equação empírica:

$$M_t/M_\infty = K.t^n \quad \text{(Equação 05)}$$

onde M_t/M_∞ é a fração de liberação no tempo *t*, *n* é o expoente de liberação e *K* a constante de liberação.

Resultados e Discussão

Significantes esforços têm sido gastos nos últimos anos com pesquisas em nanotecnologia para disponibilizar meios de vetorização de pequenas moléculas como hormônios, antitumorais, antimicrobianos, bem como macromoléculas como polissacarídeos, proteínas e peptídeos para entrega em tecidos ou alvos celulares específicos [22-25].

Diversos grupos vêm produzindo micro e nanopartículas contendo corticosteroides como a HC em sistemas lipossomais, hidroxipropilmetillcelulose (HPMC), β-ciclodextrinas e derivados, etc. Neste trabalho, pela primeira vez é apresentado o uso de PCL e o uso do método de nanoprecipitação para o preparo de nanopartículas contendo HC. Entre as vantagens, quando comparado às demais técnicas, destaca o baixo custo, maior estabilidade da suspensão coloidal, em geral um menor diâmetro de partícula (exceto

quando comparado a sistemas produzidos com derivados de β-ciclodextrinas), maior estabilidade no encapsulamento em suspensão coloidal etc. [4-6, 12, 13, 38].

Assim, o objetivo deste estudo foi formular e aperfeiçoar processos e parâmetros para nanoencapsulamento da HC em PCL baseado num planejamento fatorial 2^3. Esta é a primeira vez que o polímero PCL e o oleato de isodecila são empregados no preparo de nanopartículas contendo um corticóide como a hidrocortisona. A repetibilidade da técnica de preparo das nanopartículas em suspensão coloidal foi avaliada preparando três amostras idênticas no ponto central, sendo a quantidade de HC, do polímero e do oleato de isodecila iguais a 15, 100 e 300 mg, respectivamente. A dispersão dos resultados representado pelo DPR das variáveis dependentes pH, DP, PZ, Rec% e EE% foram 2,0%, 5,4%, 6,3%, 3,2% e 4,4%, respectivamente. Com exceção do DPR obtido para a variável pH, estes dados demonstram uma satisfatória repetibilidade no processo de preparo das nanopartículas. Além da dispersão dos resultados investigado pelo DPR, os resultados foram submetidos à análise de variância (ANOVA) obtendo conclusões similares.

De fato, a técnica de nanoprecipitação aplicada se mostrou satisfatória no preparo de nanopartículas. Imediatamente após adicionar a fase orgânica sobre a fase aquosa, todas as formulações se tornaram opacas como leite, sendo uma característica originada no efeito Tyndall que resulta da reflexão de luz pela formação das nanopartículas [10]. Através do uso da técnica de nanoprecipitação proposta por Fessi e col. foi possível produzir nanoesferas e nanocápsulas submicrômetras, carregadas com hidrocortisona utilizando PCL com polímero biodegradável [17]. A técnica de preparação se mostrou simples e facilmente reprodutível. Dentro dos limites de concentração de hidrocortisona avaliados neste trabalho (Tabela 1) foi possível preparar sistemas coloidais em meio aquoso com uma quantidade superior de 27% sobre a solubilidade máxima deste corticosteróide no meio de dispersão. Esta é uma importante característica obtida para o sistema contendo HC obtido neste trabalho. Considerando a eficiência de encapsulamento, por exemplo, de 59,6% obtida no experimento 7 (Tabela 2), a capacidade de dispersão da HC em meio aquoso pode ser ampliada à 53%, precisando apenas reduzir pela metade do volume final da dispersão coloidal.

O polímero poli-ε-caprolactona é um poliéster largamente utilizado na aplicação de sistemas de liberação de fármacos sendo escolhido por suas propriedades de biocompatibilidade e biodisponibilidade, alta permeabilidade e falta de toxicidade [26, 27]. O PCL é um polímero resistente à hidrólise química e não possui centros heterogênios, características que limitariam a possibilidade de modulação através da configuração estrutural das cadeias poliméricas [27]. Ele é um polímero hidrofóbico cristalino que degrada lentamente na ausência de enzimas [26, 28].

Contudo, sua degradação é acelerada na presença de enzimas como, por exemplo, lipases [27, 29].

Tabela 1. Variáveis investigadas na preparação de nanopartículas poliméricas de PCL carregadas com HC

Variáveis independentes	Nível inferior (−1)	Nível superior (+1)
x_1, Hidrocortisona	5,0 mg (0,01 %, m/v)	25,0 mg (0,05 %, m/v)
x_2, Polímero, PCL	30,0 mg (0,01 %, m/v)	170,0 mg (0,34 %, m/v)
x_3,Oleato de Isodecila	0,0 mg	600,0 mg (1,2 %, m/v)
Variáveis Fixadas		
Volume acetona	27,0 mL	
Span®60	80,0 mg (0,16 %, m/v)	
Volume fase aquosa	54,0 mL	
Tween®80	80,0 mg (0,16 %, m/v)	

Tabela 2. Descrição dos experimentos das variáveis independentes e respostas das variáveis dependentes observadas para o planejamento fatorial 2^3

Exp	Variáveis independentes			Variáveis dependentes [b]				
	x_1	x_2	x_3	pH	DP (nm)	PZ (mV)	(Rec%)	(EE%)
01	−1	−1	−1	6,73±0,10	67,2±2,02	-6,8±0,3	101,6±1,41	35,4±0,49
02	+1	−1	−1	6,67±0,14	56,4±1,50	-26,8±1,3	92,6±0,88	41,4±0,76
03	−1	+1	−1	6,39±0,08	149,8±5,97	-26,9±0,9	96,5±0,93	39,8±0,61
04	+1	+1	−1	6,49±0,17	163,6±12,5	-16,5±1,0	82,5±1,85	31,0±0,27
05	−1	−1	+1	6,66±0,11	254,2±6,45	-36,5±2,0	90,9±1,82	52,5±1,26
06	+1	−1	+1	6,71±0,06	235,7±4,69	-28,8±0,7	89,7±0,67	43,0±0,69
07	−1	+1	+1	6,45±0,07	228,2±11,9	-31,5±2,1	90,9±0,55	59,6±0,18
08	+1	+1	+1	6,53±0,10	227,3±9,06	-27,9±1,3	100,5±1,78	54,7±0,97
09[a]	0	0	0	6,48±0,13	211,8±6,67	-31,5±1,6	95,6±2,52	47,2±0,38
10[a]	0	0	0	6,52±0,15	189,6±5,60	-30,8±1,7	91,4±0,91	44,2±0,42
11[a]	0	0	0	6,47±0,16	201,3±4,19	-28,9±2,0	89,8±1,36	43,0±0,85

[a] Indica o ponto central do planejamento fatorial; DP, diâmetro de partícula; PZ, Potencial zeta; REC%, recuperação; EE%, eficiência de encapsulamento. [b]Réplica das análises representada como média±SD.

Para confirmar a formação de nanopartículas esféricas a morfologia foi avaliada através da microscopia eletrônica de varredura. Para se conseguir boas resoluções de imagens na avaliação morfológica das nanopartículas por MEV, após adicionar as suspensões coloidais sobre os suportes de amostras metálicos, foi necessário remover toda água das dispersões. Este processo promoveu a aglomeração das nanopartículas formando um filme polimérico. Contudo, foi possível observar nanopartículas depositadas sobre o filme polimérico, os quais mostraram uma superfície regular, homogênea e baixa dispersão no diâmetro de partícula médio (Figura 2). As fotomicrografias obtidas não demonstraram a formação de cristais. Cristais podem ocorrer quando o composto a ser nanoencapsulado está presente em excesso no meio de dispersão ou devido a uma grande polidispersão no tamanho das nanopartículas obtidas. A ausência de cristais também foi confirmada pelos resultados da Rec% e EE%.

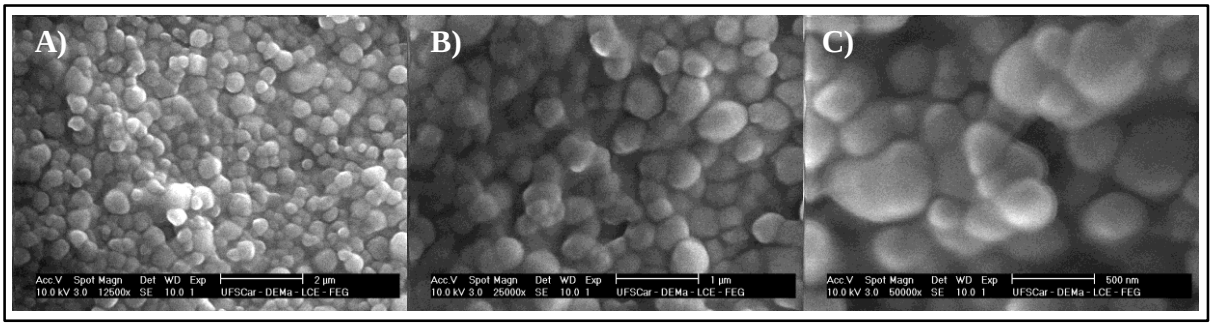

Figura 2. Fotomicroscopia de nanocápsulas de PCL carregadas com 0,05% (m/v) de hidrocortisona, 0,34% (m/v) de PCL e 1,2% de oleato de isodecila. Ampliações: A) 12.500 X; B) 25.000 X e C) 50.000 X.

Validação do método para análises cromatográficas da hidrocortisona

A validação do método analítico foi realizada de acordo com critérios propostos pela ICH (International Conference on Harmonization) [19]. As figuras de mérito investigadas na validação do método foram linearidade, seletividade, exatidão, precisão, recuperação, limites de quantificação e de detecção e repetibilidade.

Preparação das amostras

O pré-tratamento possivelmente é a etapa mais importante para análises quantitativas. Esta é a etapa crítica em análises cromatográficas, usualmente sendo a mais lenta e com maiores possibilidade de perdas analíticas no processo. Esta etapa envolve a extração de compostos ativos e a remoção de interferentes.

Deste modo foi necessário desenvolver métodos de abertura e pré-tratamento das amostras sem comprometer a recuperação. Assim, para a análise da quantidade total de HC em nanopartículas poliméricas em suspensão coloidal foi proposto uma técnica para dissolução do polímero em acetona com posterior separação do polímero e do sobrenadante. De fundamental importância foi à escolha do solvente ideal qual deve ao mesmo tempo dissolver o polímero e solubilizar a HC, contudo, sem que ocorra a saturação do sistema. Após solubilização, separou-se o polímero do sobrenadante por centrifugação. O processo utilizando etapas de secagem das amostras com posterior solubilização da HC em metanol, antes de ser analisado por CLAE, evita que resíduos de polímero comprometam a eficiência de separação e cause uma perda prematura da coluna analítica uma vez que o mesmo não é solúvel em metanol.

O preparo da amostra para análise da eficiência de encapsulamento foi mais simples, uma vez que não há necessidade da remoção do polímero ou abertura da amostra. Foi necessário desenvolver um protocolo para separação da nanopartículas do meio de dispersão sendo utilizado um sistema de filtração por centrifugação controlando-

se o tempo e a força centrífuga aplicada. Uma vez separado o meio e as nanopartículas foi possível quantificar toda HC no meio aquoso de dispersão. As amostras em meio aquoso foram secas e re-suspendidas em metanol para manter constante o coeficiente de absortividade molar da HC em comparação com as soluções padrões usadas na construção da curva de calibração.

Seletividade analítica e linearidade

A seletividade do método foi avaliada comparando cromatogramas de amostras de nanopartículas preparadas contendo hidrocortisona com relação às nanopartículas isentas de HC denominadas brancos (Figura 3). Nenhum pico interferente foi observado em 5,1 min no cromatograma do branco (tempo de retenção da HC) para o comprimento de onda de trabalho de 217 nm (Figura 3A). Os cromatogramas de amostras utilizadas nos testes de estabilidade de armazenamento e do autoinjetor também não apresentaram nenhum pico interferente no período investigado. Assim, o método pode ser considerado seletivo podendo distinguir a resposta do analito de interesse dos demais componentes da mistura.

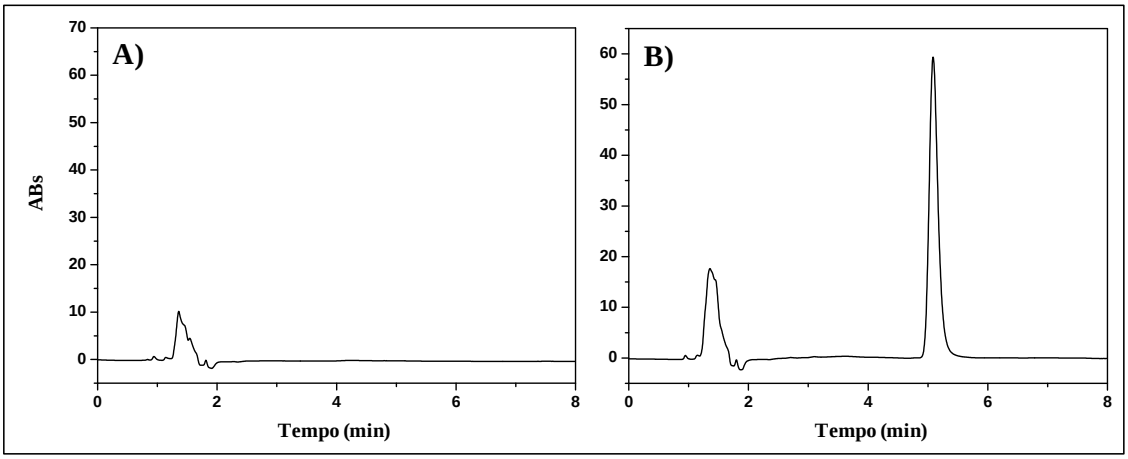

Figura 3. Cromatogramas de nanopartículas em suspensão coloidal (A) isento e (B) com hidrocortisona. As condições cromatográficas foram descritas no procedimento experimental.

A curva de calibração foi linear em toda extensão investigada, de 5,00 a 100,0 μg mL^{-1}, mostrando serem os resultados diretamente proporcionais a concentração. A linearidade foi determinada em triplicata pela avaliação visual da curva de calibração externa (Figura 4A) e pelos cálculos da equação de regressão ($A = a.x \pm b$) e do coeficiente de correlação (r^2) usando o método dos mínimos quadrados sendo:

$$A = 16{,}36(\pm 0{,}0566).\ x - 8{,}486(\pm 3{,}184); \qquad r^2 = 0.9999$$

onde A é a área da banda cromatográfica, x a concentração da amostra investigada, e a e b os coeficientes angular e de intercepto, respectivamente. Os valores do Desvio

Padrão dos coeficientes *a* e *b* estão indicados em parênteses. O valor do coeficiente de correlação (r^2) de 0,9999 indica uma boa linearidade para a faixa de trabalho proposta. A linearidade também foi avaliada pela análise do fator de resposta (valor da área da banda cromatográfica dividido pela concentração da solução padrão). A aparência visual do gráfico e o valor da regressão linear do fator de resposta (Figura 4B) mostram uma inclinação de 0,0070 (± 0,0006) próxima a zero e um DPR de 1,62% confirmando a linearidade da faixa de trabalho.

Exatidão e precisão

A exatidão [Exatidão= (média da concentração/concentração nominal).100%] pode ser avaliada calculando a porcentagem de recuperação da hidrocortisona. Três diferentes soluções de validação (6,00; 50,0; e 95,0 µg mL^{-1}), em quintuplicata cada uma, foram cuidadosamente preparadas e analisadas em dias não consecutivos (*n = 3*). As soluções foram escolhidas por abranger toda a faixa linear de trabalho. A recuperação média e DPR encontrados foram 100,2% e 2,46%, respectivamente, mostrando forte concordância entre os dados experimentais e valores nominais teóricos. Resultados detalhados para os três níveis de solução de validação podem ser observados na Tabela 3. A precisão foi determinada calculando o Desvio Padrão Relativo (DPR) para cada solução de validação analisada intra (*n = 5*) e interdias (*n = 15*). Estes resultados são apresentados na Tabela 3. O DPR de cada amostra intra e interdias foram ≤ 2,1% e ≤ 1,3%, respectivamente. Estes resultados indicam uma boa precisão para o método analítico.

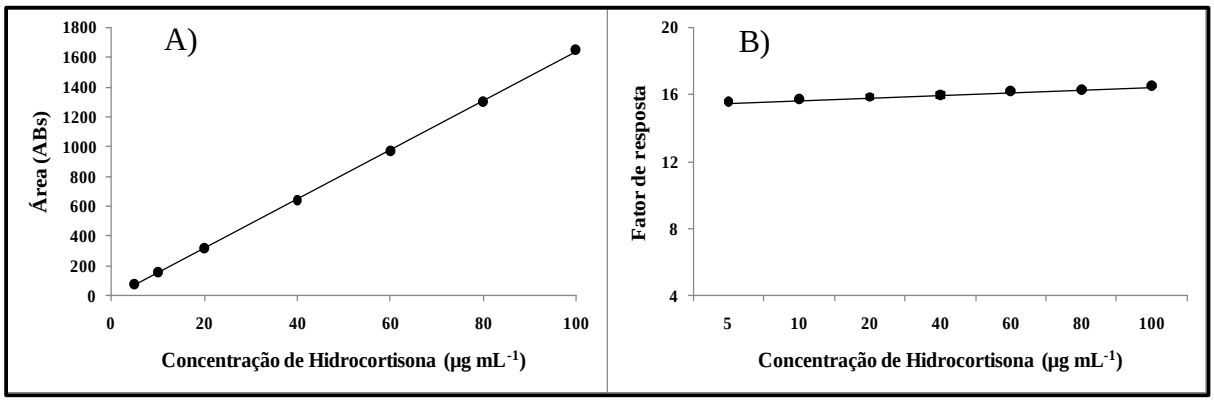

Figura 4. Linearidade do método proposto para quantificação da hidrocortisona por CLAE. (A) Curva de calibração e (B) fator de resposta (*n = 7*).

Tabela 3. Exatidão (%) e precisão (DPR%) em amostras de hidrocortisona usadas na validação do método analítico

Concentração (µg mL^{-1})	Precisão				Exatidão (*n* = 15)
	Intra-dia 1 (*n* = 5)	Intra-dia 2 (*n* = 5)	Intra-dia 3 (*n* = 5)	Inter-dia (*n* = 15)	
6,00	2,1	0,8	1,0	1,3	99,0
50,0	0,5	0,5	0,5	0,5	100,5
95,0	0,8	0,5	0,9	0,7	100,9

O Limite de Detecção do método foi estabelecido em 0,6 μg mL^{-1} (Eq. 2), enquanto o Limite de Quantificação foi 1,9 μg mL^{-1} (Eq. 3). A recuperação do método foi determinada pela comparação de resultados do conteúdo total de HC adicionado e quantificado em suspensões [30]. Os resultados de recuperação foram obtidos pela razão entre o conteúdo de HC quantificado e sua concentração nominal expresso em porcentagem. O valor médio calculado para duas diferentes concentrações (100,0 e 500,0 μg mL^{-1}) foi 99,7 ± 4,3% (n = 6) mostrando que não houve perda do analito durante as etapas de preparação das nanopartículas, pré-tratamento ou análises cromatográficas.

O método analítico depois de validado se mostrou satisfatório para análises das variáveis dependentes Rec% e EE%, fornecendo dados para investigação das variáveis independentes no preparo de nanopartículas poliméricas carregadas com hidrocortisona.

Caracterização das nanopartículas carregadas com hidrocortisona

O planejamento experimental 2^3 realizado permitiu avaliar os efeitos das variáveis independentes (quantidade de HC, polímero e do oleato de isodecila) sobre os resultados das variáveis dependentes (Tabela 2). A composição qualitativa e quantitativa das formulações foi selecionada após revisão da literatura, outros trabalhos do grupo de pesquisa e avaliação experimental da compatibilidade da formulação com a HC [10, 31].

As variáveis dependentes utilizadas para avaliar a dispersão coloidal foram o pH, DP e PZ. Por outro lado, as variáveis dependentes Rec% e EE% foram aplicadas nos estudos de estabilidade e cinética de liberação da HC.

O efeito de cada variável e suas interações foram calculados de acordo com a seguinte equação: Efeito das variáveis = $\bar{y}_+ - \bar{y}_-$, onde $\bar{y}_+$ e $\bar{y}_-$ são a média do pH, DP, PZ, Rec% e EE% no nível superior (+1) e inferior (−1), respectivamente. A Figura 5 ilustra os efeitos calculados para os dados normalizados em porcentagem para o planejamento fatorial 2^3 investigado. Na normalização os maiores valores foram tomados como 100 e os demais foram escalados proporcionalmente.

O valor do pH em todas as formulações oscilou entre 6,39 e 6,73. Modificações nos valores das variáveis independentes não apresentaram mudanças significativas no pH das suspensões coloidais. Isto pode ser indicado pela pequena inclinação das setas na Figura 5A e pelos parâmetros estatísticos.

As NS apresentaram diâmetro de partículas entre 56,4 e 163,6 nm sendo o valor médio igual a 109,2 nm. A quantidade de polímero (x_2) utilizado afetou diretamente o DP das nanoesferas. As NS preparadas no maior nível do planejamento experimental da variável PCL (x_2 = +1) foram 2,5 vezes maiores que as preparadas no menor nível (x_2 = −1). O DP das nanocápsulas variou entre 189,6 e 254,2 nm com um valor médio de

236,5 nm (Tabela 2). Estes resultados estão em conformidade com trabalhos prévios descritos aplicando a técnica de nanoprecipitação, i.e., menores que 300 nm [17, 31]. A diferença entre os tamanhos médios de NC e NS se justifica pela presença do oleato de isodecila nas formulações para preparo das NC. Utilizando o oleato de isodecila, inicialmente ocorre a formação de vesículas com a posterior precipitação do polímero na interface óleo/água conduzindo a nanopartículas de diâmetro médio superior as NS. Esses resultados são condizentes com os cálculos dos efeitos no planejamento experimental, onde se observou que o polímero e o oleato de isodecila contribuíram para um aumento de 15,5 (β_2 = 19,45) e 50,5% (β_3 = 63,55) no DP, respectivamente. Todavia, analisando a interação de segunda ordem entra estas variáveis ($x_2.x_3$), se observa que quando estão num mesmo nível (−1, −1 ou +1, +1) ocorrem uma redução no DP de 22,2% (β_6 = −28,02). Este efeito pode ser justificado para NC pelo agrupamento entre o PCL e o núcleo oleoso, aumento da tensão da interface nanopartícula/água ou mediante um efeito estabilizador do polímero ao redor das emulsões [10]. Até o momento, oleato de isodecila e o polímero PCL não foram reportados para o preparo de nanopartículas contendo corticosteróides.

Ainda em relação ao tamanho da nanopartículas, tão importante quanto o valor médio do DP é o valor de sua dispersão. Neste trabalho, a homogeneidade no diâmetro de partículas pode ser avaliada pelo índice de polidispersibilidade (IP). A polidispersão, ou índice de polidispersividade, indica a distribuição média do tamanho das nanopartículas sendo valores menores que 0,200, considerados bons indicadores de homogeneidade [32, 33]. Estes valores são desejados para manter a estabilidade da dispersão coloidal sem a formação de micropartículas ou precipitados. As dispersões coloidais preparadas não apresentaram precipitados mesmo após seis meses de armazenamento. Além disso, esta estreita distribuição no DP evita a formação de um gradiente de concentração de HC entre pequenas e grandes nanopartículas, o que poderia acarretar na cristalização de HC, com crescimento de cristais conhecidos como Ostwald Ripening [34]. As NS e NC apresentaram um valor médio do IP de 0,075 e 0,224, respectivamente, mostrando serem as dispersões coloidais de NS mais homogêneas.

Potencial Zeta, da mesma forma PS e PI, é um parâmetro importante para avaliar a estabilidade da suspensão coloidal. Quando as nanopartículas são preparadas em solução, ocorre a formação de uma dupla camada elétrica que cercam as nanopartículas. O potencial eletrostático neste limite "plano de cisalhamento hidrodinâmico" é chamado potencial zeta e está relacionado com a carga de superfície das nanopartículas [35]. Nesse sentido, o PZ indica que o grau de repulsão entre partículas semelhantes numa dispersão [36]. Nanopartículas com PZ entre +10 e −10 mV são considerados aproximadamente neutro. Por outro lado, suspensões coloidais de nanopartículas com ZP

superior +30 mV ou inferior a –30 mV são consideradas muito estáveis no meio de dispersão [34, 35]. O PZ variou entre -6,75 e -36,47 mV sendo os valores médios para

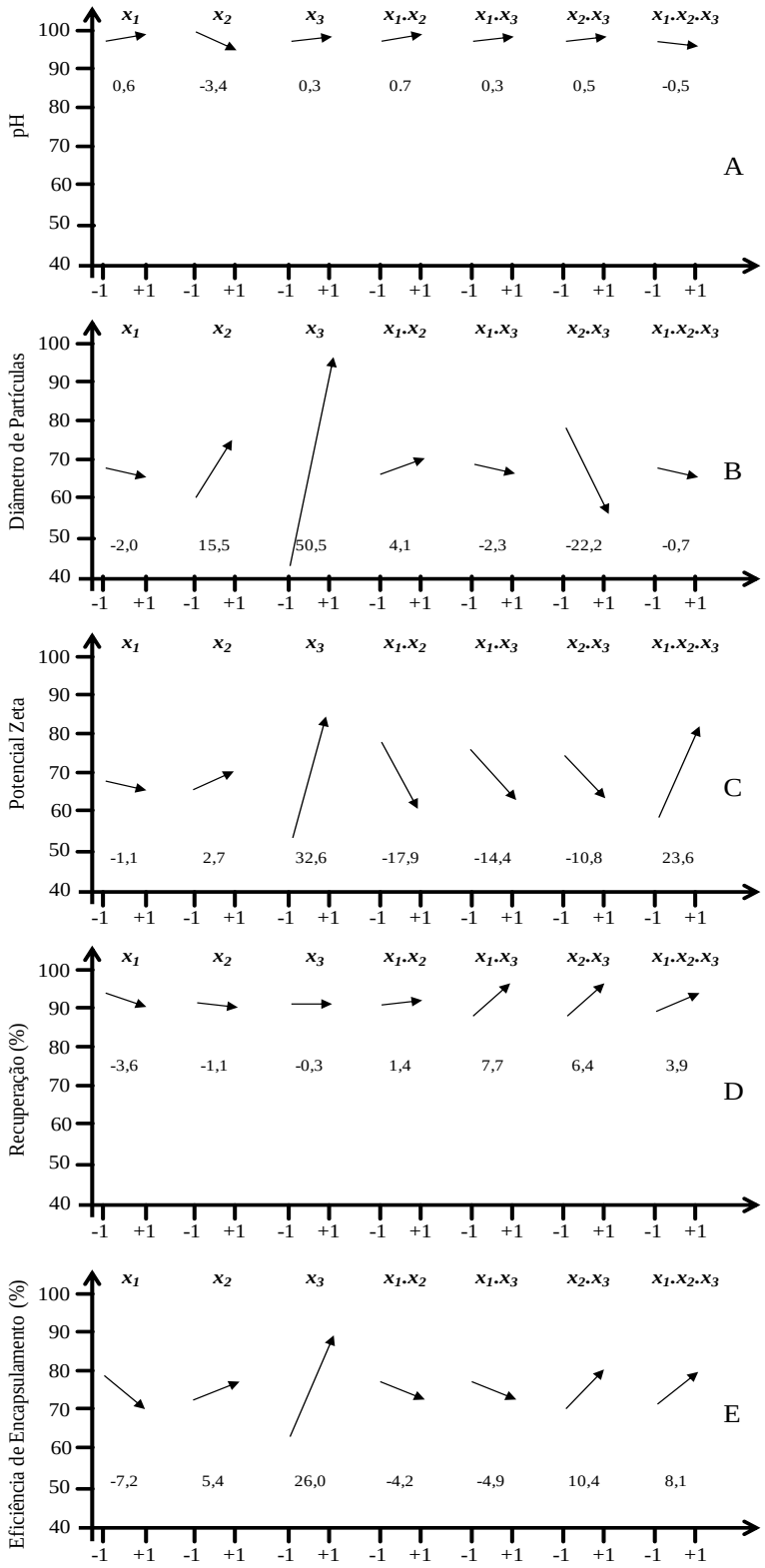

Figura 5. Cálculos dos efeitos para os experimentos realizados pelo planejamento fatorial 2^3. As setas dentro da figura representam os efeitos calculados em percentagem após a normalização dos dados. É importante observar que a inclinação das setas indica a amplitude dos efeitos.

NS e NC de −19,3 e −31,2 mV, respectivamente. Uma forte influência no PZ foi observada no cálculo do efeito para o oleato de isodecila. O oleato de isodecila (x_3) demonstrou um incremento de 32,6%, ou seja, sendo a principal variável responsável pelas NC apresentam uma maior carga de superfície que as NS. O maior PZ para as NC compensa o maior DP e IP, atribuindo as NS e NC, semelhante estabilidade coloidal.

Quando as três variáveis independentes ($x_1.x_2.x_3$) se encontram num mesmo nível (−1,−1,+1; −1,+1, −1; +1, −1, −1 ou +1,+1,+1), numa interação de terceira ordem, o potencial zeta aumentou em 23,6%. Ou seja, melhores estabilidades para a suspensão coloidal pode ser obtidas em quatro das oito principais formulações avaliadas tanto para NC quanto para NS. A análise do efeito das interações de segunda ordem ($x_1.x_2$;$x_1.x_3$;$x_2.x_3$) revelou decréscimos de −17,9, −14,4 e −10,8%, respectivamente. A redução da magnitude do PZ pela interação das três variáveis independentes em relação ao efeito individual do oleato de isodecila, de 32,7 para 23,6% colabora com a proposta da formação de uma camada polimérica ao redor do núcleo oleoso [37].

As porcentagens de recuperação nas formulações foram superiores a 82,5% mostrando uma independência com relação às variáveis investigadas. De fato, perdas na recuperação se devem principalmente a etapas de preparação das nanopartículas. A elevada recuperação analítica estabelecida durante a validação do método descarta possíveis perdas por interações irreversíveis ou erros operacionais no preparo de amostra para análises cromatográficas.

A eficiência de encapsulamento alternou entre 31,1 e 59,6% sendo, em média, 42% mais eficiente nos colóides de NC (x_3). A EE% aumentou em todos os cálculos de efeitos que envolveram o oleato de isodecila. Individualmente, o oleato de isodecila contribuiu com um aumento de 26,0% na EE%. O aumento na EE% nas NC pode ser entendido pela preferência da HC, um composto de baixa solubilidade em meio aquoso, pelo núcleo lipofílico oleoso presente nas NC [38].

Outras análises, além das acima já discutidas, de como as variáveis independentes interferem nas propriedades da nanopartículas, bem como as mesmas interagem entre si, não foram argumentadas, pois não apresentaram variações significativas. Em geral a caracterização das nanopartículas foi condizente com resultados previamente descritos na literatura empregando o PCL e a nanoprecipitação, podendo agora ser aplicados para a hidrocortisona [10]. A análise conjunta dos resultados, observando dados de estabilidade coloidal e eficiência de encapsulamento, propõe as melhores formulações para HC como sendo aquelas dos experimentos 07 e 08 ambas preparadas no nível superior das variáveis PCL (x_2) e oleato de isodecila (x_3). As mesmas conclusões foram obtidas através da análise de variância (ANOVA).

Com o propósito de avaliar a influencia de cada variável e suas interações sobre

as respostas, os coeficientes polinomiais da Equação 1 foram determinados. Quanto maior a magnitude de cada coeficiente, maior é o respectivo efeito principal sobre o sistema; um coeficiente positivo indica que ocorre um aumento no nível do parâmetro conduzindo para um acréscimo na média da variável dependente investigada. Avaliando a interação dos coeficientes, a resposta pode ser analisada em termos de como a variação de um fator modula o efeito num outro fator. Por exemplo, o sinal negativo do coeficiente sinaliza para um decréscimo na variável dependente investigada. Os valores dos coeficientes obtidos estão descritos na Tabela 4.

Tabela 4. Parâmetros de resposta para as variáveis dependentes investigadas do planejamento fatorial 2^3

Variáveis Dependentes	Coeficientes de regressão e intercepto							
	β_0	β_1	β_2	β_3	β_4	β_5	β_6	β_7
pH	6,56	0,02	-0,12	0,01	0,02	0,01	0,02	-0,02
DP	180,47	-2,05	19,45	63,55	5,28	-2,80	-28,02	-0,89
PZ	-26,64	0,21	-0,48	-5,94	3,29	2,62	1,96	-4,31
Rec%	92,91	-1,82	-0,56	-0,16	0,73	3,92	3,25	1,97
EE%	44,70	-2,15	1,60	7,77	-1,28	-1,45	3,10	2,41

Para identificar e confirmar a significância dos efeitos e suas interações, a análise de variância (ANOVA) foi aplicada para cada variável dependente investigando o significado estatístico dos modelos de interação. O *F*-valor, que é uma medida da variância dos dados da média e usado para avaliar a validade do ajuste no modelo, foi determinado com base na razão da média quadrada dos grupos e a média quadrada dos erros [39]. Quanto maior for o valor de *F* em relação a unidade, maior a certeza que as variáveis designadas (variáveis independentes) adequadamente explicam a variação na média dos dados, ou seja, indica uma boa correlação entre as respostas experimentais e preditas e que o modelo é adequado para descrever as variações nas respostas [39, 40]. Os resultados da ANOVA são apresentados na Tabela 5 para todos os modelos de interações. A tabela ANOVA sumariza a soma e média dos quadrados das regressões e residuais junto com os graus de liberdades correspondentes, valor de *F* e os coeficientes de determinação. As expressões matemáticas utilizadas para cálculos dos estimadores ANOVA são amplamente apresentados na literatura [39]. De acordo com a tabela ANOVA, com exceção dos dados de pH, os valores de *F* são elevados com valores de R^2 próximos a unidade, o que é aceitável. Previamente já foi avaliado que não houve variação significativa no valor de pH com modificações nas formulações. Pela análise de variância isto fica evidente, visto que as formulações de controle (ponto central na média) apresentaram uma dispersão nos valores de pH entre 6,29 e 6,66. Todos estes estimadores estatísticos, exceto para o pH, revelam que os modelos fatoriais das interações são aceitos estatisticamente para a predição das duas respostas na escala considerada do planejamento (região válida).

Cinética de liberação

Os perfis da cinética de liberação *in vitro* de nanocápsulas e nanoesferas poliméricas carregadas com hidrocortisona são mostrados na Figura 6. O sistema projetado em fluxo constante evita a saturação do sistema e, consequentemente, o equilíbrio de solubilidade [41]. Todavia, o sistema descreve resultados relativos comparando a cinética de liberação das nanoformulações (NC e NS) que foram investigadas nas mesmas condições. A velocidade de liberação ser alterada, por exemplo, com a modificação da vazão do tampão PBS. Amostras de 1,0 mL da suspensão coloidal foram retiradas em períodos de tempo pré-estabelecidos. Neste ensaio somente a hidrocortisona não encapsulada (livre ou liberada) possui a capacidade de permear através dos poros da bolsa de diálise. Os tempos necessários para liberação de 100% da HC de NC e NS foram de 6 e 8 horas, respectivamente. Aproximadamente 80% da hidrocortisona foi liberada nas duas primeiras horas (da suspensão coloidal para o meio de dispersão). Na Figura 6 se observa uma liberação inicial acentuada decorrente da saída para o meio de dispersão da HC não encapsulada ou apenas adsorvida na parede externa das nanopartículas. Após uma hora, a liberação assume um perfil mais lento limitado pela difusão da HC. A velocidade de liberação foi maior em NS em função da menor EE%, ou seja, maior taxa de difusão da HC não encapsulada e da capacidade de solubilização da HC no oleato de isodecila utilizado no preparo das NC.

Tabela 5. Parâmetros ANOVA para caracterização dos ajustes da Equação 1

Origem	g.l*	Soma dos quadrados	Média dos Quadrados	*F*-valor	Prob > *F*	R^2
pH						
Regressão	7	0,359	0,051	3,403	$1,08x10^{-2}$	0,488
Erro (resíduos)	25	0,377	0,015			
Total	32	0,736				
Diâmetro de Partículas						
Regressão	7	125.834,376	17.976,339	63,530	$2,42x10^{-14}$	0,947
Erro (resíduos)	25	7.073,973	282,959			
Total	32	132.908,350				
Potencial Zeta						
Regressão	7	1.816,089	259,441	27,922	$2,65x10^{-10}$	0,887
Erro (resíduos)	25	232,288	9,292			
Total	32	2.048,377				
Recuperação						
Regressão	7	814,993	116,428	27,789	$2,79x10^{-10}$	0,886
Erro (resíduos)	25	104,744	4,190			
Total	32	919,737				
Eficiência de encapsulamento						
Regressão	7	2.081,692	297,385	186,679	0,000	0,981
Erro (resíduos)	25	39,826	1,593			
Total	32	2.121,518				

* *g.l. Graus de Liberdade*

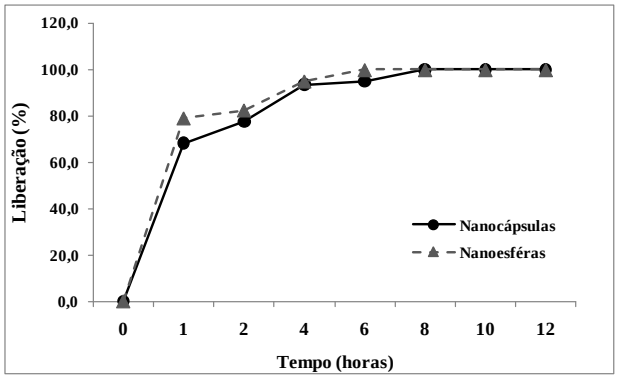

Figura 6. Perfil de liberação *in vitro* de nanopartículas poliméricas carregadas com HC.

O modelo de Korsmeyer-Peppas [21], geralmente usado para análise de mecanismos de liberação não muito bem estabelecidos ou quando há mais de um fenômeno envolvido, leva em consideração mecanismos de liberação de fármacos que não seguem a lei de Fick e segue um comportamento anômalo descrito pela Equação 5 [33, 42]. O valor de *n* é um parâmetro empírico, relacionado com a forma geométrica do sistema de liberação, e determina o mecanismo de liberação [33,43]. Os valores de *n* determinados pelos coeficientes angulares dos gráficos $ln(M_t/M_\infty)$ *vs. ln(t)* para a HC em NC e NS foram 0,187 (intervalo 1–8 h) e 0,138 (intervalo 1–6 h), respectivamente. Quando assume valores menores que 0,45 ($n \leq 0,45$) o mecanismo de liberação refere-se ao processo de difusão pura (Fickiana clássica) [10, 43, 44]. As constantes de liberação para NC e NS foram 0,689 e 0,778, respectivamente, condizentes com os perfis de liberação observados.

Conclusões

Os resultados deste trabalho demonstram que nanocápsulas e nanoesferas poliméricas carregadas com hidrocortisona podem ser preparadas utilizando o polímero pré-formado PCL pela técnica de deposição interfacial. O método cromatográfico desenvolvido e validado foi eficiente aos estudos quantitativos da HC neste trabalho. O efeito de diferentes variáveis sobre a preparação de nanopartículas foi investigado. As características físico-químicas destes sistemas foram alteradas dependendo da composição das formulações. Os resultados demonstram que partículas de pequeno diâmetro e com carga negativa de superfície foram obtidas o que confere uma boa estabilidade coloidal. As variáveis independentes PCL e oleato de isodecila foram responsáveis pelas principais alterações no diâmetro de partícula, potencial zeta e eficiência de encapsulamento. A eficiência máxima de encapsulamento foi de 59,6% sendo encontrada para nanocápsulas. A EE% foi em média 42% maior para NC quando comparada com NS. A HC pode ser dispersa em meio aquoso numa concentração 53% maior que sua solubilidade máxima. A análise do perfil de liberação utilizando o modelo de Korsmeyer-Peppas mostrou modelo de cinética condizente com um processo de

difusão pura.

Agradecimentos

À Universidade Federal de São Carlos pela bolsa PADRD e às agências de fomento CNPq, CAPES e Fapesp, pelos auxílios financeiros.

Referências e Notas

[1] Chapados, I.; Lee. T. F.; Chik, C. L.; Cheung, P. Y. *Eur. J. Pharm*. **2011**, *652,* 111. [CrossRef]

[2] Heindl, S.; Vahlkamp, K.; Weitz, G.; Fehm, H. L.; Dodt, C. *Steroids* **2006**, *71*, 206. [CrossRef]

[3] Ogias, D.; Bitencourt, B.; Alvares, E. P.; Gama, P. *Regulatory Peptides* **2006**, *135*, 17. [CrossRef]

[4] Filipović-Grčić, J.; Voinovich, D.; Moneghini, M.; Bećirević-Laćan, M.; Magarotto, L.; Jalšenjak, I. *Eur. J. Pharm. Sci*. **2000**, *9*, 373. [CrossRef]

[5] Cavalli, R.; Peira, E.; Caputo, O.; Gasco, M. R. *Int. J. Pharm*. **1999**, *182*, 59. [CrossRef]

[6] Cevc, G.; Blume, G. *Biochim. Biophys. Acta* **2004**, *1663*, 61. [PubMed]

[7] Manosroi, J.; Saowakhon, S.; Manosroi, A. *Enz. Microbial Technol*. **2007**, *41*, 322. [CrossRef]

[8] Jensen, L. B.; Magnussson, E.; Gunnarsson, L.; Vermehren, C.; Nielsen, H. M.; Petersson, K. *Int. J. Pharm*. **2010**, *390*, 53. [CrossRef]

[9] Reis, C. P.; Neufeld, R. J.; Ribeiro, A. J.; Veiga, F. *Nanomedicine: Nanotech. Biol. Med.* **2006**, 2, 8. [CrossRef]

[10] Schaffazick, S. R.; Guterres, S. S.; Freitas, L.L.; Pohlmann, A. R. *Quim. Nova* ***2003***, *26*, 726. [CrossRef]

[11] Akagi, T.; Baba, M.; Akashi, M. *Polymer* **2007**, *48*, 6729. [CrossRef]

[12] Kristmundsdóttir, T.; Loftsson, T.; Holbrook, W. P. *Int. J. Pharm*. **1996**, *139*, 63. [CrossRef]

[13] Ali, H. S. M.; York, P.; Ali, H. M. A.; Blagden, N. *J. Control. Release* **2011**, *149*, 175. [CrossRef]

[14] Zimmer, A. K.; Maincent, P.; Thouvenot, P.; Kreuter, J. *Int. J. Pharm*. **1994**, *110*, 211. [CrossRef]

[15] a) Ramanathan, S.; Block, L. H. *J. Control. Release* **2001**, 70, 109. [CrossRef]; b) Barichello, J. M.; Handa, H.; Kisyuku, M.; Shibata, T.; Ishida, T.; Kiwada, H. *J. Control. Release* **2006**, *115*, 94. [CrossRef]

[16] a) Mahnert, W.; Mäder, K. *Adv. Drug Deliv. Rev*. **2001**, *47*, 165. [CrossRef]; b) Kawashima, Y. *Adv. Drug Deliv. Rev*. **2001**, *47*, 1. [CrossRef]

[17] Fessi, H.; Puisieux, F.; Devissaguet, J-P. Ammoury, N.; Benita, S. *Int. J. Pharm*. **1989**, *55*, R1. [CrossRef]

[18] Quintanar-Guerrero, D.; Allémann, E.; Fessi, H.; Doelker, E. *Drug Dev. Ind. Pharm*. **1998**, *24*, 1113. [CrossRef]

[19] ICH [International Conference on Harmonization, FDA, USA]. Q2B: Validation of analytical procedures: methodology. 1996 (Available under: http://www.fda.gov/downloads/Drugs/GuidanceComplianceRegulatoryInformation/Guidances/UCM073384.pdf).

[20] Levy, M. Y.; Benita, S. *Int. J. Pharm*. **1990**, *66*, 29. [CrossRef]

[21] Korsmeyer, R. W.; Gurny, R.; Doelker, E.; Buri, P.; Peppas, N. A. *Int. J. Pharm*. **1983**, *15*, 25. [CrossRef]

[22] a) Wang, P. P.; Frazier, J.; Brem, H. *Adv. Drug Deliv. Rev*. **2002**, *54*, 987. [CrossRef]; b) Yan, S. S.; Gilbert, J. M. *Adv. Drug Deliv. Rev*. **2004**, *56*, 1497. [CrossRef]

[23] Dai, C.; Wang, B.; Zhao, H. *Colloids and Surfaces B: Biointerfaces* **2005**, *41*, 117. [CrossRef]

[24] Yamada, Y.; Harashima, H. *Adv. Drug Deliv. Rev*. **2008**, *60*, 1439. [CrossRef]

[25] Cassidy, C. M.; Tunney, M. M.; McCarron, P. A.; Donnelly, R. F. *J. Photochem. Photobiol. B: Biology* **2009**, *95*, 71. [CrossRef]

[26] Pitt, C. G. In: Bioderadable Polymers as Drug Delivery Systems. Langer, R.; Chasin, M., eds. New York: Marcel Decker Inc., 1990, 71.

[27] Chawla, J. S.; Amiji, M. M. *Int. J. Pharm*. **2002**, *249*, 127. [CrossRef]

[28] Ponsart, S.; Coudane, J.; Vert, M. *Biomacromolecules* **2002**, *1*, 275. [CrossRef]

[29] Fukushima, K.; Abbate, C.; Tabuani, D.; Gennari, M.; Rizzarelli, P.; Camino, G. *Mater. Sci. Eng. C* **2010**, *30*, 566. [CrossRef]

[30] Sarmento, B.; Ribeiro, A.; Veigas, F.; Ferreira, D. *Biomed. Chrom*. **2006**, *20*, 898. [CrossRef]

[31] Santos, K. C.; Da Silva, M. F. G. F.; Fernandes, J. B.; Vieira, P. C.; Polikarpov, I.; Zucolotto, V.; Forim, M. R. *Anal. Methods* **2011**, *3*, 1936. [CrossRef]

[32] Mohanraj, V. J.; Chen, Y. T. *J. Pharm. Res*. **2006**, *5*, 561.

[33] de Melo, N. F. S.; Grillo, R.; Rosa, A. H.; Fraceto, L. F.; Dias-Filho, N. L.; de Paula, E.; Araújo, D. R. *Quim. Nova* **2010**, *33*, 65. [CrossRef]

[34] Wu, L.; Zhang, J.; Watanabe, W. *Adv. Drug Deliv. Rev*. **2011**, *63*, 456. [CrossRef]

[35] Clogston, J. D.; Patri, A. K. In.: Characterization of nanoparticles intended for drug delivery. McNeil, S.E., ed. New York: Humana Press. 2011, 63. [CrossRef]

[36] Manzanilla-Granados, H. M.; Jiménez-Ángeles, F.; Lozada-Cassou, M. *Colloid Surface A* **2011**, *376*, 59. [CrossRef]

[37] Calvo, P.; Vila-Jato, J. L.; Alonso, M. J. *J. Pharm. Sci*. **1996**, *85*, 530. [CrossRef]

[38] Barichello, J. M.; Morishita, M.; Takayama, K.; Nagay, T. *Drug Dev. Ind. Pharm.* **1999**, *25*, 471. [CrossRef]

[39] Montgomery, D. C. Design and Analysis of Experiments, 5th ed. New York: John Wiley & Sons, 2001.

[40] Akhnazarova, S.; Kafarov, V. Experiment optimization in chemistry and chemical Engineering. Moscow: Mir Publisher, 1982.

[41] Alsenz, J.; Kansy, M. *Adv. Drug Deliv. Rev*. **2007**, *59*, 546. [CrossRef]

[42] Hayashi, T.; Kanbe, H.; Okada, M.; Suzuki, M.; Ikeda, Y.; Onuki, Y.; Kaneko, T.; Sonobe, T. *Int. J. Pharm*. **2005**, *304*, 91. [CrossRef]

[43] Lopes, C. M.; Lobo, J. M. S.; Costa, P. *Rev. Bras. Cien. Farm*. **2005**, *41*, 143. [CrossRef]

[44] Li, Z-Z.; Xu, X-A.; Wen, L-X.; Liu, F.; Liu, A-Q.; Wang, Q.; Sun, H-Y.; Yu, W.; Chen, J-F. *J. Control. Release* **2006**, *111*, 81. [CrossRef]

ISSN 1984-6428
ONLINE
www.orbital.ufms.br

| Vol 4 | | No. 2 | | April-June 2012 |

Full Paper

Comparative study of kinetics of adsorption of methylene blue from aqueous solutions using cinnamon plant (*Cinnamonum zeylanicum*) leaf powder and pineapple (*Ananas comosus*) peel powder

Satish D. Patil[a], S. Renukdas[b] and N. T. Patel[b]**

[a]Department of Chemistry, A. P. Science College, Nagothane – 402106 (MS), India.
[b]Department of Chemistry, Yeshwant Mahavidyalaya, Nanded – 431602 (MS), India.

Received: 01 January 2012; revised: 12 March 2012; accepted: 26 March 2012. Available online: 07 July 2012.

ABSTRACT: *Batch adsorption of methylene blue (MB) onto Cinnamon plant (Cinnamonum Zeylanicum) leaf powder (CPLP) and Pineapple (Ananas Comosus) peel powder (PPP) was investigated. Different parameters such as initial sorbate concentration, adsorbent dosage, pH, contact time, agitation speed, temperature and particle size. All isotherm models were found to be best fitting with high values of regression coefficient i.e. for Langmuir (R^2 = 0.989 to 0.994 for CPLP and 0.993 to 0.995 for PPP), for Freundlich (R^2 = 0.996 to 0.998 for CPLP and 0.995 for PPP) and for Temkin (R^2 = 0.983 to 0.995 for CPLP and 0.984 to 0.989 for PPP). The monolayer (maximum) adsorption capacities (q_m) were found to be 250 and 333.333 mg/g for CPLP and PPP respectively. Lagergen pseudo -second order model best fits the kinetics of adsorption (R^2 = 0.999 for CPLP and 1 for PPP). The amount of dye adsorbed at equilibrium $q_{e(the)}$ obtained from Lagergen pseudo -second order model were found to be nearly same with the experimental data. Intra particle diffusion plot showed boundary layer effect and larger intercepts indicates greater contribution of surface sorption in rate determining step. Adsorption was found to be directly proportional to pH and temperature but inversely proportional to particle size. Thermodynamic analysis (ΔG, ΔH and ΔS values) showed adsorption was favourable, spontaneous, endothermic physisorption and increased disorder and randomness at the solid- solution interface of MB with the adsorbents. The forward rate constant was much higher than reverse rate constant suggesting dominance of rate of adsorption. PPP was found to be better adsorbent than CPLP.*

Keywords*: adsorption; methylene blue; isotherm; adsorbent; kinetic and thermodynamic parameters*

* Corresponding author. E-mail: sdpatil72@gmail.com

Introduction

Of various pollutants contained in industrial wastewaters, colour is considered to be very important from the aesthetic point of view and is stated as visible pollutant. Almost every industry uses colouring matter to colour their products. Unspent colouring materials are usually discharged, with/without treatment into the aquatic environment. Dyes are highly coloured polymers and low biodegradable. Color/dye being one of the important recalcitrant, persist for long distances in flowing water, retards photosynthetic activity, inhibit the growth of aquatic biota by blocking out sunlight and utilizing dissolved oxygen and also decrease the recreation value of stream. Therefore it is necessary to decolorize wastewater before discharge. Colour removal was mostly studied with physiochemical methods such as adsorption, coagulation, oxidation process and biological treatment. Many researches [1-5] have conducted a great number of studies on the adsorption of dyes onto activated carbon. With the exception of activated carbon, the use of other low-cost adsorbents has also been the focus of recent research. These include silica gel, clays, sawdust, bagasse pith, peat, and fly ash [6-16].

Methylene blue (MB) is an important basic dye widely used for dyeing, printing cotton and tannin, printing calcico, dyeing leather, it causes eye burns. It also may cause cyanosis, tachycardia, if inhaled. It also causes irritation to the skin. Hence it is necessary to remove MB from wastewater.

Therefore a search of low cost and easily available biomaterials as adsorbents for removal of dyes from wastewater is a basic need. In this paper, we attempt to use CPLP and PPP as adsorbents. Cinnamon plant mature leaves were collected from one of the gardens and raw pineapple peels from one of the juice centre from Alibag - Raigad. The dried powders were used as a biosorbents for decolourisation of synthetic wastewater of MB in the present study.

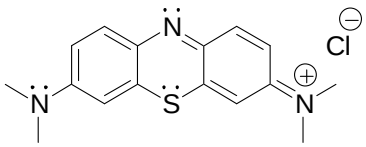

Structure of methylene blue (MB)

Material and Methods

Sorbate and chemicals

Methylene blue ($C_{16}H_{18}ClN_3S$), the sorbate used in the present study, is a monovalent cationic dye. In dye classification it is classified as C. I. Basic blue 9 and C. I. 52015. It has a molecular weight of 373.9 and was supplied by Merck.

A stock solution of 1000 mg/L was prepared and the working solutions were

prepared by diluting the stock solution by distilled water as per requirement.

Standard solution of the dye was taken and absorbance was determined at different wavelengths using Equiptronics single beam u.v. visible spectrophotometer to obtain a plot of absorbance verses wavelength. The wavelength corresponding to the maximum absorbance (λ_{max}= 665 nm) as determined from the plot, was noted and this wavelength was used for measuring the absorbance in the present study. pH of the solution was adjusted using Equiptronics pH meter.

Other chemicals such as HCl, NaOH used were of analytical grade and supplied by Merck.

Sorbent

Mature cinnamon plant leaves and pineapple peels were washed thoroughly with distilled water to remove dust and other impurities. Washed leaves and peels were dried for 5-6 days in sunlight. Dried leaves and peels were ground in a domestic mixer-grinder. After grinding, the powders were again washed and dried. Different sized CPLP and PPP were stored in plastic container for further use.

Sorption kinetics

The efficiency of adsorbents is evaluated by conducting laboratory batch mode studies. Specific amount of adsorbents were shaken in 25 mL aqueous solution of dye of varying concentration for different time periods at natural pH and temperatures. At the end of pre-determined time intervals, adsorbent was removed by centrifugation at 10000 rpm and supernatant was analyzed for residual concentration of MB spectrophotometrically at 665 nm wavelength.

Also variations in pH, adsorbent dose, particle size, agitation speed, were studied. Comparative studies of both the adsorbents (CPLP and PPP) were carried out under same experimental conditions.

Effect of contact time and initial dye concentration

Batch experiments of 25 mg of adsorbent of ≥ 120 mesh size with 25 mL of 100 and 200 mg/L dye concentration were performed at nearly 303K on a oscillator at 230 rpm for 5, 10, 15, 20, 30, 40, 50 and 60 minutes at pH = 7. Then optimum contact time was identified for further batch experimental study.

Effect of initial dye concentration

25 mg of adsorbent of ≥ 120 mesh size with 25 mL of dye solution was kept constant for batch experiments. Initial dye concentration of 100, 150, 200, 250, 300 and 350 mg/L were performed at nearly 303K on a oscillator at 230 rpm for 30 minutes at

pH = 7.

Effect of adsorbent dosage and initial dye concentration

Initial dye concentrations of 400 and 500 mg/L were used in conjunction with adsorbent dose of 1, 2, 3, 4, 5, and 6 g/L. Contact time, pH, agitation speed, temperature and particle size of 30 minutes, 7, 230 rpm, 303 K and ≥ 120 mesh respectively were kept constant.

Effect of pH

Initial pH of dye solutions were adjusted to 3, 5, 7, 9 and 11 for 200 mg/L concentration. Contact time, adsorbent dose, agitation speed, temperature and particle size of 30 minutes,1 g/L, 230 rpm, 303 K and ≥ 120 mesh respectively were kept constant.

Effect of particle size and initial dye concentration

Three different sized particles of ≥ 120, 120 ≤ 85 and 85 ≤ 60 mesh were used in conjunction with 100, 150, 200, 250, 300 and 350 mg/L dye concentration. Contact time, adsorbent dose, agitation speed, temperature and pH of 30 minutes, 1 g/L, 230 rpm, 303 K and 7 respectively were kept constant.

Effect of temperature and initial dye concentration

303 K, 313 K and 323 K temperatures were used in conjunction with 100, 150, 200, 250, 300 and 350 mg/L dye concentration. Contact time, adsorbent dose, agitation speed, particle size and pH of 30 minutes, 1 g/L, 230 rpm, ≥ 120 mesh and 7 respectively were kept constant.

Effect of agitation speed

100, 170 and 230 rpm agitation speeds were used in con junction with initial dye concentration of 100 mg/L for 5,10, 15, 20, 30, 40, 50 and 60 minutes. Adsorbent dose, pH, temperature and particle size of 1 g/L, 7, 303 K and ≥ 120 mesh respectively were kept constant.

Desorption Studies

After adsorption, the dye loaded adsorbents are separated from the solution by centrifugation and the supernatant is drained out. The adsorbent is gently washed with water to remove any unadsorbed dye. Regeneration of dye from the dye – laden adsorbent is carried out using the desorbing media - distilled water at pH 3, 7 and 11 using dilute solutions of NaOH and HCl. Then they are agitated for the equilibrium time. The desorbed dye in the solution is separated and analyzed for the residual dye.

For the desorption studies, dye loaded adsorbents from 100mg/L initial dye

concentration are used.

Results and Discussion

Effect of contact time and initial dye concentration

Effect of initial dye concentration with contact time on adsorption of MB is presented in figures 1 and 2. Uptake of MB was rapid in first 5 minutes and after 30 minutes amount of MB adsorbed was almost constant. Therefore, for batch experiments 30 minutes equilibrium time was used. Percentage sorption decreased from 83.4 to 68.35% for CPLP and 97.4 to 89.25% for PPP but amount of MB adsorbed per unit mass of adsorbent increased from 83.4 to 136.5 mg/g for CPLP and 97.4 to 178.5 mg/g with increase in MB concentration from 100 to 200 mg/L.

The rapid uptake at the beginning may be attributed to the rapid attachment of the dye molecules to the surface of the sorbent and the following slower sorption to intra particle diffusion. The initial rapid phase may also be due to the increased number of vacant sites available at the initial stage, consequently exist an increase in driving force of the concentration gradient between adsorbate in solution and adsorbate in the adsorbent [17].

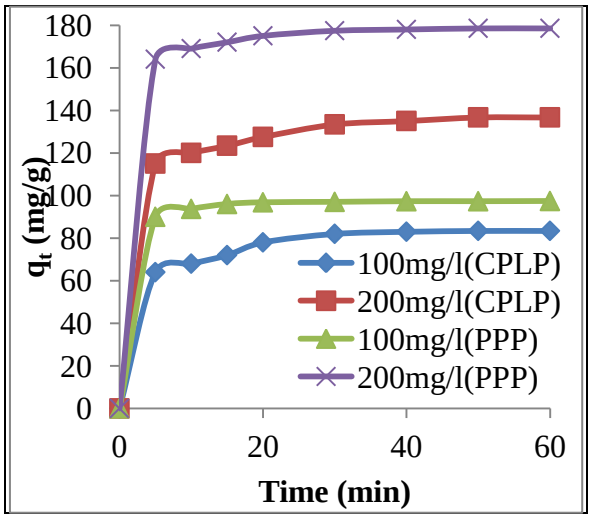

Figure 1. Effect of initial dye concentration and contact time on adsorption of MB.

To investigate the mechanism of adsorption, pseudo-first order, pseudo-second order, intra particle diffusion, Elovich, Natarajan and Khalaf first order, Bhattacharya and Venkobachar first order models were used. The Lagergen pseudo-first order rate expression is given as:

$$\log (q_e - q_t) = \log q_e - (k_1 / 2.303)\, t \quad (1)$$

Where q_e and q_t are amounts of dye adsorbed (mg/g) on adsorbent at equilibrium and at time t, respectively and k_1 is rate constant of pseudo first order adsorption (min^{-1}). The

slope and intercept values of plot log (q_e - q_t) against t, Figure 3 were used to determine pseudo first order rate constant (k_1) and theoretical amount of dye adsorbed per unit mass of adsorbent $q_{e(the)}$, respectively. $q_{e(the)}$were compared with the $q_{e(exp)}$ values in Table 1. $q_{e(exp)}$ values differ from the corresponding $q_{e(the)}$ values showed that pseudo first order equation of Langergen does not fit well with whole range of contact time and is generally applicable for initial stage of adsorption.

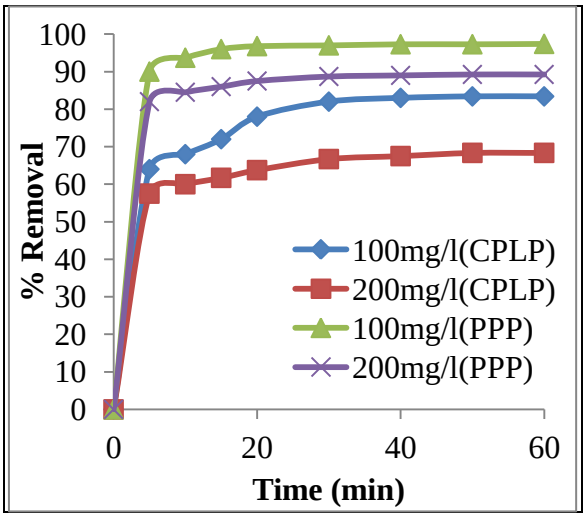

Figure 2. Effect of initial dye concentration and contact time on % removal of MB.

The Langergen pseudo- second order kinetic model is given as:

$$t/q_t = 1/(k_2 q_e^2) + t/q_e \qquad (2)$$

Where k_2 is rate constant of second order adsorption (g mg^{-1} min^{-1}). The slopes and intercepts of plot of t/q_t against t, Figure 4, were used to determine $q_{e(the)}$ and k_2 respectively. From highly linear plots it is cleared that there may be a possibility of chemisorptions playing a significant role in the rate determining step. The pseudo second order parameters, $q_{e(the)}$, h and k_2 obtained from the plot are represented in Table 1. Where h is initial adsorption rate (mg/g.min), $h = k_2 q_e^2$).

The correlation coefficient R^2 for second order adsorption model has very high values for both the adsorbents (R^2 = 1) and $q_{e(the)}$ values are consistent with $q_{e(exp)}$ showed that pseudo second order adsorption equation of Langergen fit well with whole range of contact time and dye adsorption process appears to be controlled by chemisorptions.

The adsorption of dye from aqueous solution follows first order kinetics when a single species is considered on a heterogeneous surface. The heterogeneous equilibrium between the dye solutions and adsorbent are represented as:

$$A \underset{K2}{\overset{K1}{\rightleftharpoons}} B$$

Where K_1 is forward rate constant and K_2 is the backward rate constant. A and B represents dye remaining in the aqueous solution and dye adsorbed on the surface of adsorbent respectively. The equilibrium constant (K_o) is the ratio of concentration of dye on adsorbent and in aqueous solution.

$$K_o = K_1 / K_2 \qquad (3)$$

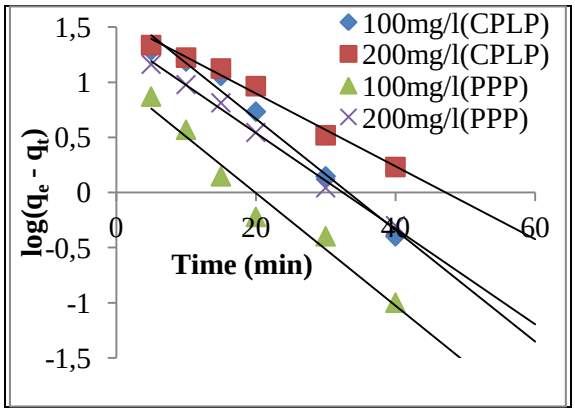

Figure 3. Pseudo first order plot of effect of initial dye concentration and contact time on adsorption of MB.

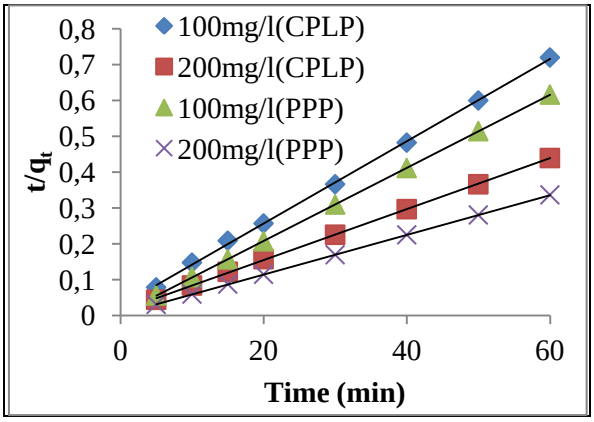

Figure 4. Pseudo second order plot of effect of initial dye concentration and contact time on adsorption of MB.

To study the kinetics of the adsorption process the kinetic equation proposed by Natarajan and Khalaf as cited in literature has been employed.

$$\log (C_o/C_t) = (K_{ad} /2.303) \qquad (4)$$

Where C_o and C_t are concentration of MB (mg/L) at time zero and time t respectively. K_{ad} is first order adsorption rate constant (min^{-1}) which was calculated from slope of the linear plot log (C_o/C_t) against t, Figure 5, for 100 to 200 mg/L MB concentrations. The rate constants are determined by the following equation:

$$K_{ad} = K_1+K_2 = K_1+ (K_1/K_o) = K_1 (1+ 1/ K_o) \qquad (5)$$

The overall rate constant K_{ad} for adsorption of dye decreases with increase in

concentration. K_{ad} is separated into rate of forward (K_1) and reverse reactions (K_2) using equation (5). K_{ad}, K_1, K_2 are given in Table 2 clearly indicate that, at all initial concentrations, the forward rate constant was much higher than the reverse rate constant suggesting that the rate of adsorption was dominant.

The linearized form of Bhattacharya and Venkobachar first order kinetic equation is presented as:

$$\log [\ 1 - U(T)\ ] = - (K /2.303)\ t \qquad (6)$$

Where $U(T) = [(C_o - C_t)\ / (C_o - C_e)]$, C_e is equilibrium MB concentration (mg/L). K is first order adsorption rate constant (min^{-1}) which was calculated from slope of the plot log [1 – U(T)] against t with $R^2 > 0.992$, Figure 6, Table 2.

Steps involved in sorption of the dye by adsorbent includes transport of solute from aqueous to surface of solid and diffusion of solute into the interior of pores, which is generally a slow process.

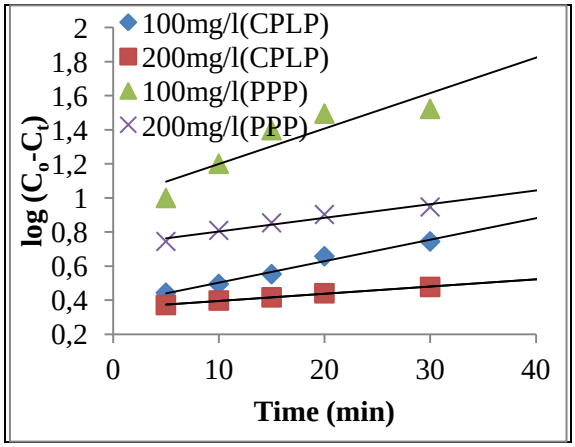

Figure 5. Natarajan and Khalaf first order plot of effect of initial dye concentration and contact time on adsorption of MB.

According to Weber and Morris, the intra particle diffusion rate constant (K_i) is given by the following equation:

$$q_t = K_i\ t^{1/2} \qquad (7)$$

K_i (mg/ g/$min^{1/2}$) values can be determined from the slope of the plot q_t against $t^{1/2}$, Figure 7 showed a linear relationship after certain time but they do not pass through origin. This is due boundary layer effect. The larger the intercept, the greater the contribution of surface sorption in rate determining step. The intercepts and K_i values of plots q_t against $t^{1/2}$ increases with increase the initial concentration of dye, Table 2. Initially there is liquid film ass transfer followed by the intra particle diffusion. The linearized form of Elovich kinetic equation is presented as:

$$q_t = 1/\ \beta[\ \ln(\alpha\beta)] + \ln t\ /\ \beta \qquad (8)$$

Where α and β are the constants calculated from the intercepts and slope of plot q_t against ln t, Figure 8, Table 2.

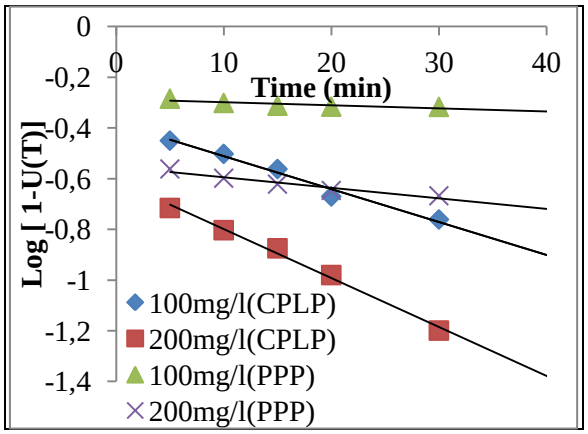

Figure 6. Bhattacharya and Venkobachar first order plot of effect of initial dye concentration and contact time on adsorption of MB.

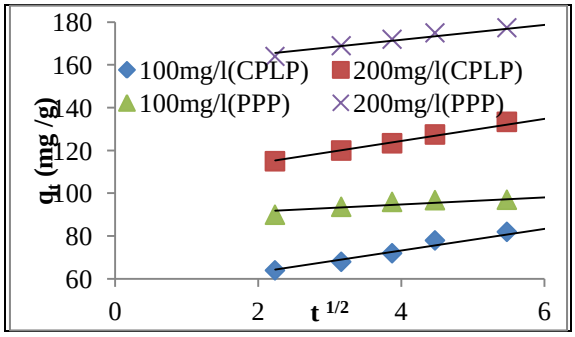

Figure 7. Intra particle diffusion plot of effect of initial dye concentration and contact time on adsorption of MB.

Mechanism of adsorption

The different functional groups such as hydroxyl, carboxylic, amino etc. from the surface of adsorbents have high affinity towards cationic dyes. The adsorption of cationic dye due to one of the following mechanisms Electrostatic attraction between oxyanion (—O^-) or carboxylate ions (—COO^-) from adsorbent surface and cationic dye molecules results into either chemisorptions (strongest among all types of forces) or electrostatic physisorption between two oppositely charged ions (strongest among the physical bonds).

(Here, S indicates surface of an adsorbent)

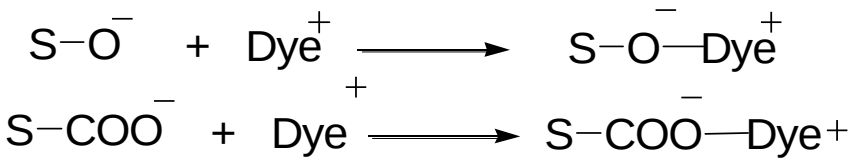

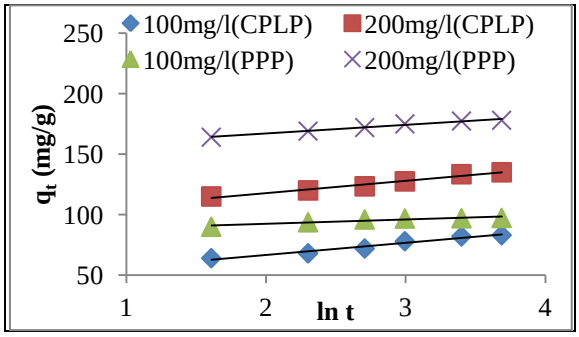

Figure 8. Elovich plot of effect of initial dye concentration and contact time on adsorption of MB.

Electrostatic physisorption between ions and dipole (second strongest among the physical bonds). Here, Electrostatic attraction between negative poles of partial polar bonds of OH, NH and CO groups of adsorbent and cationic dye molecules takes place.

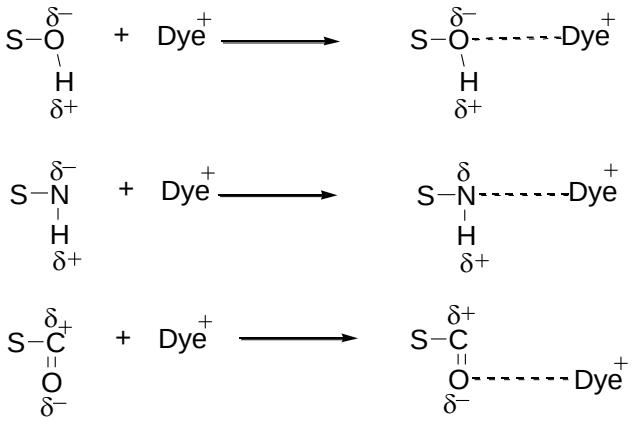

Hydrogen bonding or dipole – dipole interaction takes place between —NH and —OH groups from the surface of an adsorbent and amino groups in dye molecules. These are weaker physical interactions as compared to above ones.

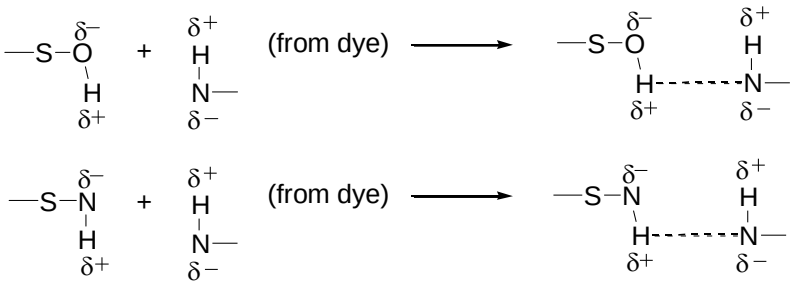

Here the adsorption of dye takes place due to exchange of ions between –OH or –COOH groups from the surface of adsorbents and cationic dye molecules. Thus, protons (H+ ions) are released into the solution [22].

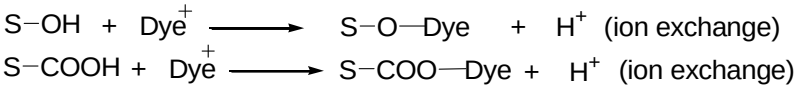

Micro–precipitation and weakest Van der Waals forces leads to multilayer formation.

Table 1. Effect of initial dye concentration and contact time on adsorption of MB

Adsor.	Initial MB Conc. (mg/l)	Pseudo -first order model				Pseudo -second order model				
		$q_{e(exp)}$ (mg/g)	K_1 (min^{-1})	$q_{e(the)}$ (mg/g)	R^2	$q_{e(exp)}$ (mg/g)	K_2 (g/mg/min)	$q_{e(the)}$ (mg/g)	h (mg/g .min)	R^2
CPLP	100	83.4	0.115	47.86	0.979	83.4	0.004	90.91	37.04	0.999
CPLP	200	136.5	0.076	36.31	0.985	136.5	0.004	142.9	83.33	0.999
PPP	100	97.4	0.117	10.35	0.961	97.4	0.033	100	333.3	1
PPP	200	178.5	0.099	25.47	0.994	178.5	0.008	200	333.3	1

Table 2. Effect of initial dye concentration and contact time on adsorption of MB

Adsorbent	Initial MB Conc. (mg/l)	Intra particle diffusion model		Elovich Model			Natarajan and Khalaf model				Bhattacharya and Venkobachar model	
		K_i ($mg/g/min^{1/2}$)	R^2	α	β	R^2	K_{ad} (min^{-1})	K_1	K_2	R^2	K (min^{-1})	R^2
CPLP	100	5.051	0.957	12.4411	0.0997	0.961	0.02764	0.02303	0.0046	0.98	0.02994	0.98
CPLP	200	5.138	0.985	11.2518	0.09862	0.977	0.00921	0.0063	0.00292	0.995	0.04376	0.993
PPP	100	1.666	0.777	3.6857	0.28281	0.892	0.04606	0.04486	0.0012	0.823	0.0023	0.743
PPP	200	3.477	0.936	7.40591	0.14142	0.985	0.01842	0.01644	0.00198	0.953	0.00921	0.939

Effect of initial dye concentration

Percentage sorption decreased from 82 to 51.43% for CPLP and 97 to 73.14% for PPP but amount of MB adsorbed per unit mass of adsorbent increased from 82 to 180 mg/g for CPLP and 97 to 256 mg/g for PPP with increase in MB concentration from 100 to 350 mg/L, Figures 9 and 10. With increasing initial concentration of dye solutions, the percent uptake of MB decreased due to the saturation and quick exhaustion of the binding sites on the sorbent as the number of dye molecules per unit volume increased. At low initial concentration, dye molecules are adsorbed on a specific binding site, however when the concentration increases, there exist reductions in immediate solute adsorption due to the lack of available binding sites.

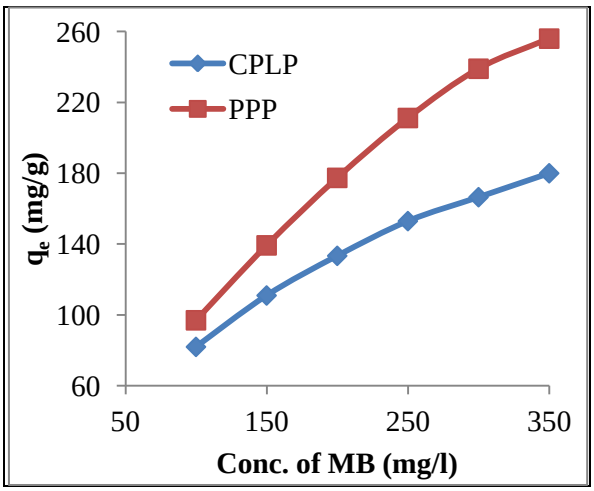

Figure 9. Effect of initial dye concentration on adsorption of MB.

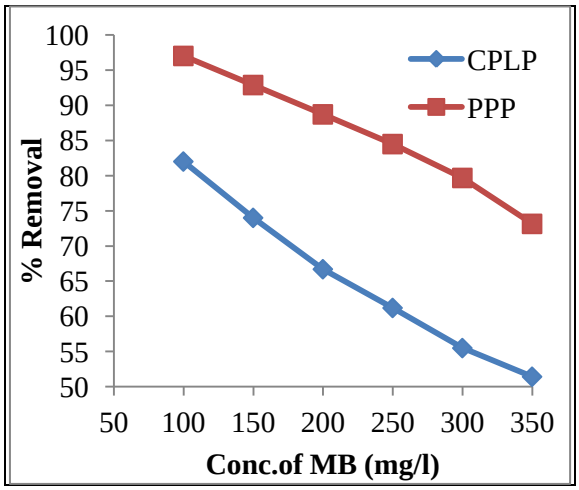

Figure 10. Effect of initial dye concentration on % removal of MB.

The Freundlich equation was employed for the adsorption of MB onto the adsorbent. The isotherm was represented by:

$$\log q_e = \log K_f + 1/n \log C_e \quad (9)$$

Where q_e is amount of MB adsorbed at equilibrium (mg/g), C_e is the equilibrium concentration of MB in solution (mg/L), K_f and n are constant incorporating factors affecting the adsorption capacity and intensity of adsorption respectively. The plots of log q_e against log C_e showed good linearity (R^2 = 0.995 to 0.996) indicating the adsorption of MB obeys the Freundlich adsorption isotherm, Figure 11. The values of K_f and n given in the Table 3. Values of n between 2 to 4 indicates an effective adsorption [20] while higher values of K_f represents an easy uptake of adsorbate from the solution [19].

The Langmuir isotherm was represented by the following equation:

$$C_e / q_e = 1/ (q_m b) + C_e /q_m \quad (10)$$

Where q_m is monolayer (maximum) adsorption capacity (mg/g) and b is Langmuir constant related to energy of adsorption (1/mg). A linear plots of C_e / q_e against C_e suggest the applicability of the Langmuir isotherms Figure 12 (R^2= 0.993 to 0.994). The values of q_m and b were determined slope and intercept of the plot, Table 3. The essential features of the Langmuir isotherm can be expressed in terms of dimensionless constant separation factor, R_L, which is defined by the following relation given by Hall:

$$R_L = 1/ (1+bC_o) \quad (11)$$

Where C_o is initial MB concentration (mg/l). The nature of adsorption if, R_L > 1 Unfavourable, R_L = 1 Linear R_L = 0 Irreversible 0 < R_L < 1 Favourable. In the present study, R_L values lies between 0 to 1 indicates favourable adsorption.

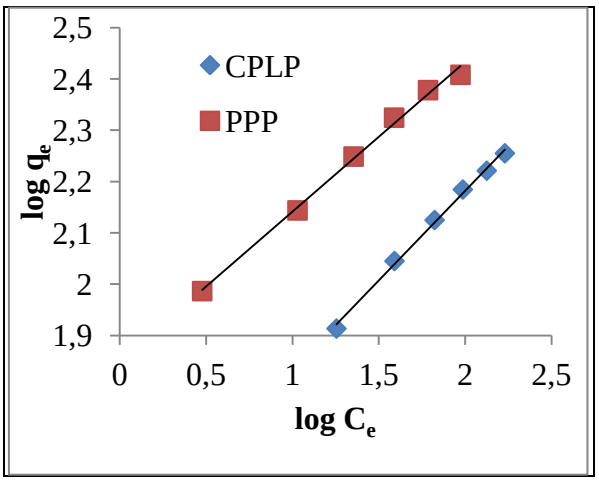

Figure 11. Freundlich isotherm plot of effect of initial dye concentration on adsorption of MB.

The Temkin isotherm is given as:

$$q_e = B \ln A + b \ln C_e \quad (12)$$

Where A (1/g) is the equilibrium binding constant, corresponding to the maximum

binding energy and constant B is related to heat of adsorption. A linear plot of q_e against ln C_e, Figure 13, enables the determination of the constants B and A from the slope and intercept. The results of the plots are given in Table 3.

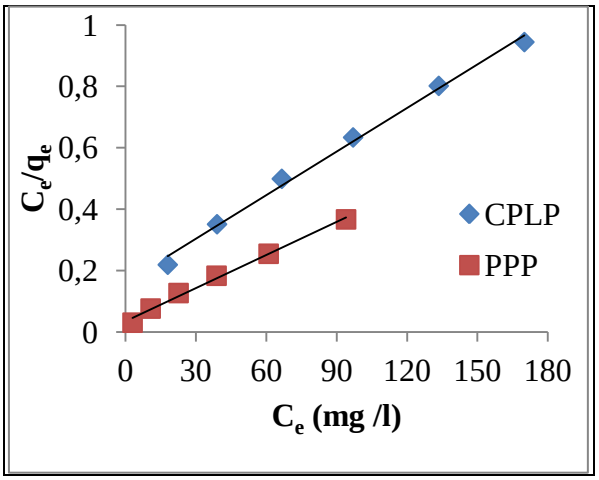

Figure 12. Langmuir isotherm plot of effect of initial dye concentration on adsorption of MB.

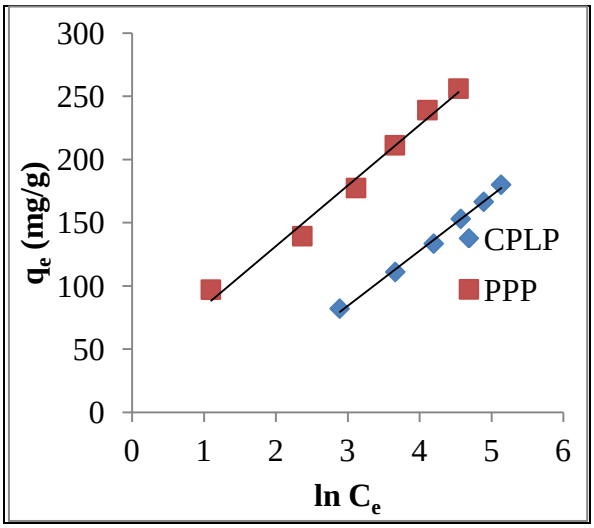

Figure 13. Temkin isotherm plot of effect of initial dye concentration on adsorption of MB.

Table 3: Effect of initial dye concentration on adsorption of MB

Adsorbent	Freundlich isotherm parameters			Langmuir isotherm parameters			Temkin isotherm parameters		
	K_f	n	R^2	q_m	b	R^2	A	B	R^2
CPLP	30.339	2.8653	0.996	250	0.0244	0.994	0.3668	43.63	0.995
PPP	70.795	3.4364	0.995	333.33	0.0857	0.993	2.1053	47.92	0.984

Effect of adsorbent dosage and initial dye concentration

The adsorption of MB on CPLP and PPP was studied by varying the adsorbent dosage. The percentage removal of MB increased but amount of dye adsorbed per unit mass of adsorbent decreased with increase in adsorbent dose from 1 to 6 g/L, Figures 14 and 15. This is due to the increase in availability of surface active sites resulting from the increased dose and conglomeration of the adsorbent [18]. For above 95% removals of MB, adsorbent dosage of 6 and 6 g/L for CPLP and 3 and 4 g/L for PPP were needed from initial MB concentrations 400 and 500 mg/L, respectively.

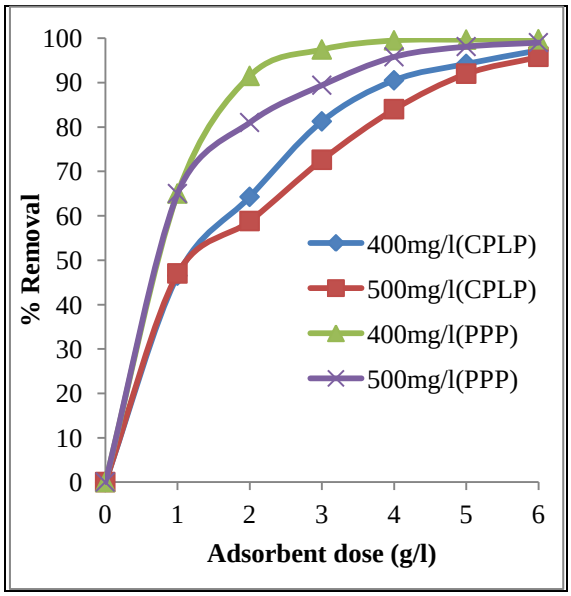

Figure 14. Effect of adsorbent dosage and initial dye concentration on % Removal of MB.

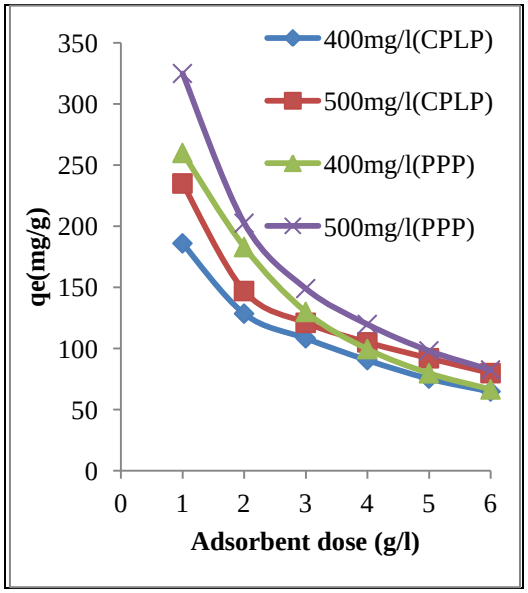

Figure 15. Effect of adsorbent dosage and initial dye concentration on amount adsorbed of MB in mg/g of adsorbent.

Effect of pH

pH is an important factor in controlling the adsorption of dye onto adsorbent. The adsorption of MB from 200mg/L concentration on CPLP and PPP was studied by varying the pH from 3 to 11. The amount of dye adsorbed per unit mass of adsorbent at equilibrium (q_e) increased from 42 to 150 mg/g for CPLP and 40 to 188 mg/g for PPP by variation in pH from 3 to 11, Figure 16.

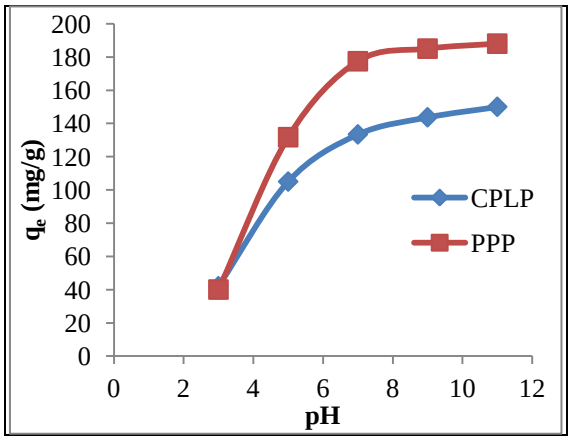

Figure 16. Effect of pH on adsorption of MB.

In acidic medium,

S-OH + $H^+ \rightarrow$ *S*-OH_2^+ (protonation) [+ Dye^+ (repulsion)]

S-C= O + $H^+ \rightarrow$ *S*-C=OH^+ (protonation) [+Dye^+ (repulsion)]

S-HN- + $H^+ \rightarrow$ *S* -H_2N^+- (protonation) [+Dye^+ (repulsion)]

In acidic medium , H^+ ions compete with the cationic dye molecules and preferably get combine with active functional group sites like –OH, C=O, -HN- of surface (*S*) of sorbent particles thus reduction in adsorption of cationic MB dye due to repulsive forces.

In basic medium,

S- OH + $OH^- \rightarrow H_2O$ + *S*-O^- (anion formation) [+ Dye^+ (attraction)]

S -COOH + $OH^- \rightarrow H_2O$ + *S*-COO^- (anion formation) [+Dye^+ (attraction)]

In basic medium, $-OH^-$ ions neutralize the functional groups of sorbents like –OH and –COOH and formation of anionic active sites on sorbents increased the adsorption of cationic dye due to increase in attractive forces. Also the –OH, C=O, -HN- of the surface of sorbent set free due to deprotonation by base and are then available for adsorption

Effect of particle size and initial dye concentration

Adsorption of MB on three sized particles ≥ 120, 120 ≤ 85 and 85 ≤ 60 mesh of adsorbents were studied for 100 to 350 mg/L concentrations of MB. The results of variation of these particle sizes on dye adsorption are shown in Figure 17. It can be

observed that as the particle size increases the adsorption of dye decreases and hence the percentage removal of dye also decreases. This is due to the decrease in available surface area. For larger particles, the diffusion resistance to mass transfer is high and most of the internal surface of the particle may not be utilized for adsorption and so the amount of dye adsorbed is small.

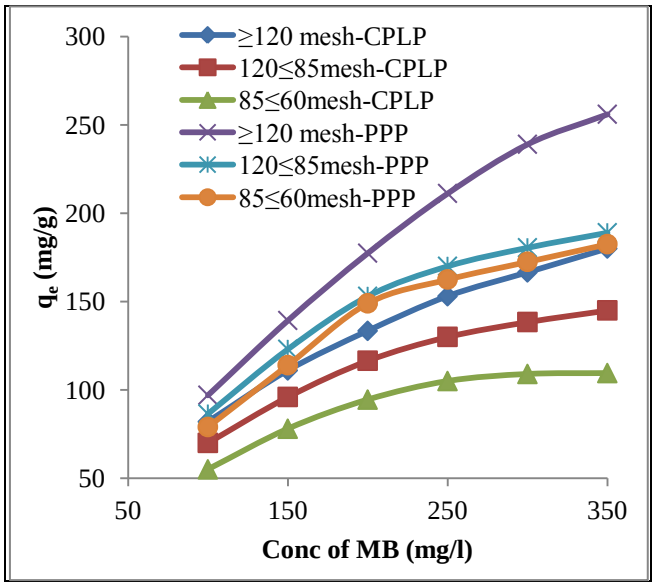

Figure 17. Effect of particle size and initial dye concentration on adsorption of MB.

Effect of temperature and initial dye concentration

Temperature has important effects on adsorption process. Thermodynamic parameters like heat of adsorption and energy of activation play an important role in predicting the adsorption behavior and both are strongly dependent on temperature. Adsorptions of MB at three different temperatures (303, 313 and 323 K) onto adsorbents were studied for 100 to 350 mg/L initial MB concentrations Figure 18. It is observed that as the experimental temperature increases from 303 to 323 K, the dye adsorption also increases. As the temperature increases, rate of diffusion of adsorbate molecules across external boundary layer and internal pores of adsorbent particle increases [22].

Changing the temperature will change the equilibrium capacity of the adsorbent for particular adsorbate [21, 22]. This is probably due to the fact that at higher temperature, an increase in free volume occurred and leading to an increment in the mobility of the solute. Alternatively, the enlargement of the pore sizes of the adsorbent particle at elevated temperatures can also be beneficial towards the dye sorption. Adsorption increased with temperature is probably due to the increase of intra particle diffusion rate of the sorbate into the interior sites of the sorbent since diffusion is an endothermic reaction.

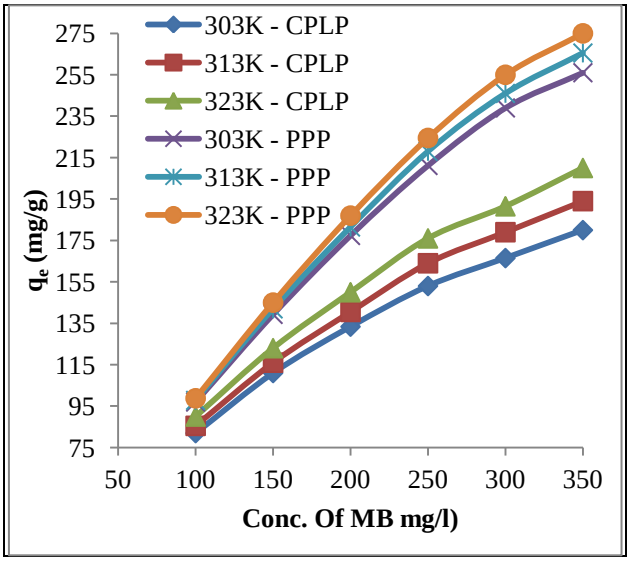

Figure 18. Effect of temperature and initial dye concentration on adsorption of MB.

Freundlich, Langmuir and Temkin adsorption isotherms were employed for 303, 313 and 323K temperatures. Plot of log q_e against log C_e, Figure 19 (R^2 = 0.995 to 0.998), plot of C_e/q_e against C_e, Figure 20 (R^2 = 0.989 to 0.995) and plot q_e against lnC_e Figure 21 (R^2 = 0.983 to 0.995) showed good linearity with regression coefficients. Freundlich constants K_f and n, Langmuir constants q_m and b, Temkin constants A and B are given in tables 4, 5, 6, respectively. Dimensionless constant separation factor (R_L) values lie between 0 to 1, Table 7. Monolayer (maximum) adsorption capacity (q_m) obtained from Langmuir plot were 250 and 333.333 mg/g remains same for all temperatures. Both Langmuir as well as Freundlich adsorption isotherms fits well for 313 to 323 K temperature range.

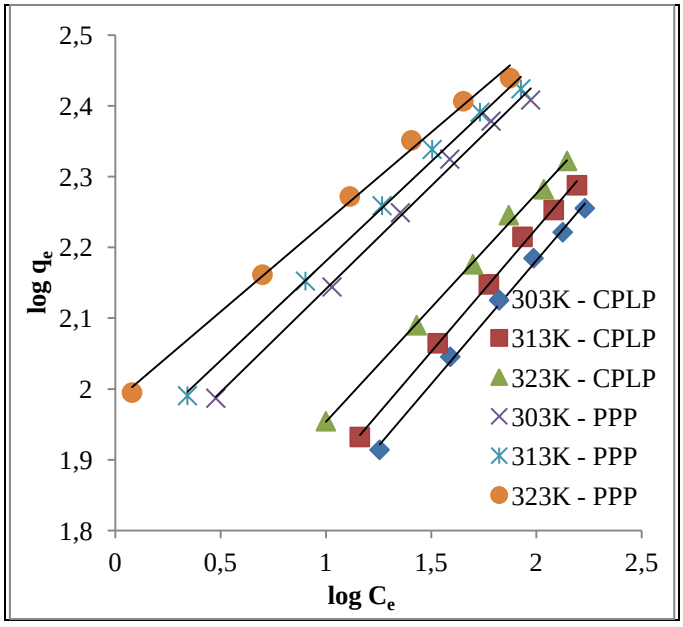

Figure 19. Freundlich isotherm plot of effect of temperature on adsorption of MB.

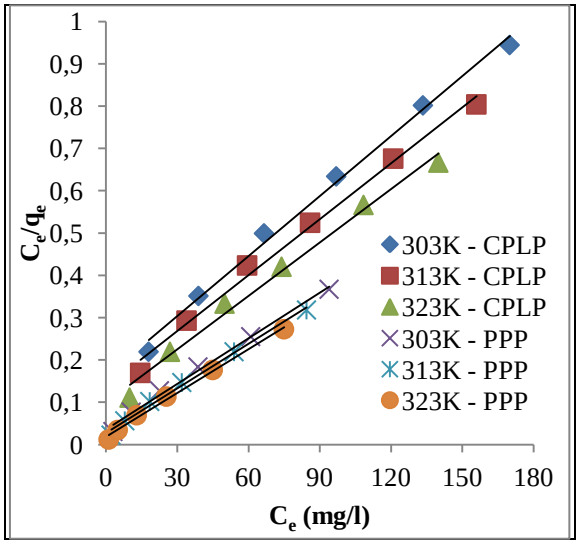

Figure 20. Langmuir isotherm plot of effect of temperature on adsorption of MB.

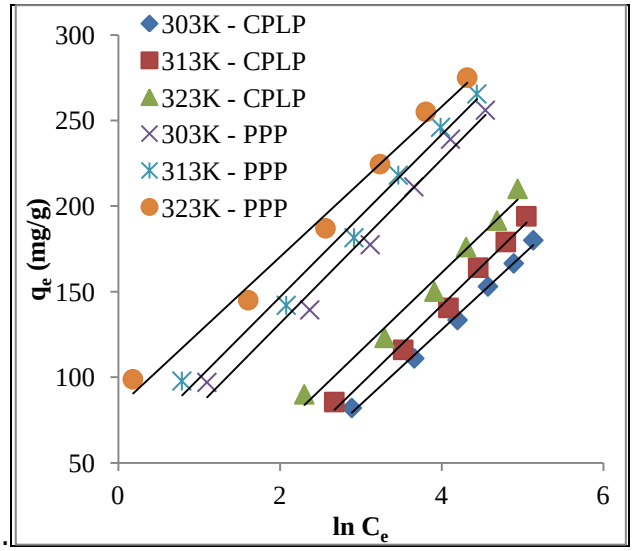

Figure 21. Temkin isotherm plot of effect of temperature on adsorption of MB.

Table 4: Effect of temperature and initial dye concentration on adsorption of MB

Temp. (Kelvin)	Freundlich isotherm parameters					
	CPLP			PPP		
	K_f	n	R^2	K_f	n	R^2
303	30.3389	2.86533	0.996	70.7946	3.43643	0.995
313	33.8844	2.88184	0.998	79.2501	3.55872	0.995
323	42.7563	3.10559	0.998	95.9401	3.95257	0.995

Table 5: Effect of temperature and initial dye concentration on adsorption of MB

Temp. in Kelvin	Langmuir isotherm parameters					
	CPLP			PPP		
	q_m	b	R^2	q_m	b	R^2
303	250	0.02469	0.994	333.333	0.08571	0.993
313	250	0.02963	0.992	333.333	0.11111	0.994
323	250	0.0404	0.989	333.333	0.16667	0.995

Table 6: Effect of temperature and initial dye concentration on adsorption of MB

Temp. in Kelvin	Temkin isotherm parameters					
	CPLP			PPP		
	A	B	R^2	A	B	R^2
303	0.34233	43.63	0.995	2.10598	47.92	0.984
313	0.39942	46.07	0.99	2.99639	47.43	0.987
323	0.63151	45.47	0.983	6.5663	43.88	0.989

Table 7: Dimensionless separation factor (R_L) calculated from Langmuir constant (b)

Initial MB Conc. (mg/L)	CPLP			PPP		
	303K	313K	323K	303K	313K	323K
100	0.28826	0.25234	0.1984	0.10448	0.08257	0.0566
150	0.2126	0.18367	0.14163	0.07216	0.0566	0.03846
200	0.1684	0.14439	0.11012	0.05512	0.04306	0.02913
250	0.13941	0.11894	0.09008	0.04459	0.03475	0.02344
300	0.11894	0.10112	0.07621	0.03743	0.02913	0.01961
350	0.10371	0.08795	0.06604	0.03226	0.02507	0.01685

Thermodynamic analysis

Thermodynamic parameters such as change in free energy (ΔG) (J/mole), enthalpy (ΔH) (J/mole) and entropy (ΔS) (J/K/mole) were determined using following equations:

$$K_o = C_{solid} / C_{liquid} \qquad (14)$$

$$\Delta G = -RT\ln K_o \qquad (15)$$

$$\Delta G = \Delta H - T\Delta S$$

$$\ln K_o = -\Delta G/RT$$

$$\ln K_o = \Delta S/R - \Delta H/RT \qquad (16)$$

Where K_o is equilibrium constant, C_{solid} is solid phase concentration at equilibrium (mg/L), C_{solid} is liquid phase concentration at equilibrium (mg/L), T is absolute temperature in Kelvin and R is gas constant. ΔG values obtained from equation (15), ΔH and ΔS values obtained from the slope and intercept of plot ln K_o against 1/T, Figure 22 presented in Table 8. The negative value of ΔG indicates the adsorption is favourable and spontaneous. ΔG values increases with increase in temperature. The low positive values of ΔH indicate endothermic nature of adsorption [12, 14]. The positive values of ΔS indicate the increased disorder and randomness at the solid solution interface of MB with the adsorbent. The adsorbed water molecules, which were displaced by adsorbate molecules, gain more translational energy than is lost by the adsorbate molecules, thus allowing prevalence of randomness in the system. The increase of adsorption capacity of

the adsorbent at higher temperatures was due to enlargement of pore size and activation of adsorbent surface [12-16].

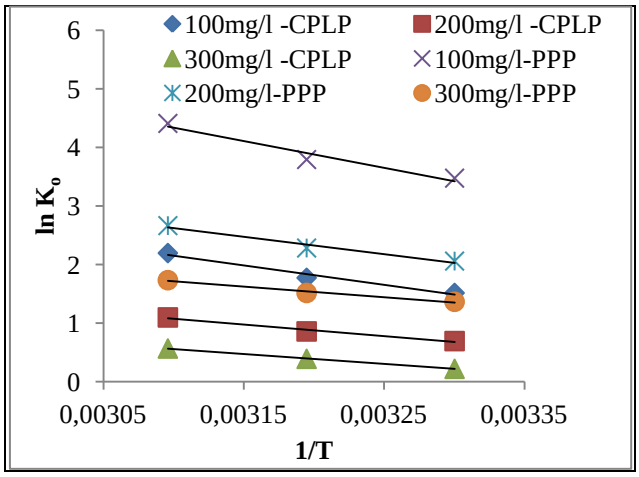

Figure 22. Von't Hoff plot of effect of temperature on adsorption of MB.

Table 8: Equilibrium constants and thermodynamic parameters for the adsorption of MB

Adsorbent	Initial MB Conc. (mg/L)	Ko			ΔG (kJ/mole)			ΔH (kJ/mole)	ΔS (J/K/mole)
		303K	313K	323K	303K	313K	323K		
CPLP	100	4.556	5.897	9	-3.820	-4.617	-5.900	27.619	103.51
CPLP	200	2.003	2.361	3	-1.750	-2.236	-2.950	16.395	59.769
CPLP	300	1.247	1.479	1.765	-0.556	-1.019	-1.526	14.117	48.412
PPP	100	32.33	44.46	82.333	-8.757	-9.874	-11.845	37.879	156.72
PPP	200	7.85	9.811	14.385	-5.191	-5.942	-7.160	24.560	97.939
PPP	300	3.918	4.556	5.667	-3.440	-3.946	-4.658	14.974	60.676

Effect of agitation speed

The sorption is influenced by mass transfer parameters. The sorption kinetics of MB by CPLP and PPP for different agitation speeds ranging from 100 to 230 rpm was studied. The amount adsorbed at equilibrium was found to increase from 68 to 83.4 mg/g for CPLP and 85 to 97.4 mg/g for PPP with increased in agitation speed from 100 to 230 rpm of an oscillator from 100 mg/L initial MB solution Figure 23. This is because with low agitation speed the greater contact time is required to attend the equilibrium. With increasing the agitation speed, the rate of diffusion of dye molecules from bulk liquid to the liquid boundary layer surrounding the particle become higher because of an enhancement of turbulence and a decrease of thickness of the liquid boundary layer. Uptake of MB increased with increasing agitation rate. Increasing agitation rate

decreases the film resistance to mass transfer surrounding the sorbent particles thus increasing sorption of dye molecules.

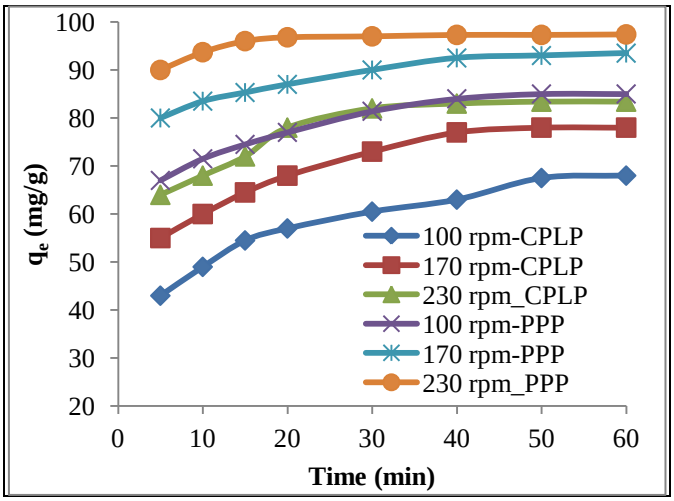

Figure 23. Effect of agitation speed on adsorption of MB.

Desorption studies

Figure 24 represents desorption of MB from dye loaded adsorbents at initial pH 3, 7 and 11. For the desorption studies, dye loaded adsorbents from 100 mg/L initial dye concentration are used. Desorption of MB was found to be maximum at pH 3 (32.44% for PPP and 44.96% for CPLP) and minimum at pH 11 (5.13% for PPP and 3% for CPLP). Percentage desorption of MB decreased with increase in pH i.e. reverse of adsorption. As percentage desorption was found to be less than 50%, adsorption process appears to be controlled by chemisorption.

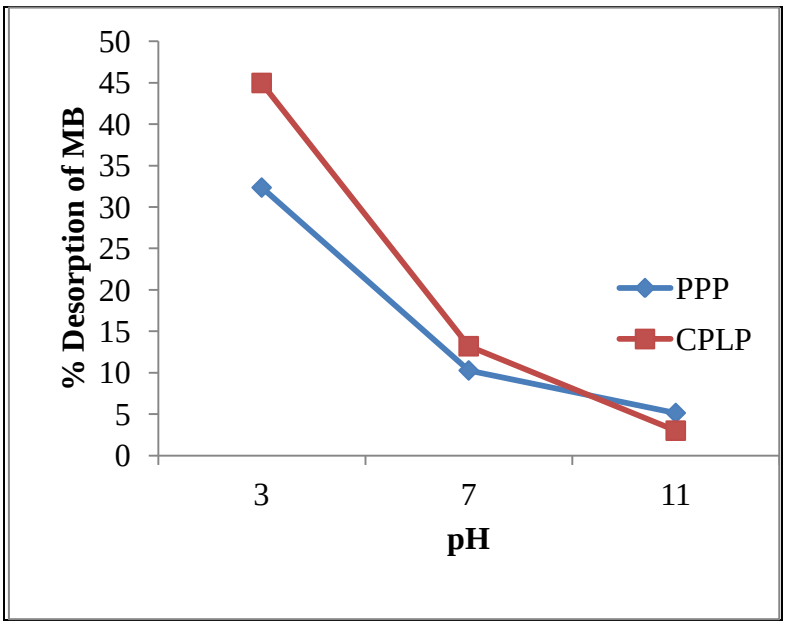

Figure 24. Effect of pH on desorption of MB.

Conclusion

In this work, two biosorbents, cinnamon plant (*Cinnamonum zeylanicum*) leaf powder (CPLP) and pineapple (*Ananas comosus*) peel powder (PPP) have been used for the removal of MB from aqueous solutions. The amount of MB adsorbed at equilibrium increased from 82 to 180 and 97 to 256 mg/g for CPLP and PPP respectively with increased in initial MB concentration from 100 to 350 mg/L.

The best fitting isotherm models were found to be of the order of Freundlich > Langmuir > Temkin. Freundlich constant n = 2.86533 to 3.4364 and R_L = 0.01685 to 0.28826 obtained from Langmuir isotherm confirmed that the adsorption of MB on both adsorbents was favourable. The monolayer (maximum) adsorption capacities (q_m) were 250 and 333.333 mg/g for CPLP and PPP, respectively. Lagergen pseudo-second order model best fits the kinetics of adsorption ($R^2 \geq 0.99$). The values amount of MB adsorbed per unit mass of CPLP as well as of PPP obtained by Lagergen pseudo-second order model, $q_{e(the)}$ were in consistent with the experimental $q_{e(exp)}$.

Intra particle diffusion plot showed boundary layer effect and larger intercepts indicates greater contribution of surface sorption in rate determining step. Adsorption was found to increase on increasing pH, temperature, agitation speed and decreasing particle size.

Percentage desorption of MB decreased with increase in pH. As percentage desorption was found to be less, adsorption process appears to be controlled by chemisorptions.

Thermodynamic analysis showed that adsorption of MB on CPLP and PPP was:

a) Favourable and spontaneous (negative values of ΔG)

b) Endothermic (positive values of ΔH)

c) Physisorption (small ΔH values < 40 kJ/mole))

d) Increased disorder and randomness at the solid- solution interface (positive values of ΔS)

e) The overall rate constant K_{ad} for adsorption of MB increased with increase in temperature suggesting adsorption was endothermic in nature. At all temperatures, the forward rate constant were much higher than the reverse rate constant suggesting that the rate of adsorption was dominant for CPLP and PPP.

These findings indicate that PPP and CPLP could be employed as effective and inexpensive adsorbents for the removal of basic dyes especially MB. PPP was found to be

better adsorbent than CPLP.

References and Notes

[1] McKay, G. *AIChE J*. **1985**, *31*, 335. [CrossRef]
[2] McKay, G.; Al-Duri, B. *Chem. Eng. Sci*. **1988**, *43*, 1133. [CrossRef]
[3] McKay, G.; Al-Duri, B. *J. Chem. Tech. Biotechnol*. **1990**, *48*, 269. [CrossRef]
[4] McKay, G.; Al-Duri, B. *Ind. Eng. Chem. Res*. **1991**, *30*, 385. [CrossRef]
[5] Juang, R.S.; Swei, S. L. *Sep. Sci. Technol*. **1996**, *31*, 2143. [CrossRef]
[6] Alexander, F.; Poots, V. J .P.; Mckay, G. *Ind. Eng. Chem. Process Res. Dev*. **1978**, *17*, 406. [CrossRef]
[7] McKay, G.; Prasad, G. R.; Mowli, P. R. *Water Air Soil Pollut*. **1986**, *29*, 273. [CrossRef]
[8] McKay, G.; Geundi, M. E.; Nassar, M. M. *Water Res.* **1988**, *22*, 1527. [CrossRef]
[9] Gupta, G. S.; Prasad, G.; Singh, V. N. *Water Res*. *1990*, *24*, 45.
[10] Nassar, M. M.; El-Geundi, M. S. *J. Chem. Tech. Biotechnol*. **1991**, *50*, 257.
[11] Wu, F. C.; Hsu, Y. C.; Tseng, R. L. *J. Chin. Inst. Environ. Eng*. **1994**, *4*, 207.
[12] El-Geundi, M. S. *Adsorp. Sci. Technol*. **1996**, *13*, 295.
[13] McKay, G.; El-Geundi, M. S.; Nassar, M. M. *Proc. Safety and Environ. Prot.:Trans. of the Inst. of Chem. Eng., Part B Proc. Safety Environ. Prot*. **1996**, *74*, 277. [CrossRef]
[14] Hsu, Y. C.; Chiang, C. C.; Yu, M. F. *Sep. Sci. Technol*. **1997**, *32*, 2513. [CrossRef]
[15] Gupta, V. K.; Mohan, D.; Sharma, S.; Sharma, M. *Sep. Sci. Technol*. **2000**, *35*, 2097. [CrossRef]
[16] Walker, G. W.; Weatherley, L. R. *Chem. Eng. J.* **2001**, *83*, 201. [CrossRef]
[17] Namasivayam, C.; Kavitha, D. *Dyes and Pigments* **2002**, *54*, 47. [CrossRef]
[18] Kannan, N.; Sundaram, M.M. *Dyes and pigments* **2001**, *51*, 25. [CrossRef]
[19] Mahvi, A. H.; Maleki, A.; Eslami, A. *Am. J. Appl. Sci.* **2004**, *1*, 321. [CrossRef]
[20] Potgeiter, J.; Potgeiter–Vermaak, S.; Kalibatonga, P. *Minerals Engineering* **2006**, *19*, 463. [CrossRef]
[21] Singh, A. K.; Singh, D. P.; Pandey, K. K.; Singh, V. N. *J. Chem. Technol*. **1988**, *42*, 39. [CrossRef]
[22] Lin, S. H. *J. Chem. Tech. Biotechnol*. **1993**, *58*, 159. [CrossRef]
[23] Weber, W. J.; Morris, J. C. *J. Sanitary Eng. Div. ASCE* **1963**, *89*, 31.
[24] Hall, K. R.; Eagleton, L. C.; Acrivos, A.; Vermeulen, T. *Ind. Eng. Chem. Fund*. **1966**, *5*, 212.
[25] Weber, W. J. Principle and Application of Water Chemistry, edited by Faust S.D. and Hunter J. V. Wiley: New York, 1967.
[26] Aslam, M. M.; Baig, M. A.; Hassan, I.; Qazi, I. A.; Malik, M.; Saeed, H. *Electronic J. Environ. Agric. Food Chem.* **2004**, 3, 804.
[27] Grau, P. *Water Sci. Technol.* **1991**, *24*, 97.
[28] Crittenden, I. C. *Water Res.* **1997**, *31*, 411. [CrossRef]
[29] Wong, Y.; Yu, J. *Water Res.* **1999**, *33*, 3512. [CrossRef]

ISSN 1984-6428
ONLINE
www.orbital.ufms.br

| Vol 4 | | No. 2 | | April-June 2012 |

Full Paper

Synthesis and antimicrobial evaluation of carbonyl isothiocyanate derivatives spiro [indoline-3,2'-[1,3,5]oxadiazin]-2-one

*Visha P. Modi and Hasmukh S. Patel**

Department of Chemistry, Sardar Patel University, Vallabh Vidyanagar-388120. Gujarat, India.

Received: 06 February 2012; revised: 26 February 2012; accepted: 25 March 2012. Available online: 07 July 2012.

ABSTRACT: *The synthesis of 6'-phenyl-3'-(thiazol-2-yl)-4'-thioxo-3',4'-dihydrospiro[Indoline-3,2'-[1,3,5]oxadiazin]-2-one* ***5a-h*** *is carried out through a three step pathway starting from acid catalyzed condensation of 2-amino thiazole* ***1*** *with indoline-2,3-dione* ***2*** *which is also called isatin yielding 3-(thiazol-2-ylimino)indolin-2-one* ***3*** *which on reaction with 4-(substituted)-cyclohexa-1,5-diene carbonyl isothiocyanate* ***4a-h*** *in the presence of anhydrous $ZnCl_2$ gives targeted compounds. All synthesized compounds have been characterized by ^{1}H-NMR, ^{13}C-NMR, IR and elemental analysis. Final compounds have been screened for antimicrobial activity.*

Keywords: aminothiazoles; benzoyl isothiocyanate; isatin; spectral study; antimicrobial screening

Introduction

The thiazole ring system is a useful structural moiety found in numerous biologically active molecules. This structure has found applications in drug development for the treatment of allergies [1], hypertension [2], inflammation [3], schizophrenia [4-5], bacterial [6] and HIV [7] infections. Aminothiazoles are known to be ligands of estrogen receptors [8] as well as a novel class of adenosine receptors antagonists [9].

In view of the importance of 2-aminothiazole and its derivatives, several methods were reported in the literature. Thiazoles containing N=C-S moiety has been employed as antipsychotic [10] and antimalarial [11]. 2-Aminothiazole derivatives are well explored as useful clinical agents and some of the derivatives of thiazoles have shown inhibition

* Corresponding author. E-mail: drhspatel786@yahoo.com or visha149@yahoo.in

towards herpes simplex virus [12]. Number of thiazole derivatives has a wide variety of biological activity [13-14]. Thiazole derivatives, particularly aminothiazoles, play vital role in pharmaceutical practice owing to their wide biological activities like fungicidal, antimicrobial, anti TB, anticancer, anti-inflammatory. The substituted thiazoles compounds have number of characteristic pharmacological features such as:

- Relative stability and ease of starting materials.
- Built in biocidal unit.
- Enhanced lipid solubility with hydrophilicity.
- Easy metabolism of compounds.

Isatin derivatives have recently received considerable attention owing to their wide applications as anti-HIV, antitubercular [15], antiplasmodical [16], anticonvulsant [17], sedative and hypnotic [18] agents. Thiazole and another class of azole group is a versatile pharmacophore, possessing diverse pharmacological properties [19-20]. Such as herbicidal [21], antitumor [22], antipsychotic [10], anticoagulant [23], antimicrobial [24-26] and antagonist [27] prompted by the aforesaid biological and pharmacological activities.

In sequel to our reported work [28] we undertake the synthesis of some new combinational molecules incorporating above moieties with a hope of augmentation in biological activities. The synthetic route of these compounds is presented in Scheme 1, as shown below.

Scheme 1

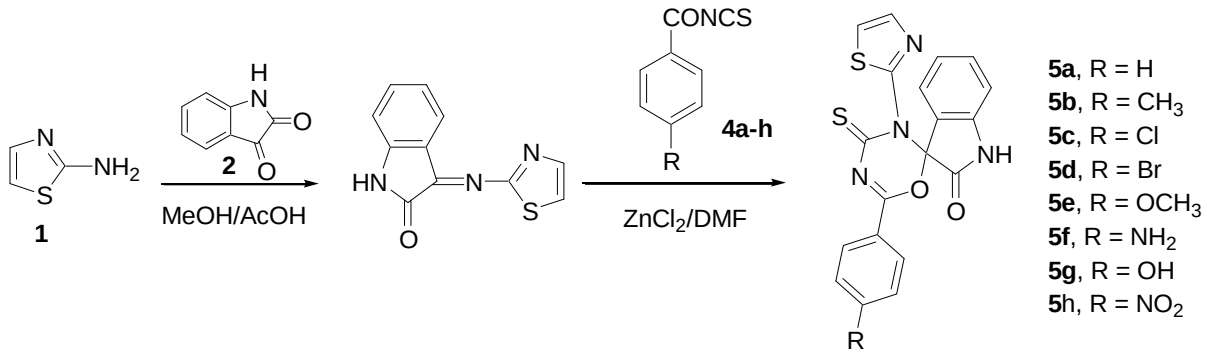

Material and Methods

General

All the chemicals used throughout were of laboratory grade. The 2-aminothiazole and isatin were procured from local market. Melting points were taken in open capillary method and were uncorrected. Purity of the compounds was checked on silica gel TLC plates of 2 mm thickness using chloroform and pet-ether as solvent system. Elemental

analysis (%C, H, N) was carried out by Perkin Elmer 2400 CHN elemental analyzer at Sophisticated Instrumentation Centre for Applied Research & Training (SICART), Vallabh Vidyanagar. IR spectra were recorded in KBr pellets on Nicolet 760D spectrophotometer. ^{1}H NMR and ^{13}C-NMR spectra were recorded on a Bruker Avance DPX 400 Spectrometer in $CDCl_3$.

General Procedure

*Synthesis of 3-(thiazol-2-ylimino) indolin-2-one (**3**):* An equimolar mixture of 2-aminothiazole and isatin were refluxed in methanol (40 mL) in presence of catalytic amount of glacial acetic acid for 3 h and allowed for cooling. Schiff bases thus obtained was filtrated from methanol and recrystallized from methanol to give compound **3**. $C_{11}H_7N_3OS$. Mol.wt.: 229.26, Yield: 71%, M.P.: 182-183 °C. IR (KBr cm^{-1}): 1567 cm^{-1} (C=N of Schiff bases), 1690 cm^{-1} (C=O of isatin), 1535 cm^{-1} (C=N of thiazole), 684 (C-S-C of thiazole). ^{1}H-NMR ($CDCl_3$) δ: 8.68 (s, 1H, NH of isatin), 7.13-7.76 (4H, m, PhH of isatin), 7.62-7.85 (H of thiazole ring). ^{13}C-NMR δ: 170.1(C_2 of thiazole), 140.9 (C_4 of thiazole), 117.1 (C_5 of thiazole) , 162.9 (C=N of isatin), 149.4 (C_2) (NH-C=O of isatin), C-Ph of isatin: 129.1 (C_4), 124.8 (C_5), 130.7 (C_6), 119.9 (C_7), 141.3 (C_8), 117.2 (C_9). Anal. Calcd. (Found%): C, 57.63; H, 3.08; N, 18.33; S, 13.99.

*Synthesis of 6′-Phenyl-3′-(thiazol-2-yl)-4′-thioxo-3′, 4′-dihydrospiro [indoline-3, 2′-[1, 3, 5] oxadiazin]-2-one (**5a**):* A well stirred solution of **3** (0.01mole) in dry DMF containing pinch of anhydrous $ZnCl_2$ and benzoyl isothiocyanate (0.02mole) was refluxed for 12 h. Excess of solvent was distilled off under reduced pressure and the residual reaction mixture was cooled and poured into ice-cold water. The separated solid was filtered washed and recrystallized from ethanol to yield **5a.** $C_{19}H_{12}N_4O_2S_2$; Mol.wt.: 392.45; Yield: 68%; M.P.: 218-223 °C, IR (KBr) cm^{-1}: 1672 cm^{-1}(C=O of isatin), 1543 cm^{-1} (C=N of thiazole), 680 (C-S-C of thiazole), 1143cm^{-1} (C=S). ^{1}H-NMR ($CDCl_3$) δ: 7.54-7.90(5H, m, PhH of phenyl ring), 8.62 (s, 1H, NH of isatin), 6.78-7.29 (H of thiazole ring), 7.08-7.36 (4H, m, PhH of isatin). ^{13}C-NMR ($CDCl_3$) δ: 159.1 (C_2 of thiazole), 136.8 (C_4 of thiazole), 111.9 (C_5 of thiazole), 168.1 (C_2) (NH-C=O of isatin), 121.3 (C_3) (C of spiro), C-Ph of isatin: 128.4 (C_4), 136.6 (C_5), 127.9 (C_6), 115.7 (C_7), 141.2 (C_8), 132.4 (C_9), 178.5 (C=S), 156.4 (C=N), C-Ar: 135.1 (C_1), 125.6 (2C), 128.3 (2C), 130.8 (C_4). Anal.Calc. (Found): C=58.15 (58.10), H=3.08 (3.10), N=14.28 (14.30), S=16.34 (16.35).

Similarly, **5b-h** were also synthesized by similar method using with minor modifications in reflux time. Their spectral data are given below:

*3′-(thiazol-2-yl)-4′-thioxo-6′-p-totyl-3′, 4′-dihydrospiro [indoline-3, 2′-[1, 3, 5] oxadiazin]-2-one **(5b)**:* $C_{20}H_{14}N_4O_2S_2$; Mol. wt.: 406.48, Yield:72%, M.P.: 283-285 °C,

IR (KBr) cm^{-1}: 1663 cm^{-1} (C=O of isatin), 1552 cm^{-1} (C=N of thiazole), 688 (C-S-C of thiazole), 1140cm^{-1} (C=S). ^{1}H-NMR ($CDCl_3$) δ: 7.26-8.05 (4H, m, PhH of phenyl ring), 2.30 (3H, s, C-CH_3), 8.57 (s, 1H, NH of isatin), 6.72-7.32 (H of thiazole ring), 7.13-7.33 (4H, m, PhH of isatin). ^{13}C-NMR ($CDCl_3$) δ: 158.9 (C_2 of thiazole), 137.1 (C_4 of thiazole), 112.4 (C_5 of thiazole), 168.4 (C_2) (NH-C=O of isatin), 121.2 (C_3) (C of Spiro), C-Ph of isatin: 128.5 (C_4), 136.8 (C_5), 127.7 (C_6), 115.3 (C_7), 141.4 (C_8), 132.7 (C_9), 178.3 (C=S), 156.5 (C=N), C-Ar: 132.3 (C_1), 128.8 (2C), 140.3 (C_4), 21.7 (C-CH_3). Anal. Calc. (Found%): C=59.10 (59.12); H=3.47 (3.44); N=13.78 (13.73); S=15.78 (15.76).

6′-(4-Chlorophenyl)-3′-(thiazol-2-yl)-4′-thioxo-3′,4′-dihydrospiro[indoline-3,2′-[1,3,5]-oxadiazin]-2-one ***(5c)****:* $C_{19}H_{11}ClN_4O_2S_2$; Mol. wt.: 426.00; Yield: 69%, M.P.: 263-265 °C, IR (KBr) cm^{-1}: 1688 cm^{-1} (C=O of isatin), 1558cm^{-1} (C=N of thiazole), 692 (C-S-C of thiazole), 1158cm^{-1} (C=S), 732cm^{-1} of (C-Cl). ^{1}H-NMR ($CDCl_3$) δ: 7.57-7.77 (4H, m, PhH of phenyl ring), 8.60 (s, 1H, NH of isatin), 6.78-7.38 (H of thiazole ring), 7.16-7.31 (4H, m, PhH of isatin). ^{13}C-NMR ($CDCl_3$) δ: 158.6 (C_2 of thiazole), 137.3 (C_4 of thiazole), 112.2 (C_5 of thiazole), 168.5 (C_2) (NH-C=O of isatin), 121.7 (C_3) (C of spiro), C-Ph of isatin: 128.6 (C_4), 136.7 (C_5), 127.3 (C_6), 115.2 (C_7), 141.6 (C_8), 132.5 (C_9), 178.7 (C=S), 156.7 (C=N), C-Ar: 133.3 (C_1), 129.3 (2C), 128.6 (C_4), 136.5 (C_4). Anal. Calc. (found%): C=53.46 (53.46); H=2.60 (2.62); N=13.12 (13.15); S= 15.02 (15.08).

6′-(4-Bromophenyl)-3′-(thiazol-2-yl)-4′-thioxo-3′,4′-dihydrospiro[indoline-3,2′-[1,3,5]-oxadiazin]-2-one ***(5d)****:* $C_{19}H_{11}BrN_4O_2S_2$; Mol.wt.: 471.35; Yield: 72%, M.P.: 237-238 °C, IR (KBr) cm^{-1}: 1682 cm^{-1} (C=O of isatin), 1545cm^{-1} (C=N of thiazole), 702 cm^{-1} (C-S-C of thiazole), 1178cm^{-1} (C=S), 578 cm^{-1} of (C-Br). ^{1}H-NMR ($CDCl_3$) δ: 7.58-7.73 (4H, m, PhH of phenyl ring), 8.83 (s, 1H, NH of isatin), 6.69-7.15 (H of thiazole ring), 7.11-7.36 (4H, m, PhH of isatin). ^{13}C-NMR ($CDCl_3$) δ: 158.1 (C_2 of thiazole), 137.6 (C_4 of thiazole), 112.8 (C_5 of thiazole), 168.9 (C_2) (NH-C=O of isatin), 121.9 (C_3) (C of spiro), C-Ph of isatin: 128.2 (C_4), 136.8 (C_5), 127.5 (C_6), 115.7 (C_7), 141.1 (C_8), 132.8 (C_9), 178.2 (C=S), 156.9 (C=N), C-Ar: 134.7 (C_1), 131.2 (2C), 131.8 (2C), 125.7. Anal. Calc. (found): C=48.41 (48.44); H=2.35 (2.37); N=11.89 (11.83); S, 13.61 (13.63).

6′-(4-methoxyphenyl)-3′-(thiazol-2-yl)-4′-thioxo-3′,4′-dihydrospiro[indoline-3,2′-[1,3,5]-oxadiazin]-2-one ***(5e)****:* $C_{20}H_{14}N_4O_3S_2$; Mol.wt.: 422.48; Yield:73%; M.P.: 273-274 °C, IR (KBr) cm^{-1}: 1692 cm^{-1} (C=O of isatin), 1554cm^{-1} (C=N of thiazole), 710 cm^{-1} (C-S-C of thiazole), 1186cm^{-1} (C=S), 2838 $cm^{-1}$of (C-OCH_3). ^{1}H-NMR ($CDCl_3$) δ: 7.06-8.03 (4H, m, PhH of phenyl ring), 3.78 (3H, m, -OCH_3), 8.52 (s, 1H, NH of isatin), 6.71-7.13 (H of thiazole ring), 7.08-7.31 (4H, m, PhH of isatin). ^{13}C-NMR ($CDCl_3$) δ: 158.9 (C_2 of thiazole), 137.1 (C_4 of thiazole), 112.3 (C_5 of thiazole), 168.3 (C_2) (NH-C=O of isatin), 121.5 (C_3) (C of spiro), C-Ph of isatin: 128.5 (C_4), 136.4 (C_5), 127.9 (C_6), 115.8 (C_7), 141.7 (C_8), 132.3 (C_9), 178.1 (C=S), 156.3 (C=N), C-Ar: 127.7 (C_1), 130.4

(2C), 114.5 (2C), 162.3 (C_4), 55.3 (-OCH_3). Anal.Calc. (found%): C=56.86 (56.83); H=3.34 (3.32); N=13.26 (13.21); S=15.18 (15.20).

6′-(4-aminophenyl)-3′-(thiazol-2-yl)-4′-thioxo-3′,4′-dihydrospiro[indoline-3,2′-[1,3,5]-oxadiazin]-2-one ***(5f)****:* $C_{19}H_{13}N_5O_2S_2$; Mol. wt.: 407.47; Yield: 74%; M.P.:282-283°C, IR (KBr) cm^{-1}:1678cm^{-1} (C=O of isatin), 1562cm^{-1} (C=N of thiazole), 698cm^{-1}(C-S-C of thiazole), 1162cm^{-1}(C=S), 3255$cm^{-1}$of (C-NH_2). ^{1}H-NMR ($CDCl_3$) δ: 6.62-7.77(4H, m, Ph.H of Phenyl ring), 6.23(2H, m, -NH_2), 8.54(s,1H, NH of Isatin),6.76-7.25(H of thiazole ring), 7.15-7.30(4H, m, Ph.H of Isatin). ^{13}C-NMR ($CDCl_3$) δ: 158.8(C_2 of thiazole), 137.7(C_4 of thiazole), 112.5(C_5 of thiazole), 168.2(C_2) (NH-C=O of Isatin), 121.3(C_3) (C of Spiro), C-Ph. Of Isatin: 128.7(C_4), 136.2(C_5), 127.6(C_6), 116.0(C_7), 140.9(C_8), 132.9(C_9), 178.4(C=S), 157.1(C=N), C-Ar: 125.1(C_1), 126.6(2C), 114.6(2C), 150.6(C_4). Anal.Calc.(found): C=56.01(56.08); H=3.22(3.18); N=17.19(17.21); S=15.74(15.73).

6′-(4-Hydroxyphenyl)-3′-(thiazol-2-yl)-4′-thioxo-3′,4′-dihydrospiro[indoline-3,2′-[1,3,5]-oxadiazin]-2-one ***(5g)****:* $C_{19}H_{11}N_5O_3S_2$; Mol.wt.:408.45; Yield:72%, M.P.: 278-279 °C. IR (KBr): 1681 cm^{-1} (C=O of isatin), 1556 cm^{-1} (C=N of thiazole), 708 cm^{-1} (C-S-C of thiazole), 1148 cm^{-1} (C=S), 3443 cm^{-1} of (O-H strec. of hydroxyl). ^{1}H-NMR ($CDCl_3$) δ: 6.68-7.92 (4H, m, PhH of phenyl ring), 8.68 (s, 1H, NH of isatin), 6.78-7.28 (H of thiazole ring), 7.13-7.36 (4H, m, PhH of isatin) 11.9 (1H, s, OH of hydroxy phenyl). ^{13}C-NMR ($CDCl_3$) δ: 158.3 (C_2 of thiazole), 137.0 (C_4 of thiazole), 111.8 (C_5 of thiazole), 168.2 (C_2) (NH-C=O of isatin), 121.6 (C_3) (C of spiro), C-Ph of isatin: 128.7 (C_4), 136.2 (C_5), 127.7 (C_6), 115.2 (C_7), 141.5 (C_8), 132.9 (C_9), 178.3 (C=S), 156.3 (C=N), C-Ar: 128.4 (C_1), 130.8 (2C), 116.2 (2C), 160.5 (C_4). Anal. Calc. (found%): C=55.87 (55.89); H=2.96 (2.92); N=13.72 (13.68); S=15.75 (15.73).

6′-(4-Nitrophenyl)-3′-(thiazol-2-yl)-4′-thioxo-3′,4′-dihydrospiro[indoline-3,2′-[1,3,5]-oxadiazin]-2-one ***(5h)****:* $C_{19}H_{11}N_5O_4S_2$; Mol. wt.: 437.45; Yield: 68%; M.P.: 253-254°C, IR (KBr): 1693 cm^{-1} (C=O of isatin), 1567 cm^{-1} (C=N of thiazole), 696 cm^{-1} (C-S-C of thiazole), 1168 cm^{-1} (C=S), 1550-1570 $cm^{-1}$of (N=O of NO_2). ^{1}H-NMR ($CDCl_3$) δ: 8.09-8.36 (4H, m, PhH of phenyl ring), 8.88 (s, 1H, NH of isatin), 6.75-7.20 (H of thiazole ring), 7.10-7.38 (4H, m, PhH of isatin). ^{13}C-NMR ($CDCl_3$) δ: 159.0 (C_2 of thiazole), 136.9 (C_4 of thiazole), 112.4 (C_5 of thiazole), 168.1 (C_2) (NH-C=O of isatin), 121.5 (C_3) (C of spiro), C-Ph of isatin: 128.5 (C_4), 136.6 (C_5), 127.2 (C_6), 115.9 (C_7), 141.3 (C_8), 132.3 (C_9), 178.8 (C=S), 156.5 (C=N), C-Ar: 141.9 (C_1), 127.4 (2C), 124.1 (2C), 150.3 (C_4). Anal. Calc. (found%): C=52.17 (52.13); H=2.53 (2.56); N=16.01 (16.07); S=14.66 (14.63).

Antimicrobial screening

Antimicrobial activity i.e. antibacterial and antifungal was screened by agar cup plate method [31] in nutrient agar and dextrose agar medium. Agar medium was sterilized by autoclaving at 15 Psi and 120 °C for 20 min. The medium was poured in Petri dishes and left to solidify. These Petri dishes were inoculated with 0.2 mL suspension of organism by spread plate method [32].

Antibacterial activities

Antibacterial activities of all the compounds were studied against gram positive bacteria and gram negative bacteria by agar cup plate method. Methanol system was used as control in this method. Under similar condition, using tetracycline as a standard drug for comparison, we carried out a control experiment. The area of inhibition of zone measured in cm. The screening result for the compound **5a-h** established that **5c**, **5e** and **5h** showed comparable activity against the entire tested microorganism as compared to the standard drugs used while other compounds were weakly active against **5c, 5e** and **5h**.

Antifungal activities

The fungicidal activity was studied at 1000 ppm concentration *in vitro*. The antifungal activity of all the compounds **5a-h** was measured on plant pathogenic strains on a potato dextrose agar (PDA) medium. Such a PDA medium contained potato 200 g, dextrose 20 g, agar 20 g and 1 L water. Five day old cultures were employed. The compounds to be tested were suspended (1000 ppm) in a PDA medium and autoclaved at 121°C for 20 min. at 15 atm pressure; the resulting product was poured into sterile Petri plates, and the organisms were inoculated after cooling the Petri plates. The percentage inhibition for fungi was calculated after five days using the formula given below:

Percentage of inhibition = 100(X-Y)/X

Where, X = area of colony in control plate; and Y = Area of colony in test plate.

Results and Discussion

In the present investigation, we aimed to synthesize derivatives of 6′-(4-(substituted)phenyl)-3′-(thiazol-2-yl)-4′-thioxo-3′,4′-dihydrospiro[Indoline-3,2′-[1, 3, 5] oxadiazin]-2-one **5a-h** through a two step process. For this purpose, Schiff base **3** was prepared from acid catalyzed condensation of 2-aminothiazole and isatin.

The ^{1}H-NMR of 2-aminothiazole shows the peak of -NH_2 group appearing at δ 6.99 ppm [29] which is disappeared in the ^{1}H-NMR spectra of 3-(thiazol-2-ylimino)indolin-2-one **3** supporting the participation of this group in the Schiff base formation. Also it is confirmed with the help of IR spectra. The peak at δ 11.98 ppm [30]

shows the –NH proton of isatin which further confirmed its formation. All the spectral data ^{1}H-NMR, ^{13}C-NMR and IR of synthesized compounds **5a-h** are shown in experimental section. All the compounds show the NMR signals for different kinds of protons at their respective positions. The structure of 6'-(4-(substituted) phenyl)-3'-(thiazol-2-yl)-4'-thioxo-3',4'-dihydrospiro[Indoline-3,2'-[1,3,5]oxadiazin]2-one **5a-h** were confirmed by spectral and elemental analysis and the proposed reaction for the formation of compound is shown in Scheme 1.

The IR spectra showing absorbing band at 1567 cm^{-1} (-HC=N of Schiff bases), 1140-1186 cm^{-1} (C=S), 1663-1693 cm^{-1} (C=O of isatin), 1535-1567 cm^{-1} (C=N), 680-710 cm^{-1} (C-S-C of thiazole), 3040-3090 cm^{-1} (C-H of Ar.), 1480-1430 cm^{-1} (C=C of Ar.), 1575-1625 cm^{-1} (C-C of Ar.), while additional peak appears due to substitution in the aromatic ring showing absorption band 3443 (O-H), 2838 (C-H of $-OCH_3$), 732 (C-Cl), 578 (C-Br), 3255 (C-NH_2 of amino phenyl) and 1550-1570 cm^{-1} (N=O of $-NO_2$).

The examination of the all data reveals that the elemental contents are consistent with the predicted structures shown in Scheme 1. The IR and NMR data also allow a direct assignment of the predicted structure. The elemental analysis values are in good agreement with theoretical data. All the compounds were screened for their antimicrobial activity.

Biological Evaluation

The antibacterial and antifungal activity displayed by various compounds **5a-h** is shown in tables 1 and 2, respectively. The antibacterial activity of series **5a-h** was carried out against some strains of bacteria. The results show that the prepared compounds are toxic against the bacteria. The comparison of the antibacterial activity of these compounds with tetracycline shows good activity against the test organisms. Antibacterial activities of all the compounds were studied against gram positive bacteria (*Bacillus subtilis* and *staphylococcus aureus*) and gram negative bacteria (*E. coli, salmonella typhi* and *Klebsiella promioe*) at a concentration of 50 µg/mL by agar cup plate method. The data in Table 1 indicate that most of the compounds show good biological activity. Further, when the substituents on the phenyl ring were changed, the inhibition activity showed significant differences. When the phenyl ring had an electron-donating group, the corresponding target compounds gave weaker activity, but when modified by the electron-attracting group at the 4th position of the phenyl ring gave good activity.

In addition, all the target compounds were screened for antifungal activities in vitro at 1000 ppm concentration. Plant pathogenic organisms used were *Penicillium expansum, Botrydepladia thiobromine, Nigrospora Sp., Trichothesium Sp.* and *Rhizopus*

nigricum. The comparison of the antifungal activity of these compounds with amphotericin B shows good activity against the test organisms. As shown in Table 2, some of the compounds displayed sensible antifungal activities. Introducing different substituted groups at the phenyl ring could enhance the fungicidal activities. As far as the relation between structure and activity are concerned the chloro, methoxy and nitro substituted compounds were found to display enhanced activity than the other substitution. This enhancement in antibacterial activity is rationalized.

Table 1. Antibacterial activity of compounds **5a-h**

Zone of inhibition mm (activity index)[std.]					
	Gram +ve		Gram –ve		
Compounds	*Bacillus subtilis*	*Staphylococcus aureus*	*Klebsiella promioe*	*Salmonella typhi*	*E.coli*
5a	26 (0.70)	25 (0.71)	26 (0.70)	26 (0.76)	27 (0.72)
5b	26 (0.70)	26 (0.74)	25 (0.67)	24 (0.70)	27 (0.72)
5c	33 (0.89)	31 (0.88)	32 (0.86)	30 (0.88)	34 (0.91)
5d	24 (0.64)	23 (0.65)	20 (0.54)	22 (0.64)	22 (0.59)
5e	30 (0.81)	28 (0.80)	29 (0.78)	27 (0.79)	30 (0.81)
5f	22 (0.59)	20 (0.57)	22 (0.59)	20 (0.58)	23 (0.62)
5g	25 (0.67)	22 (0.62)	24 (0.64)	23 (0.67)	25 (0.67)
5h	31 (0.83)	29 (0.82)	30 (0.81)	29 (0.85)	32 (0.86)
Tetracycline	37	35	37	34	37

Activity index = Inhibition zone of compound/Inhibition zone of the standard drug

Table 2. Antifungal activity of compounds **5a-h**

Zone of inhibition at 1000 ppm (%) (activity index)[std.]					
Compounds	Penicillium Expansum	Botrydepladia thiobromine	Nigrospora sp.	Trichothesium sp.	Rhizopus nigricum
5a	20 (0.57)	20 (0.62)	22 (0.64)	23 (0.69)	22 (0.64)
5b	22 (0.62)	23 (0.71)	23 (0.67)	25 (0.75)	23 (0.64)
5c	31 (0.88)	28 (0.87)	27 (0.79)	30 (0.90)	31 (0.91)
5d	24 (0.68)	22 (0.68)	21 (0.61)	24 (0.72)	25 (0.73)
5e	28 (0.80)	27 (0.84)	25 (0.73)	27 (0.81)	27 (0.79)
5f	23 (0.65)	21 (0.65)	21 (0.61)	20 (0.60)	22 (0.64)
5g	19 (0.54)	19 (0.59)	20 (0.58)	19 (0.57)	20 (0.58)
5h	30 (0.85)	28 (0.87)	26 (0.76)	29 (0.87)	30 (0.88)
Amphotericin B	35	32	34	33	34

Activity index = Inhibition zone of compound/Inhibition zone of the standard drug.

Overall activity profile of compounds **5a-h** was found to be moderate. Thus, in the present study, we attempted to increase antimicrobial activities by fusing 4-R-benzoyl isothiocyanate moiety with 3-(thiazol-2-ylimino) indolin-2-one **3** ring system in the present investigation.

Conclusion

The clubbing of 2-aminothiazole, 4-R-benzoyl isothiocyanate and isatin has been done successfully into one molecule. Their structures were verified by elemental analysis and spectral data. Bioassays showed that the title compounds show good biological activities. The compounds **5c**, **5e** and **5h** displayed good antibacterial and antifungal activity. So we can say that all the moieties have important application in medicinal use; the produced compounds act as good biological compounds. Further investigations are in progress.

Acknowledgments

We are grateful to authorities of Department of Chemistry, for providing Laboratory facilities to carry out the research work.

References and Notes

[1] Hargrave, K. D.; Hess, F. K.; Oliver, J. T. *J. Med. Chem.* **1983**, *26*, 1158. [CrossRef]

[2] Patt, W. C.; Hamilton, H. W.; Taylor, M. D.; Ryan, M. J.; Taylor, D. G.; Connolly, C. J.; Doherty, A. M.; Klutchko, S. R.; Sircar, I.; Steinbaugh, B. A.; Batley, B. L.; Painchaud, C. A.; Rapundalo, S. T.; Michniewicz, B. M.; Olson, S. C. J. *J. Med. Chem.* **1992**, *35*, 2562. [CrossRef]

[3] Haviv, F.; Ratajczyk, J. D.; DeNet, R. W.; Kerdesky, F. A.; Walters, R. L.; Schmidt, S. P.; Holms, J. H.; Young, P. R.; Carter, G. W. *J. Med. Chem.* **1988**, *31*, 1719. [CrossRef]

[4] Clemence, F.; Martret, O. L.; Delevallee, F.; Benzoni, J.; Jouanen, A.; Jouquey, S.; Mouren, M.; Deraedt, R. *J. Med. Chem.* **1988**, *31*, 1453.[CrossRef]

[5] Jaen, J. C.; Wise, L. D.; Caprathe, B. W.; Tecle, H.; Bergmeier, S.; Humblet, C. C.; Heffner, T. G.; Meltzner, L. T.; Pugsley, T. A. *J. Med. Chem.* **1990**, *33*, 311. [CrossRef]

[6] Tsuji, K.; Ishikawa, H. *Bioorg. Med. Chem. Lett.* **1994**, *4*, 1601. [CrossRef]

[7] Bell, F. W.; Cantrell, A. S.; Högberg, M.; Jaskunas, S. R.; Johansson, N. G.; Jordon, C. L.; Kinnick, M. D.; Lind, P. Jr.; Morin, J. M.; Noréen, R.; Öberg, B.; Palkowitz, J. A.; Parrish, C. A.; Pranc, P.; Sahlberg, C.; Ternansky, R. J.; Vasileff, R. T.; Vrang, L.; West, S. J.; Zhang, H.; Zhou, X. X. *J. Med. Chem.* **1995**, *38*, 4929. [CrossRef]

[8] Fink, B. A.; Mortensen, D. S.; Stauffer, S. R., Aron, Z. D.; Katzenellenbogen, J. A.

Chem. Biol. **1999**, *6*, 205. [CrossRef]
[9] Muijlwijk-Koezen Van, J. E.; Timmerman, H.; Vollinga, R. C.; Von Drabbe Kunzel, J. F.; DeGroote, M.; Visser, S.; Ijzerman, A. P. *J. Med. Chem.* **2001**, *44*, 749. [CrossRef]
[10] a) Ganjee, A.; Yuan, M.; Queener, S. F. *J. Med. Chem.* **1998**, *41*, 4533 [CrossRef]; b) *Chem. Abstr.*, **1999**, *130*, 13966x.
[11] Karade, H. N.; Acharya, B. N.; Sathe, M.; Kaushik, M. P. *Med. Chem. Res.* **2008**, *17*, 19. [CrossRef]
[12] Spector, F. C.; Liang, L. H.; Sivaraja, G.M.; Peterson, M. G. *J. Virology* **1998**, *72*, 6979.
[13] Ghorab, M. M.; El-Batal, A.I. *Boll. Chim. Farm.* **2002**, *141*, 110.
[14] Bhaskar, V.H.; Kumar, M.B.; Sangameswaran, B.; Balakrishnan, B.R. *Rasayan J. Chem.* **2008**, *1*, 218.
[15] Sriram, D.; Yogeshwari, P.; Meena, K. *Pharmazie* **2006**, *61*, 129.
[16] Chiyanzu, I.; Clarkson, C.; Smith, P. J.; Lehman, J.; Rosenthal, P. J.; Chibale, K. *Bioorg. Med. Chem.* **2005**, *13*, 3249. [CrossRef]
[17] Verma, M.; Pandey, S. N.; Singh, K. N.; Stables, J. P. *Acta Pharm*. **2004**, *54*, 49.
[18] Smitha, S.; Pandey, S. N.; Stables, J. P. *Arch. Pharm*. **2002**, *335*, 129.
[19] Moustafa, O. S.; Ahmed, R. R. *Phosphorus, Sulfur Silicon Relat. Elem*. **2003**, *178*, 475. [CrossRef]
[20] Mahadevan, K. M.; Basavaray, K. M.; Mathias, D. A. P.; Vaidya, V. P. I. *J. Chem.* **2005**, *44*, 789.[CrossRef]
[21] Zjawiony, J. K.; Dayan, F. E.; Vincent, A. C.; Romagni, J. G.; Allen, S. N.; Duke, S. O.; Duke, M. V.; Bowling, J. J. *J. Agri. Food. Chem.* **2000**, *48*, 3689.
[22] Takamoria, K.; Funakoshia, T.; Hirotaa, S.; Chakia, S.; Kameob, K. *Life Sciences*, **2002**, *71*, 947. [CrossRef]
[23] a) Quan, M. L.; Liquw, A. Y.; Pruitty, J. R.; Carini, D. S.; Bostrom, L.; Harrison, K. R.; Knabb, M. *J. Med. Chem.* **1999**, *42*, 2752. [CrossRef]; b) *Chem.Abstr.* **1999**, 131, 170287q.
[24] Pandeya, S. N.; Sriram, D.; Nath, G. *Eur. J. Pharm. Sci.* **1999**, *9*, 25. [CrossRef]
[25] Lakhan, R.; Sharma, B. P.; Shukla, B. N. *Farmaco* **2000**, *55*, 331. [CrossRef]
[26] Turan-Zitouni, G.; Kaplancikli, Z. A.; Yildiz, M. T.; Chevallet, P.; Kaya, D. *Eur. J. Med. Chem.* **2005**, *40*, 607. [CrossRef]
[27] a) Zhang, H. Li.; Chung, J. C.; Costello, T. D.; Valcis, I.; Ward, R. *J. Org. Chem.* **1997**, *62*, 2466; b) *Chem. Abstr*. **1997**, *126*, 212082y.
[28] Modi, V. P.; Jani, D. H.; Patel, H. S. *Orbital Elec. J. Chem.* **2011**, *3*, 68. [Link]
[29] Morales-Bonilla, P.; Perez-Cardena, A.; Quintero-Marmol, E.; Luis Arias-Tellez, J.; Mena-Rejon, G. J. *Heteroatom Chemistry* **2006**, *17*, 254. [CrossRef]
[30] Bekircan, O.; Bektas, H. *Molecules* **2008**, *13*, 2126. [CrossRef]
[31] Simmons, A. *Practical Medical Microbiology*, 14th Ed. Churchill Livingstone, Edinburg, 1996, 11, 163.
[32] Bisen, P. S.; Verma, K. *Hand Book of Microbiology*, 1st Ed. CBS Publishers and Distributors, New Delhi, 1996.

ISSN 1984-6428
ONLINE
www.orbital.ufms.br

| Vol 4 | | No. 2 | | April-June 2012 |

Full Paper

An efficient solvent-free synthesis of *meso*-substituted dipyrromethanes using $SnCl_2 \cdot 2H_2O$ catalysis

Kabeer A. Shaikh,[a] Vishal A. Patil[a] and B. P. Bandgar[b*]*

[a]Organic synthesis laboratory, P. G. Department of Chemistry, Sir Sayyed College of Arts, Commerce and Science. Aurangabad 431001, M.S., India.
[b]Medicinal Chemistry Research Laboratory, Solapur University, Solapur-413255, M.S., India.

Received: 24 February 2012; revised: 30 March 2012; accepted: 12 April 2012. Available online: 07 July 2012.

ABSTRACT: *Highly rapid and simple methodology has been developed for the quantitative synthesis of meso-substituted dipyrromethanes from lowest pyrrole/aldehyde ratio. The method was carried out by using $SnCl_2 \cdot 2H_2O$ as a catalyst under solvent free condition. The method is environmentally friendly, easy to workup, and gives excellent yield of the products.*

Keywords: *pyrrole; dipyrromethanes; $SnCl_2 \cdot 2H_2O$ catalysis; grinding*

Introduction

Dipyrromethanes are important building blocks for the synthesis of porphyrins [1], Calixpyrrols [2], and Corroles [3]. Dipyrromethanes are compounds known for more than a century [4]. In the past decades, a variety of conditions have been established for the synthesis of dipyrromethanes in the presence of various catalysts such as p-toluenesulfonic acid [5], $TiCl_4$ [6], CF_3COOH [7] and pyrrolidinium tetrafluoroborate [8]. In the synthesis of dipyrromethanes most of the conditions are based on the acid catalyzed condensation of pyrrole with aldehyde. Recently, several methods have been developed, for the synthesis of dipyrromethanes in various catalyst such as ionic liquid [Hmim] BF_4 [9], HCl/water [10], cation exchange resin [11], metal triflate catalysis [12], HCl [13], iodine/CH_2Cl_2 [14] and $InCl_3$ [15]. However, all of the synthetic protocols

* Corresponding author. E-mail: shaikh_kabeerahmed@rediff.com

reported so far suffer from disadvantages such as, use of metal [12], expensive reagent [11], prolonged reaction time[13], use of organic solvent [14], harsh reaction condition [13], use of excess pyrrole [12] and low yield [9]. Because of that, the researcher still continuous to have a better methodology for the synthesis of dipyrromethanes in terms of simplicity, eco-friendly, economic viability, high yielding at lowest pyrrole/aldehyde ratio which is achieved by using stannous chloride dehydrate.

In recent years, $SnCl_2 \cdot 2H_2O$ is frequently used in organic synthesis [16] as a catalyst due to its properties such as nontoxic nature, easy availability, inexpensiveness and easiness for work up. It played a great role for the synthesis of biologically active heterocycles such as benzimidazoles [17], quinoxalines [18] and functionalization of 4,5-diaminopyrazoles [19].

Material and Methods

Purity of the compounds was checked by thin layer chromatography (TLC) on Merck silica gel 60 F254 pre-coated sheets. Melting points of the synthesized compounds were determined in open-glass capillaries on a stuart-SMP10 melting point apparatus. IR absorption spectra were recorded on a Perkin Elmer 1650 FTIR using KBr pellets in the range of 4,000-450 cm^{-1}. ^{1}H-NMRs were recorded on a Bruker spectrometer operating at 400 MHz. The ^{1}H-NMR chemical shifts are reported as parts per million (ppm) downfield from TMS (Me_4Si) used as an internal standard. Mass spectra were recorded on LCQ ion trap mass spectrometer. All compounds were known, and obtained physical and spectroscopic data were compared with literatures data.

General procedure

A mixture of pyrrole (2 mmol), aldehyde (1 mmol) and $SnCl_2 \cdot 2H_2O$ (0.2 mmol) was crushed in a mortar with a pestle at room temperature. Progress of reaction was monitored by TLC. After completion of reaction (< 1 min) the crude product was washed with water, dried and purified by column chromatography using silica gel with petroleum ether/chloroform as the eluent. Pure products were obtained as solids.

*5-(4-nitrophenyl)dipyrromethane***:** Yellow powder; mp: 159–160 ^{0}C, IR (KBr) 3394, 3360, 3100, 1597, 1516, 1348, 1120, 1025, 807, 737, 660, 565 cm^{-1}; ^{1}H NMR(400 MHz, $CDCl_3$): d 5.58 (s, 1H, mesoH), 5.85 (br s, 2H, 2C3–H), 6.16 (dd, J = 2.8, 5.7, 2H, 2C4–H), 6.74 (dd, J = 2.8, 4.2, 2H, 2C5–H), 7.36 (d, J = 8.6, 2H, H-Ar), 8.0 (br s, 2H, N–H), 8.15 (d, J = 8.8, 2H, Ar-H).; MS (ES) Found [Calcd.]: m/z 267.30 [267.28] (MH^+).

5-(2-Nitrophenyl)dipyrromethane ***(1)*****:** Brown oily liquid; IR (KBr) 3402, 1602, 1534, 1340, 1134, 1029, 815, 730, 661, 567 cm^{-1}; ^{1}H NMR (400 MHz, $CDCl_3$): δ 5.87 (s,

1H, mesoH), 6.11–6.24 (m, 4H), 6.65–6.70 (m, 2H), 7.24–7.55 (m, 3H), 7.87–7.90 (m, 1H), 8.18 (brs, 2H, NH); MS (ES) Found [Calcd.]: m/z 267.26 [267.29] (MH^+).

5-(4-Fluorophenyl)dipyrromethane ***(2)****:* brown crystals; mp: 80–81 ^{0}C, IR (KBr) 3416, 2930, 1608, 1496, 1450, 1287, 1174, 1100, 964, 764, 558 cm^{-1}; ^{1}H NMR (400 MHz, $CDCl_3$): d 5.47 (s, 1H, mesoH), 5.88 (br s, 2H, 2C3-H), 6.17 (dd, J 2.7, 5.8, 2H, 2C4-H), 6.67 (br s, 2H, 2C5-H), 7.02–7.07 (m, 2H, Ar-H), 7.18–7.24 (m, 2H, Ar-H), 7.80 (br s, 2H, 2N-H); MS (ES) Found [Calcd.]: m/z 240.15 [240.27] (MH^+).

5-Phenyldipyrromethane ***(3):*** Pale yellow crystals; mp: 100 ^{0}C, IR (KBr) 3448, 2950, 1634, 1512, 1412, 1291, 1227, 1048, 761, 704, 607 cm^{-1}; ^{1}H NMR (400 MHz, $CDCl_3$): d 5.47 (s, 1H, mesoH), 5.94 (br s, 2H, 2C3-H), 6.14 (dd, J 2.8, 5.8, 2H, 2C4-H), 6.67 (dd, J 2.6, 4.2, 2H, 2C5-H), 7.20–7.37 (m, 5H, Ar-H), 7.87 (br s, 2H, 2N-H); MS (ES) Found [Calcd.]: m/z 222.31 [222.28] (MH^+).

5-(4-Methoxyphenyl)dipyrromethane ***(4):*** Pale yellow powder; mp: 98–99 ^{0}C, IR (KBr) 3407, 2965, 2934, 1615, 1507, 1455, 1298, 1246, 1174, 1105, 1025, 964, 837, 775, 722, 554 cm^{-1}; ^{1}H NMR (400 MHz, $CDCl^3$): d 3.80 (s, 3H, OCH3), 5.44 (s, 1H, mesoH), 5.90–5.93 (m, 2H, 2C3-H), 6.16 (dd, J 2.8, 5.7, 2H, 2C4-H), 6.64–6.68 (m, 2H, 2C5-H), 6.87 (d, J 8.4, 2H, Ar-H), 7.16 (d, J 8.4, 2H, Ar-H), 7.80 (br s, 2H, 2N-H); MS (ES) Found [Calcd.]: m/z 252.33 [252.31] (MH^+).

5-(2,6-Dichlorophenyl)dipyrromethane ***(5)*****:** Yellow solid. mp 102–103 ^{0}C, IR (KBr) 3412, 2925, 1612, 1495, 1447, 1282, 1175, 1101, 792, 741, 529 cm^{-1}; ^{1}H NMR (400 MHz, $CDCl_3$): δ 6.08 (s, 1H, mesoH); 6.15 (dd, J 2.4, 5.4 Hz, 2H); 6.49 (s, 1H); 6.70–6.71 (m, 2H), 7.14 (t, J 8.0 Hz, 2H), 7.30 (d, J 8.0 Hz, 2H), 8.29 (bs, 2H, NH); MS (ES) Found [Calcd.]: m/z 291.21 [291.17] (MH^+) 293.15 (MH^{+2})

5-(4-Methylphenyl)dipyrromethane ***(6):*** Pale yellow crystals; mp: 110 ^{0}C, IR (KBr) 3415, 2356, 1634, 1509, 1425, 1253, 1090, 1024, 964, 908, 791, 745, 506 cm^{-1}; ^{1}H NMR (400 MHz, $CDCl_3$): d 2.35 (s, 3H, CH3), 5.45 (s, 1H, mesoH), 5.90 (br s, 2H, 2C3-H), 6.15 (dd, J 2.7, 5.8, 2H, 2C4-H), 6.64 (dd, J 2.5, 4.0, 2H, 2C5-H), 7.10–7.14 (m, 4H, Ar-H), 7.84 (br s, 2H, 2N-H); MS (ES) Found [Calcd.]: m/z 236.28 [236.31] (MH^+).

5-(4-Chlorophenyl)dipyrromethane ***(7)*****:** Pale yellow powder; mp: 112–114 ^{0}C, IR (KBr) 3380, 2960, 2922, 2860, 1642, 1487, 1405, 1250, 1085, 1018, 765, 722, 554, 507 cm^{-1}; ^{1}H NMR (400 MHz, $CDCl_3$): d 5.40 (s, 1H, mesoH), 5.88 (br s, 2H, 2C3-H), 6.15 (dd, J 2.8, 5.6, 2H, 2C4-H), 6.67 (dd, J 2.7, 4.2, 2H, 2C5-H), 7.14 (d, J 8.1, 2H, Ar-H), 7.30 (d, J 8.1, 2H, Ar-H), 7.82 (br s, 2H, 2N-H); MS (ES) Found [Calcd.]: m/z 256.75 [256.73] (MH^+), 257.74 (MH^{+1}).

5-(4-Bromophenyl)dipyrromethane ***(8):*** yellow powder; mp: 123–124 ^{0}C, IR

(KBr) 3372, 3096, 2958, 2922, 2860, 1705, 1484, 1404, 1081, 1020, 767, 721, 645, 545, 502 cm^{-1}; ^1H NMR (400 MHz, $CDCl_3$): d 5.40 (s, 1H, mesoH), 5.92 (br s, 2H, 2C3-H), 6.15 (dd, J 2.7, 5.6, 2H, 2C4-H), 6.66 (dd, J 2.5, 4.2, 2H, 2C5-H), 7.12 (d, J 8.2, 2H, Ar-H), 7.45 (d, J 8.2, 2H, Ar-H), 7.81 (br s, 2H, 2N-H); MS (ES) Found [Calcd.]: m/z 301.15 [301.18] (MH^+).

Results and Discussion

We began our study by grinding the mixture of 2 mmol pyrrole and 1 mmol 4-nitrobenzaldehyde (Scheme 1) under the reaction conditions described in Table 1.

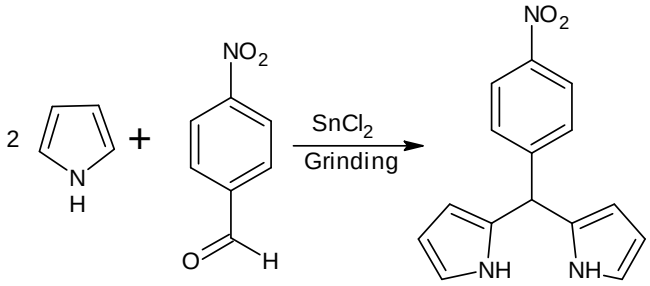

Scheme 1. Synthesis of 5-(4-nitrophenyl)dipyrromethane.

Initially, the mixture was ground in mortar with a pestle at room temperature under neat condition. However, result demonstrated the need of catalyst since the starting material was recovered (Entry 1). Thus, we chose 0.1 mmol $SnCl_2{\cdot}2H_2O$ as a catalyst. The result demonstrated that stoichiometric use of $SnCl_2{\cdot}2H_2O$ gives moderate yield of the product (Entry 2). The excellent yield was obtained at 0.2 mmol of $SnCl_2{\cdot}2H_2O$ (Entry 3) which is greater than that of 0.3 mmol of $SnCl_2{\cdot}2H_2O$ as a catalyst (entry 4). For evaluating the amount of catalyst, $SnCl_2{\cdot}2H_2O$ was employed in 0.4 and 0.5 mmol, however result demonstrated that moderate yield of product (Entry 5 and 6). Thus, from all above data, we confirmed that reaction gives excellent yield at 0.2 mmol of $SnCl_2{\cdot}2H_2O$. This study also confirmed that the $SnCl_2{\cdot}2H_2O$ played a great role as a Lewis-acid catalyst because its absence did not give desired product (Entry 1).

Table 1. Optimization for synthesis of 5-(4- nitrophenyl)dipyrromethane

Entry	$SnCl_2{\cdot}2O$ (mmol)	Time (min)	Yield[a] (%)
1	0.0	20	00[b]
2	0.1	2	62
3	0.2	< 1	98
4	0.3	< 1	84
5	0.4	< 1	78
6	0.5	< 1	78

[a]Isolated yield of the products. [b]The starting material was recovered.

Another interesting result in this article was found that we got excellent yield at lowest pyrrole/aldehyde ratio i. e. 2:1. This result was compared with the literatures best pyrrole/aldehyde ratio (Table 2). In these Littler et al [7c] and Naik et al [11] afforded moderate yield at high pyrrole/aldehyde ratio (Entry 2 and 3). Faugeras et al [14] gave good yield of the product but they had done their work at high pyrrole/aldehyde ratio (Entry 4). Rohand et al[13] also carried out good job but they did not try at lowest pyrrole/aldehyde ratio (Entry 1).

Table 2. Comparison of the pyrrole/aldehyde ratio with literature

Entry	Catalyst	Pyrrole/aldehyde ratio	Yield[a] (%)
1	HCl	3:1	97 [13]
2	TFA	25:1	56 [7c]
3	Cation exchange resin (T-63)	20:1	61 [11]
4	I_2, CH_2Cl_2	10:1	84 [14]
5	$SnCl_2$ $2H_2O$	2:1	98

[a]Isolated yield of the 5-(4-nitrophenyl)dipyrromethane.

Thus, from above data, it was cleared that none of the above best literatures can be compared with our best results i. e. use of low pyrrol/aldehyde ratio and excellent yield of the product.

In order to confirm these interesting results, we applied this method to the synthesis of various *meso*-substituted dipyrromethanes (Scheme 2) and obtained results were compared with literature best methods (Table 3).

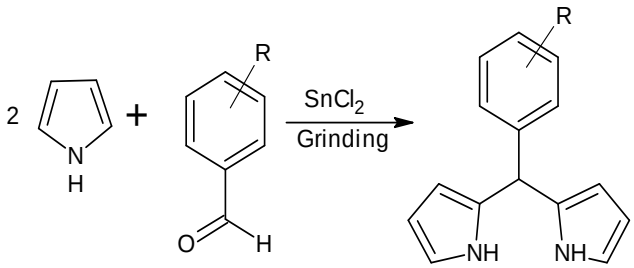

R = 2-NO_2, 4-F, H, 4-OCH_3, 2, 6-di-Cl, 4-CH_3, 4-Cl, 4-Br

Scheme 2. Synthesis of various *meso*-substituted dipyrromethanes.

Table 3 cleared that there was no influence of the electronic nature of the substituent on the reaction time or yield. Thus, it is possible to affirm that aldehydes containing electron donating or withdrawing groups reacted well in very short time (< 1 min) and gave corresponding dipyrromethanes in excellent yield (92-97%) as compared to best method found in literatures. In the case of 5-(4-metoxyphenyl)dipyrromethane, Faugeras et al. [14] gave excellent yield (90 %) in short reaction time but they performed their work by using dichloromethane as a solvent and by using microwave oven, which is always harmful to the environment and have economically higher cost. In

the another case of 5-phenyldipyrromethane and 5-(2,6-dichlorophenyl)dipyrromethane, Rohand et al. [13] gave good yields (86 and 85 %) in prolonged reaction time but they performed their work by using large quantity of strong acid which is always hazardous to the environment.

Table 3: Comparison of the yields with best methods found in the literatures

Entry	Aldehyde	Isolated Yield[a] (%) /Pyrrole:aldehyde ratio	Literature best yield (%)/Pyrrole:aldehyde ratio
1	2-nitrobenzaldehyde	94/2:1	73/20:1 [11]
2	4-fluorobenzaldehyde	95/2:1	77/20:1 [11]
3	Benzaldehyde	97/2:1	86/03:1 [13]
4	4-methoxybenzaldehyde	94/2:1	90/10:1 [14]
5	2,6-Dichlorobenzaldehyde	95/2:1	85/03:1 [13]
6	4-methylbenzaldehyde	95/2:1	83/40:1* [12]
7	4-chlorobenzaldehyde	97/2:1	77/20:1 [11]
8	4-bromobenzaldehyde	92/2:1	74/40:1* [12]

[a]products were characterized by IR, ^{1}H·NMR, MS (ES) and coincided with literature data, *pyrrole/imine ratio instead ofpyrrole/aldehyde.

Thus, from all above results and discussion it was cleared that this method is superior in terms of use of inexpensive catalyst, solvent free reaction, lowest pyrrole/aldehyde ratio, very short reaction time and excellent yield of the products.

Conclusion

In conclusion, we have discovered highly rapid and simple method for the quantitative synthesis of *meso*-substituted dipyrromethanes at lowest pyrrole/aldehyde ratio and by using $SnCl_2{\cdot}2H_2O$ as a catalyst. The use of this nontoxic, easily available and inexpensiveness catalyst make this protocol practical and economically attractive.

Acknowledgments

We would like to thank DST, New Delhi for financial assistance and Prof. Mohammed Tilawat Ali for providing necessary facilities for research work.

References and Notes

[1] Temelli, B.; Unaleroglu, C. *Tetrahedron* **2009,** *65,* 2043. [CrossRef]
[2] Gale, P. A.; Anzenbacher, P. Jr.; Sessler, J. L. *Coord. Chem. Rev.* **2001**, *222,* 57. [CrossRef]
[3] Zhan, H.-Y.; Liu, H.-Y.; Chen, H.-J. *Tetrahedron Lett.* **2009**, *50,* 2196. [CrossRef]
[4] Baeyer, A.; *Ber. Dtsch. Chem. Ges*. **1986**, *19,* 2184. [CrossRef]
[5] (a) Boyle, R. W.; Xie, L. Y.; Dolphin, D. *Tetrahedron Lett*. **1994,** *35,* 5377. [CrossRef]. (b) Mizutani, T.; Ema, T.; Tomita, T. *J. Am. Chem. Soc*. **1994**, *116,* 4240. [CrossRef]
[6] Setsune, J.-I.; Hashimoto, M.; Shiozawa, K. *Tetrahedron* **1998**, *54,* 1407. [CrossRef]

[7] (a) Srinivasan, A.; Sridevi, B.; Reddy, M. V. R. *Tetrahedron Lett*. **1997**, *38,* 4149. [CrossRef]. (b) Lee, C. H.; Lindsay, J. S. *Tetrahedron* **1994**, *50,* 11427. [CrossRef]. (c) Littler, B. J.; Miller, M. A.; Hung, C.-H. *J. Org. Chem*. **1999**, *64,* 1391. [CrossRef]
[8] Biaggi, C.; Benaglia, M.; Raimondi, L. *Tetrahedron* **2006**, *62,* 12375. [CrossRef]
[9] Gao, G. H.; Lu, L.; Gao, J. B. *Chinese Chemical Lett*. **2005**, *16,* 900.
[10] Sobral, A. J. F. N.; Rebanda, N. G. C. L.; Silva, M. D. *Tetrahedron Lett*. **2003**, *44,* 3971. [CrossRef]
[11] Naik, R.; Joshi, P.; Kaiwar, S. P.; *Tetrahedron* **2003**, *59,* 2207. [CrossRef]
[12] Tamelli, B.; Unaleroglu, C. *Tetrhedron* **2006**, *62,* 10130. [CrossRef]
[13] Rohand, T.; Dolusic, E.; Ngo, T. H. Maes, W.; Dehaen, W. *Arkivok* **2007**, *x*, 307.
[14] Faugeras, P.-A.; Boëns, B.; Elchinger, P.-H. *Tetrahedron Lett.* **2010,** *51,* 4630. [CrossRef]
[15] Laha, J. K.; Dhanalekshami, S.; Taniguchi, M. *Org. Process Res. Dev*. **2003**, *7,* 799. [CrossRef]
[16] Rai, G.; Jeong, J. M.; Lee, Y. S. *Tetrahedron Lett.* **2005**, *46,* 3987. [CrossRef]
[17] Wu, Z.; Philip, R.; Wickham, G. *Tetrahedron Lett*. **2000**, *41,* 9871. [CrossRef]
[18] Shi, D. Q.; Dou, G. L.; Ni, S. N. *Heterocyclic Chem*. **2008**, *45,* 1797. [CrossRef]
[19] Blass, B. E.; Srivastava, A.; Coburn, K. R. *Tetrahedron Lett.* **2003**, *44,* 3009. [CrossRef]

ISSN 1984-6428
ONLINE
www.orbital.ufms.br

| Vol 4 | | No. 2 | | April-June 2012 |

Full Paper

Palladium (0)-catalyzed efficient synthesis of allylic *N*- and *S*-benzoheterocycles linked to unsaturated carbohydrate derivatives

Ronaldo N. de Oliveira, Wilson S. do Nascimento, Girliane R. da Silva and Tânia Maria S. Silva*

Departamento de Ciências Moleculares, Universidade Federal Rural de Pernambuco, Rua Dom Manoel de Medeiros S/N, Dois Irmãos, 52171-900, Recife, PE, Brazil. Fax: +55(81)-33206374.

Received: 24 April 2012; accepted: 30 June 2012. Available online: 12 July 2012.

ABSTRACT: *An efficient strategy was developed to envisage the synthesis of new N- and S-benzoheterocycles attached to the C-4 position of pseudo-carbohydrates. The reaction was performed with unsaturated carbohydrates and benzoheterocycles as nucleophiles in the presence of a catalytic amount of tetrakis(triphenylphosphine)palladium(0) and chelating bidentate ligand dppb. This strategy allowed easy access to benzoheterocyclic sugars in moderate-to-good yields. A preliminary study for antioxidant activities of O-glycosides 2,3-unsaturated was evaluated based on the 1,1-diphenyl-2-picryl hydrazyl (DPPH) radical scavenging and 2,2-azinobis 3-ethylbenzothiozoline-6-sulfonic acid (ABTS) radical cation decolorization assay, and showed low-to-moderate activities.*

Keywords: *palladium; catalysis; benzoheterocycles; hexenopyranoside; carbohydrate; antioxidant activity*

Introduction

A diversity of functional moieties may be employed in the synthesis of molecular libraries for biological screening [1, 2]. Carbohydrate scaffolds possess a wide spectrum of biological activities, including enzyme inhibitory properties [3-5], antitubercular properties [6], antimicrobial [7] and antioxidant activities [8], among others [9].

The use of palladium catalyst in organic reaction is a versatile and reliable strategy for C-C, C-O, C-S and C-N bond formation, and has been employed, for example, for allylic substitution via an intermediate (π-allyl) palladium complex [10-12]. This reaction offers a potential usefulness for the functionalization of carbohydrates with

* Corresponding author. E-mail: ronaldonoliveira@dcm.ufrpe.br

excellent regio- and stereocontrol [13]. First developed by Tsuji [14] and Trost [15], this method has widespread application in organic synthesis based on chiral building blocks [16] and drug discovery [17, 18].

We have previously reported on palladium-catalyzed reactions of alkyl hex-2-enopyranosides with NaN_3 as nucleophile which resulted in a regio- and stereoselective means of obtaining aminosugar derivatives [19]. The reaction when nitrogen is connected to the allylic position of glycopyranosides in five steps from 3,4,6-tri-*O*-acetyl-D-glucal has already been described by us [20]. In this work, we repeat this methodology [20] to obtain the C-N linked compound **1** with 70% yields from cyclohexylamine and sugar-based allylcarbonates, using this protocol we achieved an overall yields of 31% (Scheme 1, route A).

In the present study, we tried to develop a stereoselective functionalization of unsaturated carbohydrate using palladium reagents resulting in an efficient strategy in two steps for constructing allylic *N*- and *S*-benzoheterocycles linked to carbohydrate moieties from D-glucal as shown in Scheme 1 (route B).

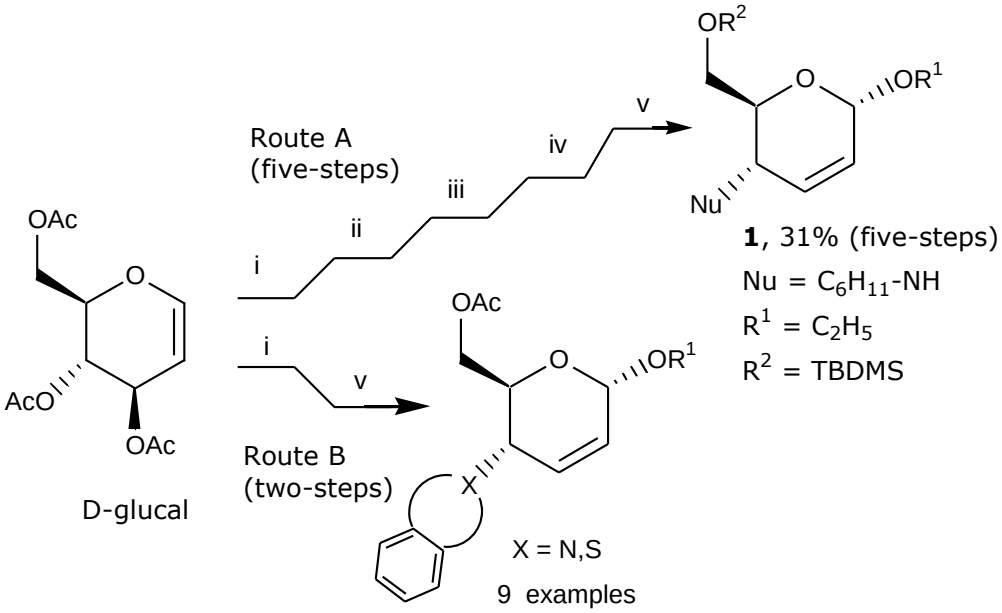

i) ROH, DCM, K10; ii) MeOH/ MeONa; iii) TBDMSCl/py; iv)CH_3OCOCl/py/DMAP/DCM; v) Pd(0)/NuH.

Scheme 1: Strategy of synthesis of benzoheterocycle-sugars

Material and Methods

General Procedure

All reactions were monitored using TLC analysis (TLC plates GF_{254} Merck). Air- and moisture-sensitive reactions were performed in an inert atmosphere of argon. All organic solvents were of analytical grade. Optical rotations were measured using a Krüss Model

P1000 polarimeter. Melting points were determined using a PFM II BioSan instrument and are uncorrected. ^{1}H (300 MHz) and ^{13}C NMR (75.5 MHz) spectra were obtained with Varian unity plus-300 spectrometers in $CDCl_3$. Elemental analyses were carried out using a CA EA1110 CHNS-O analyzer. Column chromatography was performed using Merck silica gel 60 (70-230 mesh). High resolution mass spectra HRMS were recorded on a Shimadzu Liquid Chrom MS LCMS-IT-TOF using acetonitrile or methanol as solvent. The absorbance of the solutions in the antiradical tests (DPPH) and (ABTS) were determined on an Asys HiTech UVM 340 Spectrophotometer. Ascorbic acid (for DPPH) and Trolox (ABTS) were used as standards.

Synthesis

Alkyl 4,6-di-*O*-acetyl-2,3-dideoxy-α-D-*erythro*-hex-2-enopyranoside (**2a-c**) was prepared according to literature procedure [20].

For synthesis of (**1**) see procedure in the literature [19].

Ethyl 6-O-acetyl-2,3,4-trideoxy 4-(N-cyclohexylamino)-α-D-erythro-hex-2-enopyranoside ***(1)****:* Yield= 70%; colorless oil; R_f= 0.5 (PE-EtOAc, 9:1); $[\alpha]_D^{20}$ + 85 (*c* 0.75, CH_2Cl_2). ^{1}H NMR (300 MHz, $CDCl_3$): δ= 0.00 (s, 6H, $SiMe_2$), 0.83 (s, 9H, CMe_3), 1.04-1.10 (m, 13H, $5CH_2$ and CH_3), 3.42-3.50 (m, 2H, CH- and -CH_2O), 3.60-3.83 (m, 4H, -CH_2O, H-5, H-6 and H-6'), 4.49 (d, 1H, NH, *J*= 7.2 Hz), 4.95 (br s, 1H, H-1), 5.04 (d, 1H, H-4, *J* = 9.4 Hz), 5.72 (ddd, 1H, H-2, *J* = 10.2, 2.3 Hz), 5.86 (d, 1H, H-3, *J* = 10.2 Hz). ^{13}C NMR (75.5 MHz, $CDCl_3$): δ= -4.9, -5.0, 15.6, 18.8 , 25.1, 25.8, 26.3, 33.7 (cyclohexyl), 50.3, 63.5, 64.2, 70.5, 94.3, 127.9, 130.6. Anal. Calcd. For $C_{20}H_{39}NO_3Si$: C, 64.99; H, 10.64. Found: C, 65.10; H, 10.42.

Typical procedure for the synthesis of ***4a****:* To a solution of $Pd(PPh_3)_4$ (17 mg, 14 mmol), dppb (13 mg, 28 mmol), and the unsaturated carbohydrate **2a** (100mg, 0.28 mmol) in THF (5 mL) was added the heterocyclic benzimidazole **3a** (70 mg, 1.5 equivalent). The solution was stirred at 60 °C for 2 h. Evaporation of the solvent and column chromatography on silica gel gave the corresponding unsaturated carbohydrate 4-substitued **4a**.

Ethyl 6-O-acetyl-2,3,4-trideoxy 4-(1H-benzimidazolyl)-α-D-erythro-hex-2-enopyranoside ***(4a):*** Yield= 51%; yellow oil; R_f = 0.7 (Hexane-EtOAc, 6:4); $[\alpha]_D^{20}$ + 254 (*c* 1, CH_2Cl_2). ^{1}H NMR (300 MHz, $CDCl_3$): δ= 1.29 (t, 3H, CH_3, *J* = 7.1 Hz), 2.01 (s, 3H, $COCH_3$), 3.65 (dq, 1H, OCH_2CH_3, *J* = 7.1, 9.9 Hz), 3.82-3.97 (m, 2H, H-6, OCH_2CH_3), 4.14 (dd, 1H, H-6', *J* = 12.1, 3.0 Hz), 4.50 (ddd, 1H, H-5, *J* = 9.9, 3.6, 3.6 Hz), 5.13 (br d, 1H, H-4, *J* = 9.9 Hz), 5.20 (sl, 1H, H-1), 6.01 (br d, 1H, H-3, *J* = 10.2 Hz), 6.13 (ddd, 1H, H-2, *J* = 10.2, 2.7, 2.7 Hz), 7.27-7.33 (m, 2H, H_{Ar}), 7.48-7.54 (m, 1H, H_{Ar}), 7.80-7.85 (m, 1H, H_{Ar}), 7.96 (s, 1H, N=CH).^{13}C NMR (75.5 MHz, $CDCl_3$): 15.2, 20.6, 51.0,

63.0, 64.5, 67.1, 94.1, 110.5, 120.6, 122.7, 123.4, 128.5, 128.6, 129.3, 132.1, 142.0, 170.3. Anal. Calcd. For $C_{17}H_{20}O_4N_2$: C, 64.54; H, 6.37. Found: C, 64.43; H, 6.50. m/z LC-MS $[M(C_{17}H_{20}O_4N_2)+H]^+$: 317.1501; Found: 317.1500.

(E,E) 1-(Acetyloxy) 6-ethoxy 3,5-hexadiene-2-one ***(4a'):*** Yield= 44%; colorless oil; R_f= 0.3 (PE-EtOAc, 8:2). ^{1}H NMR (300 MHz, $CDCl_3$): δ= 1.33 (t, 3H, CH_3, *J*= 7.2 Hz), 2.19 (s, 3H, $COCH_3$), 3.95 (q, 2H, OCH_2CH_3), 4.79 (s, 2H, -CH_2OAc), 5.67 (dd, 1H, *J*= 11.4, 12.3 Hz), 6.10 (d, 1H, *J*= 15.0 Hz), 6.98 (d, 1H, *J*= 12.0 Hz), 7.28 (d, 1H, J= 15.0 Hz). m/z LC-MS $[M(C_{10}H_{14}O_4)+H]^+$: 199.0970. Found:199.1021

Ethyl 6-O-acetyl-2,3,4-trideoxy 4-(1H-benzotriazolyl)-α-D-erythro-hex-2-enopyranoside ***(4b):*** Yield= 70%; colorless oil; R_f = 0.7 (Hexane-EtOAc, 6:4); $[\alpha]_D^{25}$= + 60 (*c* 0,4, $CHCl_3$). ^{1}H NMR (300 MHz, $CDCl_3$): δ= 1.27 (t, CH_3, *J*= 7.2 Hz), 1.98 (s, 3H, $COCH_3$), 3.65 (dq, 1H, O*CH*$_2$CH$_3$, *J* = 6.6, 9.6 Hz), 3.86 (dq, 1H, O*CH*$_2$CH$_3$, *J* = 6.6, 9.6 Hz), 3.93 (dd, 1H, H-6, *J* = 12.3, 5.1 Hz), 4.09 (dd, 1H, H-6', *J* = 12.3, 3.0 Hz), 4.62 (ddd, 1H, H-5, *J* = 9.9, 4.8, 2.7 Hz), 5.19 (br d, 1H, H-1, *J*= 1.2 Hz), 5.72 (ddd, 1H, H-4, *J* = 10.2, 3.6, 2.1 Hz), 6.05 (br d, 1H, H-2, *J* = 10.2, 1.2 Hz), 6.13 (ddd, 1H, H-3, *J* = 9.9, 2.7, 2.7 Hz), 7.36 (ddd, 1H, H_{arom}, *J*= 6.9, 6.9, 0.9 Hz), 7.47 (ddd, 1H, H_{arom}, *J*= 6.9, 6.9, 0.9 Hz), 7.65 (d, 1H, H_{arom}, *J*= 8.3 Hz), 8.06 (d, 1H, H_{arom}, *J*= 8.3 Hz). ^{13}C NMR (75.5 MHz, $CDCl_3$): 15.3, 20.6, 54.8, 63.0, 64.5, 66.3, 94.1, 110.3, 120.3, 124.3, 127.5, 127.7, 129.4, 132.1, 146.3, 170.3. Anal. Calcd. For $C_{16}H_{19}O_4N_3{\cdot}0.15\ H_2O$: C, 60.05; H, 6.08. Found: C, 60.11; H, 6.25. m/z LC-MS $[M(C_{16}H_{19}O_4N_3)+H]^+$ 318.1454; Found: 318.1388.

Ethyl 6-O-acetyl-2,3,4-trideoxy 4-(2H-benzotriazolyl)-α- D-erythro-hex-2-enopyranoside ***(4b'):*** Yield= 20%; colorless oil; R_f = 0.5 (Hexane-EtOAc, 6:4); $[\alpha]_D^{25}$= + 46 (*c* 0,4, $CHCl_3$). ^{1}H NMR (300 MHz, $CDCl_3$): δ= 1.27 (t, CH_3, *J*= 7.2 Hz), 2.00 (s, 3H, $COCH_3$), 3.63 (dq, 1H, O*CH*$_2$CH$_3$, *J* = 7.2, 9.6 Hz), 3.88 (dq, 1H, O*CH*$_2$CH$_3$, *J* = 7.2, 9.6 Hz), 4.07 (dd, 1H, H-6, *J* = 12.3, 4.8 Hz), 4.14 (dd, 1H, H-6', *J* = 12.3, 3.0 Hz), 4.75 (ddd, 1H, H-5, *J* = 9.9, 5.1,3.0 Hz), 5.19 (br s, 1H, H-1), 5.72 (ddd, 1H, H-4, *J* = 10.2, 3.9, 1.8 Hz), 6.05 (ddd, 1H, H-3, *J* = 10.2, 2.7, 2.7 Hz), 6.14 (br d, 1H, H-2, *J* = 10.8 Hz), 7.35-7.41 (ddd, 2H, H_{arom}, *J* = 7.2, 3.3, 1.5 Hz), 7.82-7.88 (ddd, 2H, H_{arom}, *J* = 7.2, 3.3, 1.5 Hz). ^{13}C NMR (75.5 MHz, $CDCl_3$): 15.2, 20.6, 60.6, 63.0, 64.4, 67.8, 94.3, 118.1, 126.7, 127.6, 128.0, 128.5, 132.0, 132.1, 144.4, 170.5. Anal. Calcd. For $C_{16}H_{19}O_4N_3$: C, 60.56; H, 6.03. Found: C, 60.91; H, 6.15.

N-Phthalimidomethyl 6-O-acetyl-2,3,4-trideoxy 4-(1H-benzimidazolyl)-α-D-erythro-hex-2-enopyranoside ***(5a):*** Yield= 57%; colorless solid; mp 73-75°C; R_f = 0.4 (Hexane-EtOAc, 8:2); $[\alpha]_D^{25}$= + 20 (*c* 0.3, $CHCl_3$). ^{1}H NMR (500 MHz, $CDCl_3$): δ= 2.00 (s, 3H, $COCH_3$), 3.87 (dd, 1H, H-6, *J* = 12.5, 3.0 Hz), 4.15 (dd, 1H, H-6, *J* = 12.5, 3.0 Hz), 4.54 (br d, 1H, H-5, *J* = 10.0 Hz), 5.13 (br d, 1H, H-4, *J* = 10.5, 1.5 Hz), 5.38 (m, 2H,

OCH_2Phth), 5.54 (br s, 1H, H-1), 6.02 (br d, 1H, H-2, *J* = 10.5 Hz), 6.05 (dd, 1H, H-3, *J* = 10.5, 3.0 Hz), 7.05 (m, 2H, H_{Ar}), 7.28-7.31 (m, 2H, phthalimide), 7.67-7.70 (m, 2H, phthalimide), 7.77-7.82 (m, 1H, H_{arom}), 7.92-7.93 (m, 1H, H_{arom}), 8.13 (s, 1H, H_{arom}). ^{13}C NMR (125 MHz, $CDCl_3$): 20.5, 50.1, 62.8, 64.9, 68.0, 93.5, 115.4, 120.7, 122.7, 123.3, 123.5, 123.9, 128.3, 129.6, 131.8, 134.6, 144.0, 167.5, 170.2 Anal. Calcd. For $C_{24}H_{21}O_6N_3$: C, 64.42; H, 4.73. Found: C, 64.23; H, 4.43.

N-Phthalimidomethyl 6-O-acetyl-2,3,4-trideoxy 4-(1H-benzotriazolyl)-α-D-erythro-hex-2-enopyranoside ***(5b):*** Yield= 52%; yellow solid; mp 68-70°C; R_f = 0.4 (Hexane-EtOAc, 6:4); $[\alpha]_D^{25}$= + 67 (*c* 0.3, $CHCl_3$). ^{1}H NMR (300 MHz, $CDCl_3$): δ= 1.96 (s, 3H, $COCH_3$), 3.85 (dd, 1H, H-6, *J* = 12.3, 4.8 Hz), 4.08 (dd, 1H, H-6', *J* = 12.3, 3.0 Hz), 4.70 (ddd, 1H, H-5, *J* = 9.9, 4.2, 3.3 Hz), 5.33-5.42 (2d, 2H, OCH_2Phth, *J* = 10.2 Hz), 5.56 (br s, 1H, H-1), 5.75 (br d, 1H, H-4, *J* = 10.5 Hz), 6.06-6.14 (m, 2H, H-3, H-2), 7.37 (ddd, 1H, H_{arom}, *J*= 6.9, 6.9, 0.6 Hz), 7.45 (ddd, 1H, H_{arom}, *J*= 6.9, 6.9, 0.6 Hz), 7.58 (d, 1H, H_{arom}, *J*= 8.4 Hz), 7.75-7.81 (m, 2H, phthalimide), 7.88-7.93 (m, 2H, phthalimide), 8.06 (d, 1H, H_{arom}, *J*= 8.4 Hz). ^{13}C NMR (75 MHz, $CDCl_3$): 20.5, 54.4, 62.7, 64.8, 66.8, 93.5, 110.0, 120.3, 123.8, 124.3, 127.8, 128.2, 128.5, 131.7, 134.6, 146.2, 167.5, 170.2. Anal. Calcd. For $C_{23}H_{20}O_6N_4$: C, 61.60; H, 4.50. Found: C, 61.40; H, 4,65.

Benzyl 6-O-acetyl-2,3,4-trideoxy 4-(1H-benzimidazolyl)-α-D-erythro-hex-2-enopyranoside ***(6a):*** Yield= 83%; brown oil; R_f = 0.6 (Hexane-EtOAc, 6:4); $[\alpha]_D^{25}$= + 72 (*c* 0.3, $CHCl_3$). ^{1}H NMR (200 MHz, $CDCl_3$): δ= 1.89 (s, 3H, $COCH_3$), 3.77 (dd, 1H, H-6, *J* = 12.6, 4.8 Hz), 3.95 (dd, 1H, H-6', *J* = 12.6, 2.8 Hz), 4.41 (ddd, 1H, H-5, *J* = 10.2, 5.1, 3.4 Hz), 4.62 (m, 2H, OCH_2Ph), 4.99 (br d, 1H, H-4, *J* = 9.8 Hz), 5.15 (br s, 1H, H-1), 5.90 (br d, 1H, H-2, *J* = 10.5 Hz), 6.02 (ddd, 1H, H-3, *J* = 10.5, 2.8, 2.8 Hz), 7.13-7.26 (m, 6H, H_{arom}), 7.35-7.40 (m, 2H, H_{arom}), 7.66-7.71 (m, 1H, H_{arom}), 7.81 (s, 1H, H_{arom}). ^{13}C NMR (75 MHz, $CDCl_3$): 20.6, 51.1, 62.9, 67.3, 70.4, 93.4, 110.5, 120.7, 122.7, 123.4, 128.0, 128.5, 132.0, 132.9, 137.3, 143.8, 170.3. Anal. Calcd. For $C_{22}H_{22}O_4N_2 \cdot 0.1$ H_2O: C, 69.50; H, 5.88. Found: C, 69.30; H, 5.66. m/z LC-MS $[M(C_{22}H_{22}O_4N_2)+H]^+$: 379.1580; Found: 379.1411.

Benzyl 6-O-acetyl-2,3,4-trideoxy 4-(1H-benzotriazolyl)-α-D-erythro-hex-2-enopyranoside ***(6b):*** Yield= 71 %; colorless oil; R_f = 0.6 (Hexane-EtOAc, 6:4); $[\alpha]_D^{25}$= + 92 (*c* 1, CH_2Cl_2). ^{1}H NMR (300 MHz, $CDCl_3$): δ= 1.99 (s, 3H, $COCH_3$), 3.95 (dd, 1H, H-6, *J* = 12.0, 6.4 Hz), 4.07 (dd, 1H, H-6', *J* = 12.0, 3.0 Hz), 4.66-4.98 (m, 3H, H-5, OCH_2Ph), 5.32 (br s, 1H, H-1), 5.72 (d, 1H, H-4, *J* = 8.7 Hz), 6.05 (br d, 1H, H-2, *J* = 10.2 Hz), 6.13 (ddd, 1H, H-3, *J* = 10.2, 2.7, 2.7 Hz), 7.27-7.48 (m, 9H, H_{arom}), 7.65 (d, 1H, H_{arom}, *J*= 8.4 Hz), 7.65 (d, 1H, H_{arom}, *J*= 8.3 Hz), 7.95 (m, 1H, H_{arom}) 8.08 (d, 1H, H_{arom}, *J*= 7.1 Hz). ^{13}C NMR (75.5 MHz, $CDCl_3$): 20.6, 54.6, 62.9, 66.5, 70.3, 93.3, 110.2, 114.8, 120.2, 124.4, 126.5, 127.7, 127.8, 128.0, 128.5, 129.1, 132.1, 137.2, 146.0, 170.4.

Anal. Calcd. For $C_{21}H_{21}O_4N_3$: C, 66.48; H, 5.58. Found: C, 66.34; H, 5.51.

For the preparation of the compounds **4c**, **5c** and **6c** the typical procedure was used except that Et_3N (1.5 equivalent on **3c**) was added to the mixture.

Ethyl 6-O-acetyl-2,3,4-trideoxy 4-(benzimidazol-2-ylsulfanyl)-α-D-erythro-hex-2-enopyranoside ***(4c):*** Yield= 97%; yellow solid; mp 80-81°C; R_f = 0.3 (Hexane-EtOAc, 8:2); $[\alpha]_D^{25}$= + 81 (*c* 0.3, $CHCl_3$). ^{1}H NMR (300 MHz, $CDCl_3$): δ= 1.24 (t, 3H, CH_3, *J* = 6.9 Hz), 2.04 (s, 3H, $COCH_3$), 3.58 (dq, 1H, OCH_2CH_3, *J* = 7.2, 9.6 Hz), 3.86 (dq, 1H, OCH_2CH_3, *J* = 7.2, 9.6 Hz), 4.26 (ddd, 1H, H-5, *J* = 10.2, 3.6, 3.6 Hz), 4.39 (br d, 1H, H-4, *J* = 10.2 Hz), 4.43 (m, 2H, H-6, H-6'), 5.08 (br s, 1H, H-1), 5.88 (ddd, 1H, H-3, *J* = 10.2, 2.4, 2.4 Hz), 6.15 (br d, 1H, H-2, *J* = 10.2 Hz), 7.21-7.25 (m, 3H, H_{Ar}, NH), 7.51-7.54 (m, 2H, H_{Ar}).^{13}C NMR (75.5 MHz, $CDCl_3$): 15.2, 20.8, 41.6, 63.9, 64.1, 68.7, 93.7, 114.4, 122.8, 127.6, 130.4, 138.5, 146.6, 171.1. Anal. Calcd. For $C_{17}H_{20}O_4N_2S \cdot 0.4\ H_2O$: C, 57.42; H, 5.90. Found: C, 57.73; H, 5.59. m/z LC-MS $[M(C_{17}H_{20}O_4N_2S)+H]^+$: 349.1222. Found: 349.0956.

N-Phthalimidomethyl 6-O-acetyl-2,3,4-trideoxy 4-(benzimidazol-2-ylsulfanyl)-α-D-erythro-hex-2-enopyranoside ***(5c):*** Yield= 83%; Yellow solid; mp 82-84°C; R_f = 0.4 (Hexane-EtOAc, 6:4); $[\alpha]_D^{20}$ + 52 (*c* 1, MeOH). ^{1}H NMR (300 MHz, $CDCl_3$): δ= 2.04 (s, 3H, $COCH_3$), 4.22 (ddd, 1H, H-5, *J* = 10.5, 5.4, 2.1 Hz), 4.32-4.42 (m, 2H, H-4 and H-6), 4.48 (dd, 1H, H-6, *J* = 12.0, 1.8 Hz), 5.22 (d, 1H, OCH_2Phth, *J* = 10.2 Hz), 5.29 (d, 1H, OCH_2Phth, *J* = 10.2 Hz), 5.34 (br d, 1H, H-1, *J*= 2.7 Hz), 5.78 (ddd, 1H, H-3, *J* = 10.1, 3.0, 3.0 Hz), 6.17 (br d, 1H, H-2, *J* = 10.1 Hz), 7.16-7.19 (m, 2H, H_{arom}), 7.50-7.53 (m, 3H, H_{arom}, NH), 7.74-7.77 (m, 2H, H_{arom}), 7.87-7.90 (m, 2H, H_{arom}). ^{13}C NMR (75 MHz, $CDCl_3$): 20.9, 41.8, 63.9, 64.4, 69.3, 93.0, 114.0, 123.0, 123.8, 126.4, 131.1, 131.7, 134.5, 145.8, 167.4, 171.4. Anal. Calcd. For $C_{24}H_{21}O_6N_3S$: C, 60.12; H, 4.41. Found: C, 59.81; H, 4.54.

Benzyl 6-O-acetyl-2,3,4-trideoxy 4-(benzimidazol-2-ylsulfanyl)-α-D-erythro-hex-2-enopyranoside ***(6c):*** Yield= 65 %; colorless oil; R_f = 0.6 (Hexane-EtOAc, 6:4); $[\alpha]_D^{25}$= + 55 (*c* 0.5, CH_2Cl_2). ^{1}H NMR (400 MHz, $CDCl_3$): δ= 2.02 (s, 3H, $COCH_3$), 3.91 (dd, 1H, H-6, *J* = 12.0, 4.4 Hz), 4.04 (dd, 1H, H-6', *J* = 12.0, 2.1 Hz), 4.54 (dl, 1H, H-5, *J* = 9.9 Hz), 4.68 (d, 1H, OCH_2Ph, *J* = 12.0 Hz), 5.12 (br d, 1H, H-4, *J* = 10.0 Hz), 5.23 (br s, 1H, H-1), 6.02 (br d, 1H, H-2, *J* = 10.0 Hz), 6.14 (ddd, 1H, H-3, *J* = 10.0, 2.1, 2.1 Hz), 7.28-7.39 (m, 8H, H_{arom}), 7.83 (d, 1H, H_{arom}, *J* = 7.6 Hz), 7.97 (s, 1H, NH). ^{13}C NMR (100 MHz, $CDCl_3$): 20.6, 51.2, 62.9, 67.2, 70.4, 93.4, 110.6, 120.6, 122.8, 123.5, 128.1, 128.4, 128.6, 128.9, 129.2, 132.1, 137.2, 142.0, 170.3. m/z LC-MS $[M(C_{22}H_{22}O_4N_2S)-OCH_2Ph]^+$: 303.0803; Found:303.0806. m/z LC-MS $[M(C_{22}H_{22}O_4N_2S)+CH_3OH-H]^+$:441.1370; Found: 441.1484.

Biological activity assays

DPPH$^{\bullet}$ Radical Scavenging Assay

The free radical scavenger activity was determined using the DPPH assay as previously described [30]. The antiradical activity was evaluated using a dilution series to obtain five concentrations. This involved mixing the DPPH solution (60 µM in ethanol) with an appropriate amount of the compounds (standard and samples). After 30 min, quantification of the remaining DPPH radicals was recorded using absorption at 517 nm. The percentage of inhibition was given by the following formula: Percent inhibition (%) = $[(A_0 - A_1) / A_0] \times 100$ in which A_0 is the absorbance of the control and A_1 is the absorbance in the presence of the sample and standards. The tests were performed in triplicate. The statistical analysis was carried out using the Microsoft Excel software package (Microsoft Corp., Redmond, WA).

ABTS$^{+\bullet}$ Radical Cation Decolorization Assay

The radical cation decolorization assay was based on a method previously reported in the literature [31]. ABTS was dissolved in water to yield a final concentration of 7 mM. The ABTS radical cation (ABTS$^{+\bullet}$) was produced by reacting an ABTS stock solution with 2.45 mM potassium persulfate (final concentration) and allowing the mixture to stand in the dark at room emperature for 12–16 h before use. The ABTS$^{+\bullet}$ solution was diluted with ethanol to give an absorbance of 0.700 ± 0.025 at 734 nm prior to its use. Then, the appropriate amounts of the ABTS$^{+\bullet}$ solution were added to sample solutions in ethanol (5 mL) of the compounds (standard and samples). After 10 min, the percentage inhibition of absorbance at 734 nm was calculated for each concentration relative to the blank absorbance (ethanol). The capability of scavenging the ABTS$^{+\bullet}$ radical was calculated using the following equation:

ABTS$^{+\bullet}$ scavenging effect (%) = $[(A_0 - A_1 / A_0) \times 100]$

in which A_0 is the initial concentration of the ABTS$^{+\bullet}$ and A_1 is the absorbance of the remaining concentration of ABTS$^{+\bullet}$ in the presence of the sample. All samples were analyzed in triplicate. The statistical analysis was carried out using the Microsoft Excel software package (Microsoft Corp., Redmond, WA).

Results and Discussion

The alkyl 4,6-di-*O*-acetyl-2,3-dideoxy-α-D-*erythro*-hex-2-enopyranosides **2a-c** were prepared by reacting 3,4,6-tri-*O*-acetyl-D-glucal with ethanol (81%), *N*-hydroxymethyl-phthalimide (87%) or benzyl alcohol (75%) via a Ferrier rearrangement protocol [21]. After column chromatographic of the crude mixture, the compounds were crystallized in ethyl acetate to obtain the α-D-*erythro*-hex-2-enopyranoside **2a-c** in good yields 75-87% (Scheme 2).

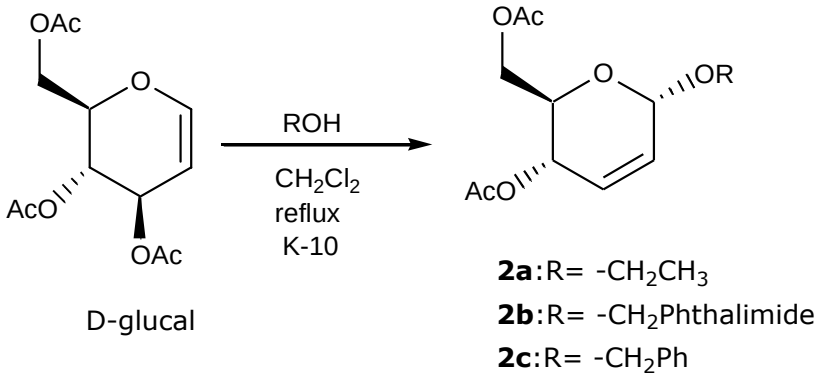

Scheme 2: Synthesis of *O*-glycoside 2,3-unsaturated (**2a-c**).

We have focused our attention on the details of the reaction on the substitution of allylic acetate **2a-c** by *N*- or *S*-benzoheterocycles **3a-c** (Scheme 3).

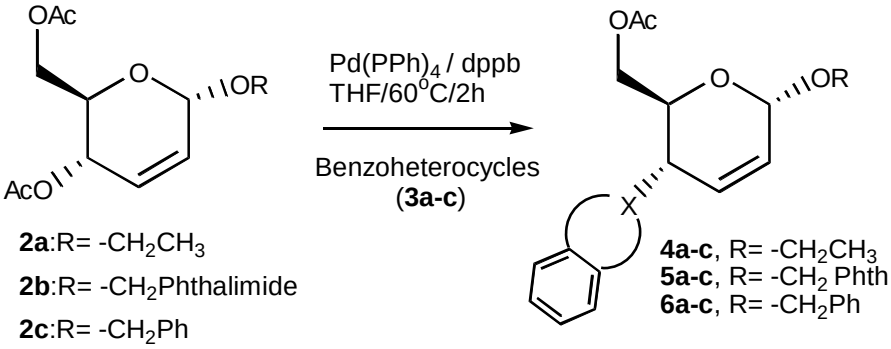

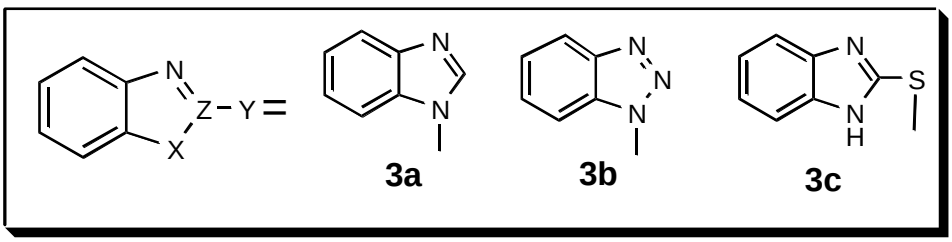

Scheme 3 : Synthesis of allylic *N*- and S-benzoheterocycle-sugars.

We treated the unsaturated carbohydrates **2a-c** with the *N*-benzoheterocycles benzimidazole **3a** and benzotriazole **3b**, and *S*-benzoheterocycle benzimidazole-2-thiol **3c**. We examined this reaction using the $Pd(PPh_3)_4$ system and dppb [1,4-bis(diphenylphosphino)butane] as the catalyst model because it had been employed previously with success with allylic carbonate of hexenopyranosides [20]. The reaction was performed in THF at 60 °C and the contents were stirred during 2 h. The results listed in Table 1 show that the reactions of unsaturated carbohydrate **2a-c** and benzoheterocycles **3a-c** produced allylic 4-substituted sugars **4-6** in moderate-to-excellent yields of 51-97%.

Firstly, we examined the substitution of ethyl 4,6-di-*O*-acetyl-2,3-dideoxy-α-D-*erythro*-hex-2-enopyranoside **2a** with benzoheterocycles **3a-b**. Reaction of benzimidazole **3a** (1.5 mol equivalent) with unsaturated acetate **2a** (1 mol equivalent) in the presence of 5 mol% (w/w of **2a**) $Pd(PPh_3)_4$ and dppb (2 equivalent of ligand per Pd) in THF at 60 °C produced the compound **4a** with a 51% yield (Table 1, entry 1). In order to rationalize the moderate yield for **4a** we analyzed the second spot in TLC. We believe that this compound is the diene conjugate **4a'** after elimination and rearrangement for *trans*-diene [22] in 44% yield after column chromatography (Table 1, entry 1). The compound **4a'** has also been described by Baer and Hanna using amines and hexenopyranoside **2a** as reagents under similar conditions [23].

Next, when benzotriazole **3b** was employed under the same conditions, the product **4b** yielded 70% and another allylated product 2*H*-triazole **4b'** yielded 20% (Table 1, entry 2). This latter compound **4b'** was formed during isomerization of the benzotriazole **3b**, this isomerization has been reported in the literature [24, 25].

There are only few reports in the literature about C-S connection [12, 26, 27]. Thus, we decided study more examples using the benzimidazol-2-ylsulfanyl **3c** as a sulfur nucleophile. Nevertheless, when we tried to repeat the same conditions using **3c** as nucleophile, we did not obtain any conversion monitored by TLC. Taking into account the poor reactivity of benzimidazole-2-thiol **3c**, a further experiment was carried out with bases. Initially, we chose the bases NaH or *tert*-BuOK, but no reaction occurred. Thus, only when triethylamine (TEA) was added to raise the nucleophilicity of **3c**, the desired product **4c** was formed with an excellent yield of 97% (Table 1, entry 3).

Table 1: Palladium-catalyzed synthesis of **4-6**

Entry	Products (yields, %)[a]	Overall yields (%)[d]
1	**4a** (51) + **4a'** (44)	(**4a**) 41
2	**4b** (70) + **4b'** (20)	(**4b**) 61
3	**4c** (97)[b]	73
4	**5a** (57)[c]	46
5	**5b** (52)[c]	45
6	**5c** (83)[b]	62
7	**6a** (83)	67
8	**6b** (71)	62
9	**6c** (70)[b]	53

[a]isolated yield after column chromatography. [b]In these cases the reaction was performed using Et_3N. [c]Low yields because it was recovered starting material. [d]Total yields in two-steps to form **4-6** from D-glucal.

With the successful synthesis of **4a-c** in mind, we decided investigate others

aglycons in the hex-2-enopyranoside structure. Thus, we examined the reaction starting from *N*-phthalimidomethyl 4,6-di-*O*-acetyl-2,3-dideoxy-α-D-*erythro*-hex-2-enopyranoside **2b** and benzoheterocycles **3a-c**, under optimized conditions to obtain the heterocycle-sugars **5a-c** in moderate to good yields of 52-83% (entries 4-6). In two cases, we recovered approximately 30% of the unchanged substrate **2b** after column chromatography (entries 4 and 5). Attempts for complete conversion of **2b** were unsuccessful even when the catalytic system was changed to Pd_2dba_3/dppb.

In order to test more one aglycon, we use the benzyl 4,6-di-*O*-acetyl-2,3-dideoxy-α-D-*erythro*-hex-2-enopyranoside **2c** to react with benzimidazole **3a**, benzotriazole **3b** and benzimidazole-2-thiol **3c** producing *N*- and *S*-carbohydrates **6a-c** in good yields 83%, 71% and 70%, respectively (entries 7, 8 and 9).

The structure of the new compounds **1**, **4a-c**, **5a-c** and **6a-c** were assigned by ^{1}H NMR and ^{13}C NMR spectral analysis. In order to confirm the configuration at C-4 in 2,3-unsaturated compounds we investigated the coupling constant between H-4 and H-5. The vicinal $^{3}J_{4,5}$ ranged between 9.9-10.2 Hz, indicative of *trans* stereochemistry. Thus, this configuration is in agreement with similar structures of α-D-*erythro*-hex-2-enopyranosides [19, 20, 28, 29].

We were attracted to substrate that can be susceptible to an allylic hydrogen abstraction to form an allylic radical based on our compounds that containing an allylic *N*- or *S*-substituent. Thus, all the compounds **(4-6) (a-c)** have been evaluated for $DPPH^{\cdot}$ radical scavenging and $ABTS^{\cdot+}$ radical-cation decolorization assay [30, 31]. The preliminary results showed that percentage of inhibition at 50 μg/mL ranged from 11% to 23% for DPPH and 9% to 68% for ABTS assays. For the most active compound (**5c**) was calculated the EC_{50} values which showed values of 40.3±3.4 μg/mL and 31.3±0.18 μg/mL for DPPH and ABTS assays, respectively. Further tests are under development, and we believe that this class of the allylic compounds may be a new promising prototype for antioxidant activity.

Conclusion

In conclusion, we developing a concise means for the synthesis of new unsaturated sugars **4-6,** substituted at the allylic position by *N*- or *S*-benzoheterocycles, that was easily available in a two-step reaction, starting from D-glucal with 41-73% overall yields. Preliminary study showed that there are some interesting antioxidant activities, which may be due to the facile release of a hydride radical from an allylic substrate.

Acknowledgments

The authors are grateful to FACEPE-PRONEM (APQ-1232.106/10) for financial support, and FACEPE and CAPES for providing fellowships (W. S. N. and G. R. S.). Our thanks are also due to Analytical Centers CENAPESQ-UFRPE and DQF-UFPE.

References and Notes

[1] Silverman, R. B. *The Organic Chemistry of Drug Design and Drug Action*; Elsevier Academic Press: Burlington (MA), **2004**.
[2] Barbosa, F. C. G.; de Oliveira, R. N. *J. Braz. Chem. Soc.* **2011**, *22*, 592. [CrossRef]
[3] Cheng, K.; Liu, J.; Liu, X.; Li, H.; Sun, H.; Xie, J. *Carbohydr. Res.* **2009**, *344*, 841. [CrossRef]
[4] Dodela, S.; Hughes, D. L.; Nepogodiev, S. A.; Rejzek, M.; Field, R. A. *Carbohydr. Res.* **2010**, *345*, 1123. [CrossRef]
[5] Bokor, É.; Docsa, T.; Gergely, P.; Somsák, L. *Bioorg. Med. Chem.* **2010**, *18*, 1171. [CrossRef]
[6] Ferreira, M. L.; de Souza, M. V. N.; Wardell, S. M. S. V.; Wardell, J. L.; Vasconcelos, T. R. A.; Ferreira, V. F.; Lourenço, M. C. S. *J. Carbohydr. Chem.* **2010**, *29*, 265. [CrossRef]
[7] Xavier, N. M.; Silva, S.; Madeira, P .J. A.; Florêncio, M. H.; Silva, F. V. M.; Justino, J.; Thiem, J.; Rauter, A. P. *Eur. J. Org. Chem.* **2008**, 6134. [CrossRef]
[8] Rajaganesh, R.; Jayakumar, J.; Sivaraj, C.; Raaman, N.; Das, T. M. *Carbohydr. Res.* **2010**, *35*, 1649. [CrossRef]
[9] Fürstner, A. *Eur. J. Org. Chem.* **2004**, 943. [CrossRef]
[10] Kallinen, A.; Tois, J.; Sjöholm, R.; Franzén, R. *Tetrahedron: Asymmetry* **2010**, *21*, 2367. [CrossRef]
[11] Comely, A. C.; Eelkema, R.; Minnaard, A. J.; Feringa, B. L. *J. Am. Chem. Soc.* **2003**, *125*, 8714. [CrossRef]
[12] Divekar, S.; Safi, M.; Soufiaoui, M.; Sinou, D. *Tetrahedron* **1999**, *55*, 4369. [CrossRef]
[13] Frappa, I.; Sinou, D. *J. Carbohydr. Chem.* **1997**, *16*, 255. [CrossRef]
[14] Tsuji, J.; Yamakawa, T.; Kaito, M.; Mandai, T. *Tetrahedron Lett.* **1978**, *19*, 2075. [CrossRef]
[15] Trost, B. M.; Verhoeven, T. R.; Fortunak, J. M. *Tetrahedron Lett.* **1979**, *20*, 2301. [CrossRef]
[16] Borisova, S. A.; Guppi, S. R.; Kim, H. J.; Wu, B.; Penn, J. H.; Liu, H.-w.; O'Doherty, G.A. *Org. Lett.* **2010**, *12*, 5150. [CrossRef]
[17] Simila, S. T. M.; Martin, S. F. *J. Org. Chem*. **2007**, *72*, 5342. [CrossRef]
[18] Fuertes, M. J.; Kaur, J.; Deb, P.; Cooperman, B. S.; Smith, A. B., III. *Bioorg. Med. Chem*. *Lett.* **2005**, *15*, 5146. [CrossRef]
[19] de Oliveira, R. N.; Cottier, L.; Sinou, D.; Srivastava, R. M. *Tetrahedron* **2005**, *61*, 8271. [CrossRef]
[20] de Oliveira, R. N.; Mendonça Jr., F. J. B.; Sinou, D.; de Melo, S. J.; Srivastava, R. M. *Synlett* **2006**, 3049.

[21] Toshima, K.; Ishizuka, T.; Malsuo, G.; Nakata, M. *Synlett* **1995**, 306. [CrossRef]
[22] Takenaka, H.; Ukaji, Y.; Inomata, K. *Chem. Lett.* **2005**, *34*, 256. [CrossRef]
[23] Baer, H. M.; Hanna, Z. S. *Can. J. Chem.* **1981**, *59*, 889. [CrossRef]
[24] Katritzky, A. R.; Rachwal, S. *Chem. Rev.* **2010**, *110*, 1564. [CrossRef]
[25] Liu, W.; Zhang, D.; Zheng, S.; Yue, Y.; Liu, D.; Zhao, X. *Eur. J. Org. Chem.* **2011**, 6288. [CrossRef]
[26] Neirabeyeh, M. Al; Rollin, P. *J. Carbohydr. Chem.* **1990**, *9*, 471. [CrossRef]
[27] Valverde, S.; Bernabé, M.; Garcia-Uchoa, S.; Gómez, A. M. *J. Org. Chem.* **1990**, *55*, 2294. [CrossRef]
[28] de Oliveira, R. N.; Sinou, D.; Srivastava, R. M. *J. Carbohydr. Chem.* **2006**, *25*, 407. [CrossRef]
[29] de Oliveira, R. N.; de Melo, A. C. N.; Srivastava, R. M.; Sinou, D. H*eterocycles* **2006**, *68*, 2607. [CrossRef]
[30] Freire, K. R. L.; Lins, A. C. S.; Dórea, M. C.; Santos, F. A. R.; Camara, C. A.; Silva, T. M. S. *Molecules* **2012**, *17*, 1652. [CrossRef]
[31] Re, R.; Pellegrini, N.; Proteggente, A.; Pannala, A.; Yang, M.; Rice-Evans, C. *Free Radic. Biol. Med.* **1999**, *26*, 1231. [CrossRef]

ISSN 1984-6428
ONLINE
www.orbital.ufms.br

| Vol 4 | | No. 2 | | April-June 2012 |

Full Paper

Pyrazine carboxylic acid derivatives of dichlorobis(cyclopentadienyl)titanium (IV)

Satish Chandra Dixit[a*] *and Rohit Kumar Singh*[b]

[a]Department of Chemistry, D.B.S. Post-graduate College, Kanpur-208006, India
[b]Department of Chemistry, Pt. Jawahar Lal Nehru P.G. College, Banda (U.P.), India

Received: 29 March 2012; revised: 01 June 2012; accepted: 15 June 2012. Available online: 12 July 2012.

ABSTRACT: *Reactions of dichlorobis(cyclopentadienyl)titanium (IV) with pyrazine carboxylic acids viz. 2-pyrazine carboxylic acid (2-PzCH), 5-methyl-2-pyrazine carboxylic acid (MPzCH) and 2,3-pyrazine dicarboxylic acid (2,3-PzDCH$_2$) were carried out in different stoichiometric ratios. Complexes of the type Cp$_2$Ti(2-PzC)Cl, Cp$_2$Ti(2-PzC)$_2$, Cp$_2$Ti(MPzC)Cl,Cp$_2$Ti(MPzC)$_2$, Cp$_2$Ti(2,3-PzDCH)Cl and Cp$_2$Ti(2,3-PzDCH)$_2$ were obtained. These newly synthesized complexes were characterized on the basis of elemental analyses, electrical conductance, magnetic moment and spectral data.*

Keywords: *Cp$_2$TiCl$_2$; tumour; complexes; characterization; synthesis; pyrazine carboxylic acids*

Introduction

Pyrazine carboxylic acids have been found on the basis of the reported x-ray molecular structures to be interesting and versatile ligands [1-9]. Several complexes of copper (II) and cobalt (II) with pyrazine carboxylic acids have been reported in the literature [10-14]. Much interest has been generated in the biological field after the reports that Cp_2TiCl_2 shows antitumour activity [15]. A large number of unbridged titanocene analogues containing aromatic groups attached to the cyclopentadienyl ligand have been synthesized [16]. One of the most promising drugs of this series was bis-[(p-methoxybenzyl)cyclopentadienyl]titanium dichloride (titanocene Y) and its antiproliferative activity has been studied in 36 human tumour cells [17] and in explanted human tumours [18-21]. These *in vitro* and *ex vivo* experiments showed that prostate, cervix and renal cancer cells are prime targets for these novel classes of

* Corresponding author. E-mail: satishdixit1@gmail.com

titanocenes.

A survey of the literature reveals that no work has been carried out on the reactions of Cp_2TiCl_2 with 2-pyrazine carboxylic acid (2-PzCH), 5-methyl-2-pyrazine carboxylic acid (MPzCH) and 2,3-pyrazine dicarboxylic acid (2,3-$PzDCH_2$). It was, therefore, considered worthwhile to study the reactions of dichlorobis(cyclopentadienyl)titanium (IV) with different said pyrazine carboxylic acids.

The structure of the ligands used is given below:

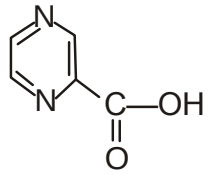

2-pyrazine carboxylic acid
(2-PzCH)

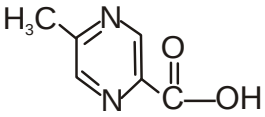

5-methyl-2-pyrazine carboxylic acid
(MPzCH)

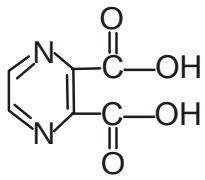

2, 3-pyrazine dicarboxylic acid
(2,3-$PzDCH_2$)

Material and Methods

Dichlorobis(cyclopentadienyl)titanium (IV) (Aldrich), 2-pyrazine carboxylic acid (Aldrich), 5-methyl-2-pyrazine carboxylic acid (Aldrich) and 2,3-pyrazine dicarboxylic acid (Aldrich) were used as supplied. Triethylamine and *n*-Hexane were dried by the standard method [22]. THF (Ferak, Berlin) was dried according to the method described [23]. Stringent precautions were taken to exclude the moisture from the system. The reactions were carried out under dry nitrogen with system well protected from atmospheric moisture by means of calcium chloride guard tubes.

Analysis for carbon, hydrogen and nitrogen were carried out at the Central Micro-Analytical Laboratory of IIT, Kanpur. Titanium was estimated gravimetrically as TiO_2. Chlorine was determined as AgCl. The IR spectra were recorded on a Perkin- Elmer 1710 Infrared Fourier Transform Spectrometer in the region 400-4000 cm^{-1} in KBr pellets. The ^1H NMR spectra were recorded on a Hitachi R-600 FT NMR spectrometer using $CDCl_3$ as solvent (TMS as the internal standard). The electronic spectra of the complexes in chloroform were recorded on a Shimadzu UV-260 spectrophotometer.

Preparation of complexes

A general procedure was followed to synthesize the complexes of Cp_2TiCl_2 with 2-pyrazine carboxylic acid, 5-methyl-2-pyrazine carboxylic acid and 2,3-pyrazine dicarboxylic acid which involved the mixing of the reactants in anhydrous tetrahydrofuran at room temperature in the presence of triethylamine . The reaction mixture was stirred for ~35 h. The precipitated $Et_3N.HCl$ was filtered off and the solvent was removed under reduced pressure. The product so obtained was recrystallised from a

n-hexane/THF mixture. The relevant details of the preparative method used and the complexes obtained are summarized in Table 1. The analytical data of these complexes are tabulated in Table 2.

Table 1. Reactions of Cp_2TiCl_2 with pyrazine carboxylic acids

Reactants, g			Molar Ratio	Stirring Time(hrs)	Product, Colour, Decomposition temp(℃)
Cp_2TiCl_2	Acid	Et_3N			
0.82	2-PzCH 0.41	0.33	1:1:1	30	$(C_5H_5)_2Ti(2\text{-}PzC)Cl$ Reddish brown, 105 (M.P.)
0.79	2-PzCH 0.79	0.64	1:2:2	32	$(C_5H_5)_2Ti(2\text{-}PzC)_2$ Brick red, 115
0.75	MPzCH 0.42	0.31	1:1:1	35	$(C_5H_5)_2Ti(MPzC)Cl$ Orange, 114
0.72	MPzCH 0.80	0.59	1:2:2	38	$(C_5H_5)_2Ti(MPzC)_2$ Reddish brown, 118 (M.P.)
0.69	2,3-$PzDCH_2$ 0.47	0.28	1:1:1	] 30	$(C_5H_5)_2Ti(2,3\text{-}PzDCH)Cl$ Brick red, 108
0.83	2,3-$PzDCH_2$ 1.11	0.67	1:2:2	35	$(C_5H_5)_2Ti(2,3\text{-}PzDCH)_2$ Brick red, 120

Where 2-PzCH= 2-pyrazine carboxylic acid; MPzCH= 5-methyl-2-pyrazine carboxylic acid and 2,3-PzDCH2 = 2,3-pyrazine dicarboxylic acid.

Table2. Characterization data

Complex	Analysis, Found(Calcd.)%					λ_{max} (nm) (in $CHCl_3$)	C_5H_5 (δ)
	Ti	C	H	N	Cl		
$(C_5H_5)_2Ti(2\text{-}PzC)Cl$	14.21 (14.24)	51.99 (53.51)			10.49 (10.55)	245.0	6.8
$(C_5H_5)_2Ti(2\text{-}PzC)_2$	10.93 (11.3)	55.28 (56.62)	3.42 (3.78)		-------	248.2	6.7
$(C_5H_5)_2Ti(MPzC)Cl$	13.61 (13.67)		4.23 (4.28)	7.86 (7.99)	9.93 (10.13)	250.4	
$(C_5H_5)_2Ti(MPzC)_2$	10.56 (10.60)	57.68 (58.42)	4.32 (4.43)		------	255.2	
$(C_5H_5)_2Ti(2,3\text{-}PzDCH)Cl$	12.51 (12.59)		3.35 (3.42)	7.29 (7.36)	9.12 (9.33)	255.0	
$(C_5H_5)_2Ti(2,3\text{-}PzDCH)_2$	9.31 (9.36)	50.93 (51.57)	2.93 (3.13)		--------	252.6	

Results and Discussion

The reactions of Cp_2TiCl_2 with different pyrazine carboxylic acids viz. 2-pyrazine carboxylic acid, 5-methyl-2-pyrazine carboxylic acid and 2,3-pyrazine dicarboxylic acid in 1:1 and 1:2 molar ratio in anhydrous THF in the presence of triethylamine at room temperature may be represented by the following general equations:

$$Cp_2TiCl_2 + LH + Et_3N \xrightarrow[r.t.]{THF} Cp_2Ti(L)Cl + Et_3N.HCl$$

$$Cp_2TiCl_2 + 2LH + 2Et_3N \xrightarrow[r.t.]{THF} Cp_2Ti(L)_2 + 2Et_3N.HCl$$

(Where Cp= cyclopentadienyl; LH= 2-PzCH or MPzCH or 2,3-$PzDCH_2$)

All these complexes are crystalline and extremely sensitive to hydrolysis. These new complexes are soluble in tetrahydrofuran and chloroform but insoluble in *n*-hexane and petroleum ether. Magnetic susceptibility measurements show their diamagnetic nature. The electrical conductance measurements of these complexes in acetone showed them to be non-electrolyte.

The IR spectra of these complexes invariably show the usual absorptions due to cyclopentadienyl groups at ~3100 cm^{-1} [ν(C-H)], ~1435 cm^{-1} [ν(C-C)], ~1020 cm^{-1} [$\delta_{i.p.}$(CH)] and ~810 cm^{-1} [$\delta_{o.p.}$(CH)] [23]. The persistence of the bands of cyclopentadienyl rings in the complexes indicate that these groups remain delocalized and π-bonded to the metal and retain their aromatic character. In the IR spectra of the free acids viz. 2-pyrazine carboxylic acid and

5-methyl-2-pyrazine carboxylic acid, the absorption bands due to ν(OH) and ν(C=O) appear in the regions 3000-2800 cm^{-1} and 1710-1700 cm^{-1} respectively. The band due to ν(OH) disappears in the complexes which indicate the complete removal of the hydroxyl proton of the acid. The bands at 1710 cm^{-1} and 1700 cm^{-1}due to ν(C=O) exhibit a downward shift of ~90 cm^{-1} and appear in the region 1630-1620 cm^{-1} in the complexes indicating that carbonyl oxygen is coordinated to the metal. This suggests that bonding of the carboxylate group to the metal is bidentate in these complexes. The ν(C=N) band occurring at about 1598 cm^{-1}in the free acids does not show any shift in the complexes confirming the non-participation of heterocyclic nitrogen in the bonding.

The IR spectral data for the dicarboxylate complexes show the presence of both the "free" carboxylic and coordinated carboxylate groups at ~1710 cm^{-1} and ~1620 cm^{-1} respectively. This indicates that only one of the two carboxylic groups is bonded to the metal.

The absorption bands in the region 590-550 cm^{-1} are assigned to ν(Ti-O) stretching vibration [25,26].

^{1}H NMR spectra of the free ligand 2-pyrazine carboxylic acid show a signal at δ 7.46 ppm due to hydroxyl proton of the carboxylic groups which is absent in the titanium complexes which confirms the removal of the hydroxyl proton of the carboxylic groups in the complexes. The ^{1}H NMR spectra of all the complexes show a signal due to cyclopentadienyl groups in the region δ 6.8-6.7 ppm [27, 28].

The electronic spectra of all the complexes are recorded in the chloroform. They show fairly intense bands between 255.2 – 245 nm which can be assigned to the charge transfer band [29] and is in accord with their (n-1)d^0, ns^0 electronic configuration (the position of the absorption bands in the UV and visible regions of the electronic spectra of the complexes are given in Table 2).

On the basis of the elemental analyses, spectral data, electrical conductance and magnetic susceptibility measurements, the following structures (I and II) may tentatively be assigned for $(C_5H_5)_2Ti(L)Cl$ and $(C_5H_5)_2Ti(L)_2$ complexes respectively.

I II

(Where L = 2-PzCH or MPzCH or 2, 3-PzDCH$_2$)

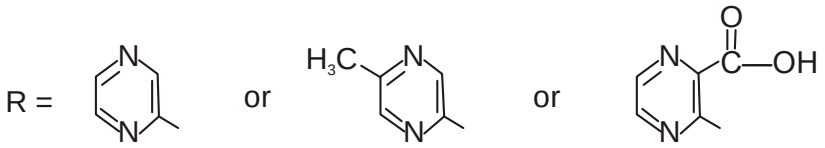

References and Notes

[1] Anagnostopulos, A.; Drew, M. G. B.; Walton, R. A. *Chem. Comm.* **1969**, 1241.
[2] Cinai, M. B.; Manfredotti, A. G.; Musatti, A.; Nardelli, M. Gazz. *Chim. Ital.* **1971**, *101*, 815.
[3] Cox, E. G.; Wardlaw, W.; Webster, K. C. *J. Chem. Soc.* **1936**, 775. [CrossRef]
[4] Faure, R.; Loiseleur, H.; David, G. T. *Acta. Cryst.* **1973**, *B29*, 1890.
[5] Loiseleur, H.; Thomas, G. *Chem. Comm.* **1967**, 182.
[6] Lumme, P.; Lundgren, G.; Mark, W. *Acta Chem. Scand.* **1969**, *23*, 3011. [CrossRef]
[7] Deloume, J. P.; Faure, R.; Loiseleur, H. *Acta Cryst.* **1977**, *B23*, 2709.
[8] Deloume, J. P.; Loiseleur, H. *Acta Cryst.* **1974**, *B30*, 607.
[9] O´ Connor, C. J.; Sinn, E. *Inorg. Chem.* **1981**, *20*, 545. [CrossRef]
[10] Tenhunen, A. *Acta Chem. Scand.* **1972**, *26*, 1291. [CrossRef]
[11] O´ Connor, C. J.; Klein, C. L.; Majeste, R. J.; Trefonas, L. M. *Inorg. Chem.* **1982**, *21*, 64. [CrossRef]
[12] Cariati, F.; Naldini, L. Gazz. *Chim. Ital.* **1965**, *95*, 3.
[13] Cariati, F.; Naldini, L. *J. Inorg. Nucl. Chem.* **1966**, *28*, 2243. [CrossRef]
[14] Pratap, C.; Shigeru, K.; Toshinori, K.; Shigeo, S. *Polyhedron* **2009**, *28*, 370. [CrossRef]
[15] Koepf, H.; Kopf-Maier, P. *Angew. Chem. Int. Ed. Engl.* **1979**, *18*, 477. [CrossRef]
[16] Strohfeldt, K.; Tacke, M. *Chem. Soc. Rev.* **2008**, *37*, 1174. [CrossRef]
[17] Kelter, G.; Sweeney, N.; Strohfeldt, K.; Fiebig, H. H.; Tacke, M. *Anti-Cancer Drugs* **2005**, *16*, 1091. [CrossRef]
[18] Oberschmidt, O.; Hanauske, A. R.; Rehmann, F. J. K.; Strohfeldt, K.; Sweeney, N. J.; Tacke, M. *Anti-Cancer Drugs*, **2005**, *16*, 1071. [CrossRef]
[19] Fichtner, I.; Pampillon, C.; Sweeney, N. J.; Tacke, M. *Anti-Cancer Drugs* **2006**, *17*, 333. [CrossRef]

[20] Beckhove, P.; Oberschmidt, O.; Hanauske, A. R.; Pampillon, C.; Schirrmacher, V.; Sweeney, N. J.; Strohfeldt, K.; Tacke, M. *Anti- Cancer Drugs* **2007**, *18*, 311. [CrossRef]
[21] Top, S.; Kaloun, E. B.; Vessieres, A.; Leceroq, G.; Jaouen, G. *J. Organomet. Chem.* **2002**, *643*, 350. [CrossRef]
[22] Vogel A.I. *A Text Book of Practical Organic Chemistry*, Longmon Green, London, 1948.
[23] Dixit, S. C.; Sharan, R.; Kapoor, R. N. *J. Organomet. Chem.* **1987**, *332*, 135. [CrossRef]
[24] Fritz, H. P. *Adv. Organomet. Chem.* **1964**, *262*, 1.
[25] Kher, S.; Verma, V.; Kapoor, R. N. *Transition Met. Chem.* **1983**, *8*, 163. [CrossRef]
[26] Sharan, R.; Gupta, G.; Kapoor, R. N. *J. Less. Common. Met.* **1978**, *60*, 171. [CrossRef]
[27] Samuel, E. *Bull. Soc. Chim. Fr.* **1966**, 3548.
[28] Elder, M.; Evans, J. C.; Graham, W. A. G. *J. Am. Chem. Soc.* **1969**, *91*, 1245. [CrossRef]
[29] Dixit, S. C.; Singh, R. K. *E-J. Chem.* **2012**, *9*, 277.

ISSN 1984-6428
ONLINE
www.orbital.ufms.br

| Vol 4 | | No. 2 | | April-June 2012 |

Full Paper

Los biossensores electroquímicos, basados en los polímeros conductores, con la etapa autocatalítica en su función y la descripción matemática de su desempeño

Volodymyr Tkach*, Vasyl´ Nechyporuk, Petro Yagodynets´ y Ihor Rusnak

58012, Calle de Kotsyubyns´ky, 2, Universidad Nacional de Chernivtsi, Ucrania

Received: 31 January 2012; revised: 16 April 2012; accepted: 03 July 2012. Available online: 12 July 2012.

ABSTRACT: *The electroanalytic process of the detection of biosubstances, realized by the biosensor, based in conducting polyheterocyclic compounds, the function of which contained autocatalytic stage, was mathematically described. The correspondent mathematical model was analyzed by linear stability theory and bifurcational analysis. The electrochemical instabilities, capable to succeed in this process, were explained in the terms of this model.*

Keywords: *electrochemical sensors; biosensors; conducting polymers; enzyme sensors; oscillatory instability*

Introducción

La química electroanalítica, siendo uno de los capítulos importantes de las ciencias químicas, porque aplica los conocimientos electroquímicos para las finalidades analíticas, es uno de los ramales más importantes de electroquímica, ya que los métodos de la análisis electroquímica tienen la posibilidad de ser aplicados en la detección de las substancias diferentes.

Actualmente una de las áreas de la química electroanalítica es traer los conocimientos electroanalíticos para nano- y biotecnología, que da la posibilidad de confeccionar nano- y biosensores electroquímicos del vasto y rico espectro de su uso [1, 2].

* Corresponding author. E-mail: volodya@llanera.com, nightwatcher2401@gmail.com

Entre los sensores electroquímicos usados los sensores baseados en los polímeros electroconductores (SCP) del tamaño y finalidad diferente ya han sido usados en las técnicas diferentes de análisis, porque ellos son fáciles de modificarse, la señal electroquímica es es más o menos clara y puede ser facilmente interpretada. [1-4].

Los polímeros conductores pueden ser usados como los compuestos activos (que participan en la reacción) [2, 3, 4], catalizadores y también mediadores [1,3 -6].

Si el polímero conductor es modificado (por ejemplo, con un fragmento de la encima) para participar en la reacción y se oxida electroquimicamente en el potencial del trabajo, el sensor no tiene mediador y su esquema de desempeño es

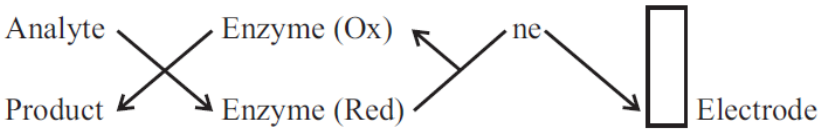

Pero si las moléculas de la encima estén adsorbidas sobre el polímero conductor, o estén presentes como dopantes, hay mas una etapa en su desempeño y el esquema será:

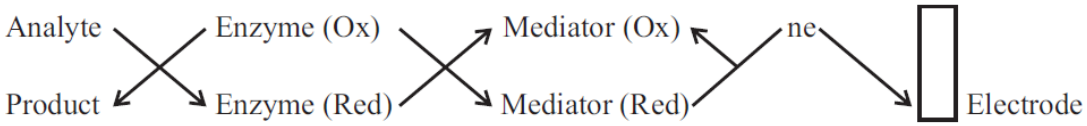

siendo el polímero conductor el mediador[3-6, 8-9].

Entre los métodos de la modificación de los polímeros los más usados son:

- La adsorción de la encima sobre la superficie polimérica
- La funcionalización química (es posible funcionalizar tanto los polímeros (ya sintetizados) cuanto los monómeros (modificándolo antes de la electropolimerización).
- La inmovilización de los compuestos capaces de implementar las funciones del sensor [(a través de la dopación [5, 6] o atrapación [1]).

Por ejemplo, el artículo de revisión [3] describe los tipos diferentes de los biosensores electroquímicos baseados en el polipirrol. Uno de sus ejemplos habiendo sido descrito en [3] fueron los sensores modificados por el factor PQQ con y sin mediador.

El artículo [5] describe el transporte directo del electrón de la GOx inmovilizada en el electrodo de vidrio, modificado por la polifenantrolina. El sensor obtenido demonstró la selectividad excelente y agió como el biosensor de la glicose de la

"respuesta directa".

La tesina [6] y las referencias por dentro describe la preparación (tanto química cuanto electroquímica) de los electrodos sensitivos de oro y polipirrol, capaces de reconocer las cadenas complementarias.

La tesina [1] indica el uso práctico de los politiofenos con las biosubstancias atrapadas. A veces los politiofenos sobreoxidados también se usan.

Actualmente la meta de las investigaciones de los SCP es sintetizar los electrodos baratos que puedan reconocer selectivamente los compuestos específicos.

Los procesos autocatalíticos durante la oxidación de las biosubstancias ya son conocidos y también algunos modelos fueron propuestos para explicar ese tipo del comportamiento [10-11].

Pero a veces el proceso de la detección puede ser acompañado por las inestabilidades electroquímicas. Hay casos en los cuales su presencia es importante porque ella demuestra la mudanza de la resistencia causada por la formación o muerte de algunos compuestos intermedios pero generalmente su aparecida no es deseada. Por ejemplo, la inestabilidad osciladora puede ser observada como:

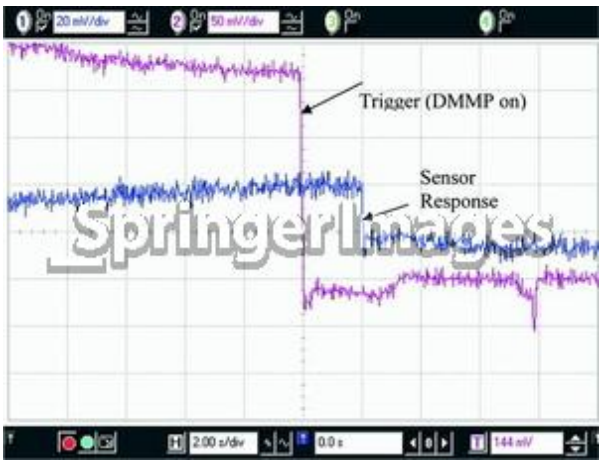

Para encontrar las condiciones de ella, nosotros describimos matemáticamente la función de los sensores y analizamos el modelo matemático a través de los métodos de la teoría de la estabilidad linear y del análisis de bifurcaciones.

Nosotros ya hemos hecho la tentativa de describir matemáticamente la función de algunos tipos de los revestimientos sensorios obtenidos por la electropolimerización de los compuestos heterocíclicos (por ejemplo, los SPC modificado por el factor PQQ) [7,8,9]. Ahora nuestra meta es describir matemáticamente la función de los sensores electroquímicos sin mediador, cuyo desempeño contiene las etapas autocatalíticas.

Encontrar las condiciones del estado estacionario estable e inestable es preciso para encontrar los valores de parámetros en los cuales las respuestas de sensores se

interpretan mejor y desde entonces se puede prever los parámetros del trabajo de sensor.

Materiales y Métodos

El desempeño del sensor en las condiciones potentiotáticas

Ahora describimos el sensor cuya función consiste de las tres etapas

I. Análito + Pol – Enz → Pol – Enz – Análito (el complejo preliminar, proceso autocatalítico, químico)

II. Pol – Enz – Análito → Análito (ox.) + Pol – Enz (red) (químico)

III. Pol – Enz (red) – ne^- → Pol – Enz (Ox) (electroquímico)

Para describirla usamos 3 variables:

c – la concentración del análito en la camada pre-superficial;

C –la concentración superficial del complejo preliminar

E – la concentración superficial del polímero conteniendo la encima en la forma reducida

Para simplificar el modelo nosotros suponemos que:

- El líquido en este sistema se está mezclando intensamente, desde entonces se puede menospreciar la influencia de la convección.
- El electrolito de suporte está en exceso y podemos menospreciar la influencia del flujo de la migración.
- La distribución de la concentración del analito en la camada pre-superficial es linear. La espesura de la camada es constante e igual a δ.
- Las moléculas de la encima son orientadas en la posición que no deja afectar mucho a la difusión del analito y al transporte de electronos
- Las camadas de la encima y del polímero son supuestas a ser monomoleculares.
- Las reaciones químicas son supuestas a ser de la orden uno para cada substancia.

El analito en la camada pre-superficial. El analito entra la camada pre-superficial difundiendo para ella y se pierde en la etapa 1. Entonces, la ecuación del balanzo del analito se describirá como:

$$\frac{dc}{dt} = \frac{2}{\delta}\left(\frac{\Delta}{\delta}(c_b - c) - r_1\right) \equiv F_1$$

Siendo Δ el coeficiente de la difusión, c_b la concentración del analito en el interior

de la solución y r_1 la velocidad de la reacción en la primera etapa.

El complejo preliminar

El complejo de forma durante la etapa I y se pierde en la etapa II. Entonces la reacción en la segunda etapa será descrita como:

$$\frac{dC}{dt} = r_1 - r_2$$

Siendo r_2 la velocidad de la reacción en la segunda etapa.

Se puede escribir esta ecuación de otra manera usando el grado del recubrimiento. Entonces, la ecuación del balanzo de la forma reducida de la encima será decrtita como:

$$\frac{d\varepsilon}{dt} = \Gamma^{-1}{}_{\max 1}\left(r_1 - r_2\right) \equiv F_2$$

Siendo Γ_{max1} la concentración maximal de la encima reducida que quepa en la matriz polimérica. En este caso θ se puede entender como el grado de la reducción de la encima.

La concentración de la forma reducida de la encima

La escoja del PC y los métodos de su síntesis y modificación es prevista por sus funciones. El polímero escogido debe implementar las funciones del mediador: él debe contener los grupos funcionales capaces de oxidar la forma reducida de la encima y entretanto capaces de se oxidar electroquímicamente en los potenciales del trabajo para reformar la forma oxidada. La forma reducida del CP se forma durante la etapa 2 y se oxida electroquímicamente (terminando el transporte de electronos en el sistema sensitivo) en la superficie del electrodo. Entonces, la ecuación de la balanza de la forma reducida de la encima será descrita como

$$\frac{dE}{dt} = r_2 - r_3$$

Siendo r_3 la velocidad de la etapa tercera.

O, si usáremos el grado de la reducción del mediador μ:

$$\frac{d\mu}{dt} = \Gamma^{-1}{}_{\max 2}\left(r_2 - r_3\right) \equiv F_3$$

Siendo $\Gamma^{-1}{}_{\max 2}$ es la concentración maximal del polímero conductor que quepa en la superficie.

Las velocidades de las reacciones en las etapas uno dos y tres se calculan como:

$$r_1 = k_1 \varepsilon c(1-\varepsilon); \qquad r_2 = k_2 \varepsilon(1-\mu); \qquad r_3 = k_3 \mu \exp\left(-\frac{zF}{RT}\phi_0\right)$$

Siendo k_1, k_2 and k_3 las constantes de las velocidades de los procesos correspondientes, z la cantidad de los electrones transportados durante el proceso de la detección, F la constante de Faraday ($F = N_A * e$), R la constante universal de gases, T la temperatura absoluta, φ_0 el salto del potencial en la CED relativamente al potencial de la carga cero.

La carga del electrodo consiste de la carga de la parte oxidada y reducida del electrodo:

$$Q = K_1(\varphi_0-\varphi_1)\mu + K_0\varphi_0(1-\mu)$$

Siendo φ_1 el salto del potencial en la CED entre las partes oxidada y reducida de ella, K_1 y K_0 describen las capacidades integrales de las partes respetivas de la CED.

Entonces, el valor del salto del potencial depende del grado de la reducción de la superfície y el derivativo parcial de la función correspondiente puede ser descrita como:

$$\frac{\partial\phi_0}{\partial\mu} = \frac{\phi_0(K_0 - K_1) + K_1\phi_1}{K_1\mu + K_0(1-\mu)}$$

Resultados y Discusión

Nosotros describimos el comportamiento en este sistema usando la teoría de la inestabilidad linear. La matriz funcional de Jacobi puede ser descrita como:

$$J = \begin{pmatrix} a_{11} & a_{12} & a_{13} \\ a_{21} & a_{22} & a_{33} \\ a_{31} & a_{32} & a_{33} \end{pmatrix}$$

Siendo:

$$a_{11} = \frac{\partial F_1}{\partial c} = \frac{2}{\delta}\left(-k_1(1-\varepsilon) - \frac{\Delta\alpha_1}{\delta}\right)$$

$$a_{12} = \frac{\partial F_1}{\partial \varepsilon} = -\frac{2}{\delta}k_1 c(1-2\varepsilon)$$

$$a_{13} = \frac{\partial F_1}{\partial \mu} = 0$$

$$a_{21} = \frac{\partial F_2}{\partial c_r} = \tilde{A}^{-1}_{\max 1}\left(k_1(1-\varepsilon)\right)$$

$$a_{22} = \frac{\partial F_2}{\partial \varepsilon} = \tilde{A}^{-1}_{\max q}\left(k_1 c(1-2\varepsilon) - k_2(1-\mu)\right)$$

$$a_{23} = \frac{\partial F_2}{\partial \mu} = \tilde{A}^{-1}_{\max 1}\left(k_2 \varepsilon\right)$$

$$a_{31} = \frac{\partial F_3}{\partial c} = 0$$

$$a_{32} = \frac{\partial F_3}{\partial \varepsilon} = \tilde{A}^{-1}_{c,\max}\left(-k_2(1-\mu)\right)$$

$$a_{32} = \frac{\partial F_3}{\partial \mu} = \tilde{A}^{-1}_{c,\max}\left(-k_2\varepsilon - k_3 \exp\left(-\frac{zF}{RT}\phi_0\right) - k_3\mu \exp\left(-\frac{zF}{RT}\phi_0\right)\frac{\phi_0(\mathrm{K}_0 - \mathrm{K}_1) + K_1\phi_1}{\mathrm{K}_1\mu + \mathrm{K}_0(1-\mu)}\right)$$

Las condiciones del estado estacionario estable

La ecuación característica para este sistema se describirá como

$$l^3 + Al^2 + Bl + C = 0$$

siendo que:

$$A = -\left(a_{11} + a_{22} + a_{33}\right)$$

$$B = \begin{vmatrix} a_{11} & a_{12} \\ a_{21} & a_{22} \end{vmatrix} + \begin{vmatrix} a_{11} & a_{32} \\ a_{31} & a_{33} \end{vmatrix} + \begin{vmatrix} a_{22} & a_{23} \\ a_{32} & a_{33} \end{vmatrix}$$

$$C = -\begin{vmatrix} a_{11} & a_{12} & a_{13} \\ a_{21} & a_{22} & a_{23} \\ a_{31} & a_{32} & a_{33} \end{vmatrix}$$

Para investigar la instabilidad linear, nosotros usamos el critério de Rauss y Gurwitz. Él require que para un estado estacionário estabil los menores de los membros de la diagonal principal de la matriz de Gurwitz

$$\begin{pmatrix} A & 1 & 0 \\ C & B & A \\ 0 & 0 & C \end{pmatrix}$$

sean positivos. Los menores de los membros de la diagonal principal se ven como:

$$\Delta_1 = A,\ \Delta_2 = \begin{vmatrix} A & 1 \\ C & B \end{vmatrix},\ \Delta_3 = \begin{vmatrix} A & 1 & 0 \\ C & B & A \\ 0 & 0 & C \end{vmatrix}$$

Se puede ver que $\Delta_3 = C\Delta_2$, entonces, la condición de la estabilidad será descrita

como C>0. Para hacer el Jacobiano más compacto, se puede introducer las variables siguientes:

$$-k_1(1-\varepsilon) = f \;;\; \frac{\Delta}{\delta} = \kappa\,; k_1 c(1-2\varepsilon) = g\;;\; k_2(1-\mu) = h;\; k_2\varepsilon = s\,;$$

$$k_3 \exp\left(-\frac{zF}{RT}\phi_0\right) = u\,;\; k_3\mu\exp\left(-\frac{zF}{RT}\phi_0\right)\frac{\phi_0(\mathrm{K}_0-\mathrm{K}_1)+K_1\phi_1}{\mathrm{K}_1\mu+\mathrm{K}_0(1-\mu)} = v\,; w = u+v\,;$$

Es obvio que f es siempre negativo, κ, g, h, s y u son positivos. La variable v puede tener tanto positivos cuanto negativos valores dependiendo del sistema.

Como los miembros de la matriz a_{13} y a_{31} en este caso son iguales al cero, se puede encontrar las condiciones del estado estacionario con más simplicidad y reescribir la condición del estado estacionario como:

$$fsw < \kappa(gs + gw + wh)$$

Estos valores de los parámetros son las de mejor respuesta y del trecho linear de la curva I(c) si se dice sobre un sensor amperométrico. Se puede hacer conclusión, que la estabilidad del estado estacionario en este sistema es más controlado por la reacción en la primera etapa, por la difusión y por la reacción electroquímica en la tercera etapa.

La inestabilidad del oscilador

Se realiza en las condiciones de la bifurcación de Hopf. Para encontrar las condiciones de la inestabilidad del oscilador, se debe resolver la ecuación:

$$\frac{B_3}{B_1} - B_2 = 0$$

Siendo B_1 = -A; B_2= B; B_3= -C, y la condición obligatoria es B_2>0.

La condición precisa se realice si la diagonal principal de Jacobi contiene los elementos positivos. Se puede ver que el element

$$-k_3\mu\exp\left(-\frac{zF}{RT}\phi_0\right)\frac{\phi_0(\mathrm{K}_0-\mathrm{K}_1)+K_1\phi_1}{\mathrm{K}_1\mu+\mathrm{K}_0(1-\mu)}$$

podrá ser positivo si φ_0 fuere negativo (eso usualmente acontece cuando se oxidante los reducientes fuertes que tienen el momento del dipolo). Cuánto más fuerte reduciente es el análito, cuanto menor es φ_0 (los potenciales de los pares de las 3 reacciones son casi iguales), como describimos también en el artículo [8].

Una causa a más de la inestabilidad osciladora, imposible para el caso del artículo [8], es el desenvolvimiento de la formación autocatalítica del complejo intermediario,

que puede ser descrito por la condición g>0. Según la misma, este factor sólo podrá accionar como la causa del comportamiento oscilador, si ε<0,5, porque si él tuviere el valor mayor, la expresión (1-2ε) será negativa y portanto perderá la positiva conexión de vuelta

El ciclo oscilador existe por causa de la mudanza cíclica de la conducción eléctrica de la superficie. Ella cambia durante las reacciones químicas y vuelve al valor inicial después de la etapa electroquímica. Este ciclo se repite cuando el analito está presente en este sistema, entonces el comportamiento superficial para este sistema es importante.

La inestabilidad monotónica en este sistema es posible también. Sus condiciones pueden ser definidas como Tr J<0, Det J =0. Como la condición Tr J <0 se realice para la mayoridad de los sistemas, se puede dar atención a la condición principal Det J = 0. La inestabilidad monotónica se realiza en las condiciones de:

$$f = \frac{\kappa(gs + gw + wh)}{ws}$$

En esta condición el sistema existe en la multiplicidad de los estados estacionarios entre los cuales sólo escoge un y él se destruye si las condiciones mudan. La inestabilidad monotónica existe en el valor crítico de la velocidad de la reacción química en la etapa uno.

Conclusiones

1. La función de los sensores y biossensores basados en los PCs, en el modo potenciostático fue descrita matemáticamente. El modelo matemático fue analizado usando la teoría de la inestabilidad linear y la análisis de bifurcaciones
2. Las condiciones del estado estacionario estable pueden ser encontradas usando el criterio de Rauss e Gurwitz. La estabilidad de los estados estacionarios es controlada por la difusión del analito, la velocidad de la reacción en la primera etapa y en la tercera etapa.
3. La inestabilidad oscilatoria podrá suceder si el analito fuere el reductor fuerte que tiene el momento del dipolo y también podrá ser causada por la reacción autocatalítica.
4. La inestabilidad monotónica para este sistema puede suceder en el valor crítico de la velocidad de la reacción química en la primera etapa.

Referencias y Notas

[1] de Andrade, V. M. [Doctoral dissertation]. Porto Alegre, Brazil: UFRGS. 2006 and references cited therein.
[2] Tyler, D. M.; Pullen, A.; Swager, T. M. *Chem. Rev.* **2000***, 100*, 2537. [CrossRef]
[3] Ramanavicius, A.; Ramanaviciene, A.; Malinauskas, A. *Electrochimica Acta* **2006**, *51*, 6025*,* and references cited therein. [Link]
[4] Gupta, N.; Sharma, S.; Mir, I. A.; Kumar, D. *J. Sci. Ind. Res*. **2006**, *65*, 549.
[5] Oztekin, Y.; Ramanaviciene, A.; Yazicigil, Z.; Solak, A. O.; Ramanavicius, A. *Biosens. Bioelectr.* **2011**, *26*, 6. [CrossRef]
[6] Tosar, J. P. Thesis Lic. Bioquím., Universidade de la República, Montevideo, 2008 and references cited therein.
[7] Tkach, V.; Nechyporuk, V.; Yagodynets', P. Abstract 7th Nanoscience and Nanotechnology conference, Istanbul, 2011, 173.
[8] Tkach, V.; Nechyporuk, V.; Yagodynets, P.; Yu, M. *Rev. Soc. Quím. Perú* **2011**, *77*, 259. [Link]
[9] Tkach, V.; Nechyporuk, V.; Yagodynets, P.; Yu, M. Abstract 2nd International Conference in Organic Chemistry "Advances in heterocyclic chemistry", Tbilisi, 2011, p. 101–102
[10] С.Д. Варфоломеев, С.О. Бачурин и Ч.Д. Тоай., Мол. Биол. **1977**, *11*, 423.
[11] Tien, J. H.; Hazelton, W. D.; Sparks, R.; Ulrich, C. M. *Bul. Math. Biol.* **2005***, 67*, 683. [CrossRef]